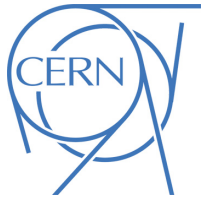




JHEP 07 (2019) 117
DOI: [10.1007/JHEP07\(2019\)117](https://doi.org/10.1007/JHEP07(2019)117)



CERN-EP-2018-300
1st August 2019

Search for scalar resonances decaying into $\mu^+\mu^-$ in events with and without b -tagged jets produced in proton–proton collisions at $\sqrt{s} = 13$ TeV with the ATLAS detector

The ATLAS Collaboration

A search for a narrow scalar resonance decaying into an opposite-sign muon pair produced in events with and without b -tagged jets is presented in this paper. The search uses 36.1 fb^{-1} of $\sqrt{s} = 13$ TeV proton–proton collision data recorded by the ATLAS experiment at the LHC. No significant excess of events above the expected Standard Model background is observed in the investigated mass range of 0.2 to 1.0 TeV. The observed upper limits at 95% confidence level on the cross section times branching ratio for b -quark associated production and gluon–gluon fusion are between 1.9 and 41 fb and 1.6 and 44 fb respectively, which is consistent with expectations.

1 Introduction

This paper presents a search, in proton–proton (pp) collision data at a centre-of-mass energy of 13 TeV, targeting a scalar particle Φ with a mass in the range 0.2–1.0 TeV decaying into two opposite-sign muons. The natural width of the particle is assumed to be much narrower than the experimental resolution, such that it is the latter that dominates the distribution of the dimuon invariant mass in signal events. To maximize the sensitivity to the presence of b -quarks, the analysis is performed in two data categories. The first search category requires at least one jet tagged as containing b -hadrons (b -tagged) in the final state. The second category requires exactly zero b -tagged jets in the event. Simultaneous fits to these two categories are used to search for both the gluon–gluon fusion and b -associated production mechanisms of the scalar particle. This work is primarily motivated as a signature-based search; the event selection is not designed to target any specific model and instead facilitates the comparison of the data with predictions from various theoretical models.

The discovery of the 125 GeV Higgs boson at the Large Hadron Collider (LHC) [1, 2] was a significant step in understanding the mechanism of electroweak symmetry breaking (EWSB). Measurements of the properties of this particle [3–7] are so far consistent with expectations for the Standard Model (SM) Higgs boson [8–13]. However, the observed Higgs boson could be only a part of an extended scalar sector, as predicted by several theoretical models beyond the SM. For example, such an extended scalar sector is predicted by a class of extensions of the SM known as the two-Higgs-doublet models (2HDM) [14, 15].

The 2HDM posit the existence of three neutral bosons with properties and coupling strengths differing from those of the SM Higgs particle. One of the higher-mass neutral Higgs bosons may couple to muons at a higher rate than to τ -leptons, in contradiction to the SM Yukawa ordering. This is the case in the Flavourful Higgs model [16], for example. The search described in this paper sets limits on the cross-section times branching ratio of Φ decaying into muon pairs which are more stringent than the equivalent limits for Φ decaying into τ -lepton pairs [17]. This is due to higher identification efficiency and lower background rate for muons than for τ -leptons, and the invariant-mass resolution being better for muon pairs than for τ -lepton pairs. Similarly, the coupling of these higher-mass neutral Higgs bosons to b -quarks could be enhanced relative to the SM Higgs boson coupling. Hence, the production of Φ in association with b -quarks ($bb\Phi$), shown in Figure 1(a), could be more abundant than the production of Φ by gluon–gluon fusion (ggF), shown in Figure 1(b). The $\Phi \rightarrow b\bar{b}$ decay mode, where Φ is produced in associations with b -quarks, is investigated by CMS in Ref. [18].

Additional interest for the search for an excess of events with respect to the SM predictions in the dimuon plus b -tagged jets final state arises from Z' and leptoquark models [19], which could result in either resonant or non-resonant contributions to the $pp \rightarrow t\bar{t}\mu^+\mu^- \rightarrow WbW\bar{b}\mu^+\mu^-$ final state. This work complements the search for Z' candidates decaying into muon pairs presented in Ref. [20]: by classifying events in terms of the presence or absence of a b -tagged jet, it may be sensitive to signatures not observable with an inclusive selection.

Previous similar searches focused explicitly on beyond-the-SM Higgs bosons decaying into muon pairs, in the mass range 90–500 GeV [21, 22] using $\sqrt{s} = 7$ and 8 TeV data. This work extends the exclusion limits for new scalar resonances with masses up to 1.0 TeV.

The analysis described in this paper makes use of a fit to the observed dimuon invariant mass ($m_{\mu\mu}$) spectra. The presence of a signal produced either in association with b -quarks or via gluon–gluon fusion is tested with simultaneous fits to the two data regions (with and without a b -tagged jet) separately for $bb\Phi$ and

ggF production modes. No assumptions are made about the relative contributions of the $bb\Phi$ and ggF cross-sections.

This paper is structured as follows. Section 2 describes the ATLAS detector. Section 3 discusses the data and the simulated event samples used to model the signal and the background processes. The event reconstruction is discussed in Section 4, while Section 5 describes the background estimate and introduces the signal interpolation procedure used to model the $m_{\mu\mu}$ distribution for resonance mass hypotheses for which no simulated sample was generated. The event yields and the description of the statistical analysis are discussed in Section 6, followed by Section 7, which provides an overview of the systematic uncertainties. Section 8 summarizes the results.

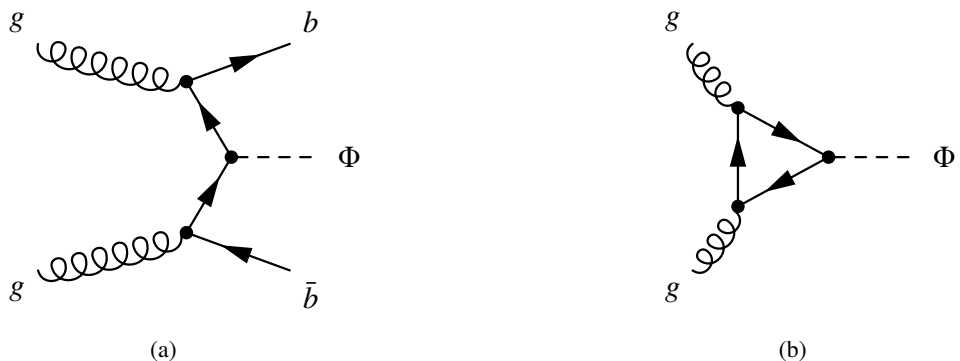


Figure 1: Feynman diagrams for (a) the b -quark associated production mode and (b) the gluon-gluon fusion production mode.

2 ATLAS detector

ATLAS [23], [24] is a multipurpose particle detector with a forward–backward symmetric cylindrical geometry and near 4π coverage in solid angle.¹ It consists of an inner tracking detector surrounded by a thin superconducting solenoid, electromagnetic and hadronic calorimeters, and a muon spectrometer.

The inner tracking detector (ID) covers the pseudorapidity range $|\eta| < 2.5$, and is surrounded by a superconducting solenoid providing a 2 T magnetic field. At small radii, a high-granularity silicon pixel detector covers the vertex region and typically provides four measurements per track. It is followed by the silicon microstrip tracker, which provides eight measurement points per track. The silicon detectors are complemented by a gas-filled straw-tube transition radiation tracker, which extends the tracking capability radially with typically 35 measurements per track for particles at $|\eta| = 2.0$.

Electromagnetic (EM) calorimetry, within the region $|\eta| < 3.2$, is provided by barrel and endcap high-granularity lead/liquid-argon (LAr) sampling calorimeters, with an additional thin LAr presampler covering

¹ ATLAS uses a right-handed coordinate system with its origin at the nominal interaction point (IP) in the centre of the detector and the z -axis along the beam pipe. The x -axis points from the IP to the centre of the LHC ring, and the y -axis points upward. Cylindrical coordinates (r, ϕ) are used in the transverse plane, ϕ being the azimuthal angle around the z -axis. The pseudorapidity is defined in terms of the polar angle θ as $\eta = -\ln \tan(\theta/2)$. The angular distance is measured in units of $\Delta R = \sqrt{(\Delta\eta)^2 + (\Delta\phi)^2}$.

$|\eta| < 1.8$ to correct for energy loss in the upstream material. For $|\eta| < 2.5$ the EM calorimeter is divided into three layers in depth. A steel/scintillator-tile calorimeter provides hadronic calorimetry for $|\eta| < 1.7$. LAr ionization, with copper as absorber, is used for the hadronic calorimeters in the endcap region $1.5 < |\eta| < 3.2$. The solid-angle coverage is completed with forward copper/LAr and tungsten/LAr calorimeter modules in $3.1 < |\eta| < 4.9$, optimized for EM and hadronic measurements, respectively.

The muon spectrometer (MS) surrounds the calorimeters and comprises separate trigger and high-precision tracking chambers measuring the deflection of muons in a magnetic field provided by one barrel and two end-cap toroid magnets. The precision chamber system covers the region $|\eta| < 2.7$ with three layers of monitored drift tubes, complemented by cathode-strip chambers in the forward region. The muon trigger system covers the range $|\eta| < 2.4$ with resistive-plate chambers in the barrel and thin-gap chambers in the endcap regions.

A two-level trigger and data acquisition system is used to record events for offline analysis [25]. The level-1 trigger is implemented in hardware and uses a subset of the detector information to reduce the event rate to a value of at most 100 kHz. It is followed by a software-based high-level trigger which filters events using the full detector information and outputs events for permanent storage at an average rate of 1 kHz.

3 Data and simulated event samples

This search is performed with a sample of pp collision data recorded at a centre-of-mass energy $\sqrt{s} = 13$ TeV corresponding to an integrated luminosity of 36.1 fb^{-1} collected during 2015 and 2016. Events are considered for further analysis only if they were collected under stable LHC beam conditions and the relevant detector components were fully operational.

The data used in this analysis were collected using a combination of muon triggers. For the 2015 dataset an isolated muon with transverse momentum p_T greater than 20 GeV was required, while for 2016 this requirement was raised to 26 GeV. To avoid inefficiencies due to the isolation requirement, these triggers were complemented by a trigger requiring a reconstructed muon with p_T greater than 50 GeV, without any isolation requirements.

Simulated signal events were generated similarly to the SM Higgs boson H , where H was replaced by a higher-mass scalar boson Φ with a constant width of 4 MeV. Nine Monte Carlo (MC) samples were generated in the mass range 0.2–1.0 TeV at intervals of 100 GeV. Both the ggF and bb Φ production modes were considered. Events were generated at next-to-leading order (NLO) with PowHEG-Box 2 [26–29] and MADGRAPH5_AMC@NLO [30, 31], for ggF and bb Φ respectively. The CT10 [32] set of parton distribution functions (PDFs) was used in the generation of ggF events while CT10NLO_NF4 [33] PDFs were used to produce the b -quark associated signal samples in the four-flavour scheme. In the gluon–gluon fusion production mode, PYTHIA 8.210 [34] with the AZNLO [35] set of tuned parameters was used together with the CTEQ6L1 [36] PDF set for the parton shower, underlying event and hadronization simulation. For the b -quark associated production, PYTHIA 8.210 with the A14 [37] set of tuned parameters was used together with the NNPDF2.3LO [38] PDF set for the parton shower, underlying event, and hadronization simulation. The EvtGen v1.2.0 program [39] was used to model the properties of the bottom and charm hadron decays in all signal samples.

Since the generated signal samples are spaced equally in m_Φ while the experimental resolution increases with m_Φ , signal distributions for intermediate mass hypotheses were obtained using an interpolation procedure, described in Section 5.

Events containing $Z/\gamma^* + \text{jets}$ were simulated using PowHEG-Box 2 [28, 40] interfaced to the PYTHIA 8.186 parton shower model and the CT10 PDF set. The AZNLO tune was used, with PDF set CTEQ6L1 for the modelling of non-perturbative effects. The EvtGen v1.2.0 program was used to model the properties of the bottom and charm hadron decays. Photos++ 3.52 [41] was used for photons radiated from electroweak vertices and charged leptons. Generator-level filters are employed to enhance the fraction of simulated events in the phase-space region that is most relevant for the analysis. Event yields were corrected with a mass-dependent rescaling at next-to-next-to-leading order (NNLO) in the QCD coupling constant, computed with VRAP 0.9 [42] and the CT14NNLO PDF set [33]. Mass-dependent electro-weak (EW) corrections were computed at NLO with mcsanc-1.20 [43], along with photon-induced contributions ($\gamma\gamma \rightarrow \ell\ell$ via t - and u -channel processes) computed with the MRST2004QED PDF set [44].

Additional $Z/\gamma^* + \text{jets}$ events, used to evaluate the systematic uncertainty from the modelling of the fitted $m_{\mu\mu}$ distribution, were simulated with SHERPA 2.2.1 [45] and with MADGRAPH5_AMC@NLO interfaced with PYTHIA 8.186. In SHERPA, $Z/\gamma^* + \text{jets}$ matrix elements were evaluated with up to two extra partons at NLO, and three or four extra partons were included at LO in QCD. The merging of different parton multiplicities was achieved through a matching scheme based on the CKKW-L [46] [47] merging technique using a merging scale of $Q_{\text{cut}} = 20$ GeV. The models used for the parton shower and underlying event are the ones provided internally by SHERPA. The SHERPA 2.2.1 generator adopts a full five-flavour scheme, with massless b -quarks and c -quarks in the matrix elements. These quarks are given mass in the final state and massive quarks can be produced directly via the parton shower. The MADGRAPH5_AMC@NLO v2 generator merges the LO (QCD) matrix-element calculations for $Z/\gamma^* + \text{jets}$ with up to four additional partons (higher jet multiplicities are modelled by the parton shower algorithm). The merging scheme applied to combine different parton multiplicities is the CKKW-L scheme with a merging scale of $Q_{\text{cut}} = 30$ GeV. For the LO matrix-element calculation the NNPDF2.3 LO PDFs were used (with $\alpha_S = 0.13$). The A14 tune, together with the NNPDF2.3 LO PDFs, was used for the parton shower. Similarly to SHERPA 2.2.1, MADGRAPH5_AMC@NLO adopts a full five-flavour scheme.

For the generation of $t\bar{t}$ and single top-quark production in the Wt - and t -channel, the PowHEG-Box 2 generator with the CT10 PDF set was used for the matrix element calculations. The parton shower, fragmentation, and the underlying event were simulated using PYTHIA 6.428 with the CTEQ6L1 PDF set and the corresponding Perugia 2012 tune [48]. The top-quark mass was set to 172.5 GeV. For the generation of $t\bar{t}$ events, the h_{damp} parameter of PowHEG-Box, which controls the transverse momentum of the first additional emission beyond the Born configuration, was set to the mass of the top quark. The main effect of this parameter is to regulate the high transverse momentum emission against which the $t\bar{t}$ system recoils. The $t\bar{t}$ production sample was normalized to the predicted production cross-section as calculated with the TOP++2.0 program to NNLO in perturbative QCD, including soft-gluon resummation to next-to-next-to-leading-log (NNLL) order [49]. The normalization of the single top-quark event samples used an approximate calculation at NLO in QCD for the t -channels [50, 51] while NLO+NNLL predictions were used for the Wt -channel [51]. The EvtGen v1.2.0 program was used to describe the properties of the bottom and charm hadron decays.

Diboson processes were modelled using the SHERPA 2.1.1 [45] generator and they were calculated for up to one (ZZ) or zero (WW , WZ) additional partons at NLO and up to three additional partons at leading order (LO) using the Comix [52] and OpenLoops [53] matrix-element generators. The matrix element calculation was merged with the SHERPA internal parton shower [54] using the ME+PS@NLO prescription [55]. The CT10 PDF set was used in conjunction with dedicated parton shower tuning developed by the SHERPA authors. The generator cross-sections, calculated at NLO, were used in this case.

The generated signal samples were simulated with the fast simulation [56, 57] framework of ATLAS, which replaces the full simulation of the electromagnetic and hadronic calorimeters by a parameterized model. The background samples were simulated using the full Geant4-based simulation of the detector [58]. Finally, the simulated events were processed through the same reconstruction software as the data. The effects of pile-up from multiple proton–proton interactions in the same and neighbouring bunch crossings were accounted for by overlaying minimum-bias events simulated using PYTHIA 8 with the A2 tune [59] and interfaced with the MSTW2008LO PDFs. Simulated events were then reweighted to match the pile-up conditions observed in the data.

4 Event reconstruction

Interaction vertices are reconstructed [60] from tracks measured by the inner detector. The primary vertex is defined as the vertex with the largest $\sum p_T^2$ of its associated tracks. It must have at least two associated tracks, each with transverse momentum $p_T > 400$ MeV.

Muon candidates are reconstructed from an ID track combined with a track or track segment detected in the muon spectrometer [61]. These two tracks are used as inputs to a combined fit (for p_T less than 300 GeV) or to a statistical combination (for p_T greater than 300 GeV) [61]. The combined fit takes into account the energy loss in the calorimeter and multiple-scattering effects. The statistical combination for high transverse momenta is performed to mitigate the effects of relative ID and MS misalignments. High- p_T muon candidates are required to have at least three hits, one in each of the three layers of precision chambers in the MS. For these muons, specific regions of the MS where the alignment is suboptimal are vetoed as a precaution, as well as the transition region between the MS barrel and endcap ($1.01 < |\eta| < 1.10$). Further quality requirements are applied to the consistency of the ID and MS momentum measurements, and to the measured momentum uncertainty for the MS track.

The reconstructed muon candidates are required to have transverse momentum, p_T , greater than 30 GeV and pseudorapidity $|\eta| < 2.5$. They are further required to be consistent with the hypothesis that they originate from the primary vertex by applying selections on the transverse (d_0) and longitudinal (z_0) impact parameters, defined relative to the primary vertex position: $|d_0/\sigma_{d_0}| < 3$ and $|z_0 \sin \theta| < 0.5$ mm where σ_{d_0} denotes the uncertainty in the transverse impact parameter. A loose isolation requirement is applied, based on the sum of the momenta of inner detector tracks which lie within a variable-sized cone, with $\Delta R_{\max} = 0.3$, around the muon track. This isolation requirement is tuned to yield a 99% efficiency over the full range of muon p_T .

Jets are reconstructed from noise-suppressed energy clusters in the calorimeter [62] with the anti- k_t algorithm [63, 64] with radius parameter $R = 0.4$. The energies of the jets are calibrated using a jet energy scale (JES) correction derived from both simulation and in situ studies using data [65]. All jets are required to have $p_T > 25$ GeV and $|\eta| < 4.5$. A multivariate selection that reduces contamination from pile-up [66] is applied to jets with $p_T < 60$ GeV and with $|\eta| < 2.4$ utilizing calorimeter and tracking information to separate hard-scatter jets from pile-up jets.

Selected jets in the central region can be tagged as containing b -hadrons (b -tagged) by using a multivariate discriminant (MV2c10) [67, 68] that combines information from an impact-parameter-based algorithm, from the explicit reconstruction of a secondary vertex and from a multi-vertex fitter that attempts to reconstruct the full b - to c -hadron decay chain. At the chosen working point, the algorithm provides nominal light-flavour (u,d,s -quark and gluon) and c -jet misidentification rates of 3% and 32%, respectively,

for an average 85% b -jet tagging efficiency, as estimated from simulated $t\bar{t}$ events for jets with $p_T > 20 \text{ GeV}$ and $|\eta| < 2.5$. The flavour-tagging efficiencies from simulation are corrected separately for b -, c - and light-flavour jets, based on the respective data-based calibration analyses [69].

Simulated events were corrected to reflect the muon and jet momentum scales and resolutions, b -jet identification algorithm calibration, as well as the muon trigger, identification, and isolation efficiencies measured in data.

An overlap removal procedure is applied to avoid a single particle being reconstructed as two different objects as follows. Jets not tagged as b -jets, but which are reconstructed within $\Delta R = 0.2$ of a muon, are removed if they have fewer than three associated tracks or if the muon energy constitutes more than 50% of the jet energy. Muons reconstructed within a cone of size $\Delta R = \min(0.4, 0.04 + 10 \text{ GeV}/p_T)$ around the jet axis of any surviving jet are removed. Jets are also discarded if they are within a cone of size $\Delta R = 0.2$ around an electron candidate. Electrons are reconstructed from clusters of energy deposits in the electromagnetic calorimeter that match ID tracks, and are identified as described in Ref. [70]. For electrons with transverse energy $E_T > 10 \text{ GeV}$ and pseudorapidity of $|\eta| < 2.47$, a likelihood-based selection is used at the “loose” operating point defined in [70].

Following the overlap removal, jet cleaning criteria are applied to identify jets arising from non-collision sources or noise in the calorimeters, and any event containing such a jet is removed [71].

The missing transverse momentum, E_T^{miss} , is defined as the negative vector sum of the transverse momenta of muons, electrons and jets associated with the primary vertex. A soft term [72] is added to include well-reconstructed tracks matched to the primary vertex that are not associated with any of the objects.

At least two reconstructed muons are required in the event, and the two highest- p_T muons of the event are used to form a dimuon candidate. If these muons do not have opposite charges, the event is rejected.

5 Signal and background estimate

Events satisfying the preselection criteria of Section 4 are considered for further analysis. Depending on the value of the reconstructed dimuon invariant mass and the number of b -tagged jets, they are classified as being in either a control region, used to measure the rate of the dominant backgrounds ($Z/\gamma^* + \text{jets}$ and $t\bar{t}$) or a signal region, used to search for the $\Phi \rightarrow \mu\mu$ signal. All signal and control regions are designed to be orthogonal.

Selected events are retained in the signal region if the dimuon invariant mass, $m_{\mu\mu}$, exceeds 160 GeV, while they are retained in the control region if $100 \text{ GeV} < m_{\mu\mu} < 160 \text{ GeV}$. The control regions do not include the Z -boson peak; this avoids constraints on systematic uncertainties in a region of phase space which may behave differently with respect to the high mass tails where the signal search is focused.

Events in the signal region are further classified as “SRbTag”, if at least one b -tagged jet is identified in the event, or “SRbVeto”, otherwise. No further optimization of the signal region definition is considered, in order to minimize the assumptions made about the signal kinematics.

Events in the control region are further classified as “CRbVeto” if there is no b -tagged jet identified in the event, while remaining control region events are classified as “CRbTag”, if the missing transverse momentum is less than 100 GeV, or “CRttbar” otherwise.

The dominant background sources for this signature are muon pairs through $Z/\gamma^* +$ jets, top-quark pair, and diboson production. $W +$ jets and QCD multi-jet events contribute less than 0.01% to the total background in signal regions, and therefore are neglected. All relevant background contributions were modelled using simulated samples as described in Section 3.

Simulated $Z/\gamma^* +$ jets events were categorized depending on the generator-level “truth” labels of the jets in the event. Simulated jets were truth-labelled according to which hadrons with $p_T > 5 \text{ GeV}$ were found within a cone of size $\Delta R = 0.3$ around the jet axis. If a b -hadron was found, the jet was truth-labelled as a b -jet. If no b -hadron was found, but a c -hadron was present, then the jet was truth-labelled as a c -jet. Otherwise the jet was truth-labelled as a light-flavour (i.e., u,d,s -quark, or gluon) jet. The $Z/\gamma^* +$ jets events were classified as $Z +$ heavy flavour ($Z + \text{HF}$) if a b -jet or c -jet was found at generator level and $Z +$ light flavour ($Z + \text{LF}$) otherwise. These two categories of simulated events were treated as different background components.

The predictions for the expected numbers of $t\bar{t}$, $Z + \text{HF}$ and $Z + \text{LF}$ events are adjusted to match the number of events in data in the control regions via a global fit (see Section 6), while the other backgrounds are normalized to their expected cross-section, discussed in Section 3.

The expected invariant mass distribution of the narrow resonance signal m_Φ is modelled with a double-sided Crystal Ball (DSCB) [73] function in the mass range $0.2 \text{ TeV} < m_\Phi < 1.0 \text{ TeV}$ for all nine simulated MC samples. The width of the $m_{\mu\mu}$ distribution is dominated by the experimental resolution, which can be described by a Gaussian distribution. The power-law asymmetric terms of the DSCB have enough degrees of freedom to model the $m_{\mu\mu}$ tails for signals in the 0.2 – 1.0 TeV mass range. In order to interpolate the signal parameterization to any mass value in this fit range, second-order polynomial parameterizations of all six signal-shape parameters as a function of m_Φ are obtained from a simultaneous fit to all the generated mass points m_Φ , separately for events with and without at least one b -tagged jet. Since all signal samples are scaled to the same arbitrary cross-section, any differences in the number of events are due to differences in the acceptances of the selection. The fitted normalization is parameterized with a second-order polynomial in a similar way to the other DSCB parameters. As a result of this procedure, the $m_{\mu\mu}$ distribution for an arbitrary hypothesis mass can be found by constructing a DSCB from parameters calculated using the fitted coefficients and the hypothesized mass m_Φ . The interpolation is performed separately for each systematic variation, and for the gluon–gluon fusion and b -quark associated production signal samples. Binned templates are then generated from the DSCB. To validate the interpolation procedure, one simulated sample at a time is removed from the simultaneous fit, and the template generated from the DCSB is compared with the $m_{\mu\mu}$ distribution from the corresponding simulated sample and they agree within 2–5%, the size of the bin-by-bin MC statistical uncertainty. Nine MC samples were generated in the mass range 0.2 – 1.0 TeV , every 100 GeV . The interpolation procedure was used to generate signal templates every 10 GeV between 0.2 and 0.3 TeV , every 20 GeV between 0.3 and 0.6 TeV , and every 50 GeV between 0.6 and 1.0 TeV .

The acceptance of b -quark associated production in the SRbTag region varies in the range 11–19% depending on m_Φ . The acceptance in the SRbVeto region, which is inversely correlated with the SRbTag one, varies from 20% to 15%. For this reason, both SRbTag and SRbVeto are included in the global fit (see Section 6). The acceptance of gluon–gluon fusion in the SRbVeto region varies in the range 31–35%. The acceptance in the SRbTag is less than 2% for all masses.

6 Statistical analysis

The test statistic \tilde{q}_μ as defined in Ref. [74] is used to determine the probability that the background-only model is compatible with the observed data, to extract the local p -value, and, if no hint of a signal is found in this procedure, to derive exclusion intervals using the CL_s method. The binned likelihood function is built as the product of Poisson probability terms associated with the bins in the $m_{\mu\mu}$ distribution in the 0.16–1.5 TeV range. It depends on the parameter of interest, on the normalization factors of the dominant backgrounds and on additional nuisance parameters (representing the estimates of the systematic uncertainties) that are each constrained by a Gaussian prior. The bin-by-bin statistical uncertainties of the simulated backgrounds are also considered. Separate fits are performed to test the different hypotheses: only $bb\Phi$ signal, only ggF signal, and signal composed of different mixtures of the two production modes. Data are fitted in the 0.16–1.5 TeV range to check that the background description is correct and to constrain systematic uncertainties, while the signal presence is tested in a narrower 0.2–1.0 TeV range.

Logarithmic binning in $m_{\mu\mu}$ is chosen to scale with experimental dimuon mass resolution (defined as full-width at half-maximum), which varies from 5% at $m_{\mu\mu} = 200$ GeV to 14% at $m_{\mu\mu} = 1$ TeV, while ensuring that the number of simulated background events in each bin is sufficient to reliably predict the background. The numbers of events in the CRbVeto, CRbTag, and CRttbar control regions are also included in the maximum-likelihood fit. Data in these regions are used to constrain the normalizations of the dominant background processes: $Z+LF$, $Z+HF$, and $t\bar{t}$. The normalization factors used to scale the expected number of events for each process to match the data are free parameters in the fit. Their expected uncertainty is estimated using an Asimov dataset [74], a pseudo-data distribution equal to the background plus signal expectation for a given value of the signal cross-section times branching ratio. The expected and measured normalization factors are shown in Table 1. They are measured in a fit to data under the background plus signal hypothesis, where the signal corresponds to $bb\Phi$ production with mass $m_\Phi = 480$ GeV.

Table 1: Normalization factors of the dominant backgrounds as measured in a fit to data under the background plus signal hypothesis (480 GeV $bb\Phi$ signal). The uncertainty includes both the statistical and systematic sources: the latter ones dominate. The reduction of the observed relative uncertainty of the $Z+HF$ normalization in the data fit is due to the large increase in the number of $Z+HF$ events when the data in signal regions are included.

Background	Asimov data	Observed data
$Z+HF$	1.00 ± 0.23	1.47 ± 0.26
$Z+LF$	1.00 ± 0.02	1.02 ± 0.02
$t\bar{t}$	1.00 ± 0.04	1.02 ± 0.04

As discussed in Section 7, the experimental uncertainties are treated as fully correlated among different processes and regions, while the theoretical uncertainties are mostly uncorrelated among processes.

The numbers of observed events in the signal regions together with the predicted event yields from signal and background processes are shown in Table 2. The numbers are the results of the maximum-likelihood fit to data under the background plus signal hypothesis, where the signal corresponds to $bb\Phi$ production with $m_\Phi = 480$ GeV. The number of predicted signal events corresponds to the expected upper limit (UL) times the cross-section: this highlights the comparison between signal and background at the edge of the analysis sensitivity.

The observed numbers of events are compatible with those expected from SM processes, within uncertainties. The $m_{\mu\mu}$ distribution in the SRbTag region is shown in Figure 2(a) for a $bb\Phi$ -only fit. The $m_{\mu\mu}$ distribution in the SRbVeto region is shown in Figure 2(b), for a ggF-only fit. Each background process is normalized according to its post-fit cross-section. The templates for the $m_\Phi = 200$ GeV, $m_\Phi = 480$ GeV and $m_\Phi = 1$ TeV mass hypotheses are normalized to the expected upper limit.

Table 2: Post-fit numbers of events from the combined fit under the background plus signal hypothesis (480 GeV $bb\Phi$ signal). Here ‘‘Total Bkg’’ represents the sum of all backgrounds. The quoted uncertainties are the combination of statistical and systematic uncertainties. The uncertainty in the total background determined by the fit is smaller than the sum in quadrature of the individual components due to the normalization factors and systematic uncertainties that introduce correlation between them. The number of signal events corresponds to the expected upper limit (UL) times the cross-section. The uncertainties in the expected signal yields are from fits using the Asimov dataset.

Sample	SRbTag	SRbVeto	CRbTag	CRbVeto	CRttbar
$t\bar{t}$	$16\,490 \pm 240$	$2\,090 \pm 300$	$16\,300 \pm 600$	$2\,320 \pm 350$	$4\,160 \pm 70$
Single top	$1\,470 \pm 100$	480 ± 50	$1\,340 \pm 100$	530 ± 50	297 ± 22
Diboson	176 ± 23	$2\,570 \pm 180$	280 ± 40	$4\,550 \pm 310$	19 ± 5
Z+ HF	$1\,920 \pm 320$	$3\,400 \pm 700$	$13\,300 \pm 1\,900$	$25\,000 \pm 5\,000$	18 ± 9
Z+ LF	$1\,060 \pm 330$	$57\,700 \pm 900$	$6\,300 \pm 2\,000$	$501\,000 \pm 5\,000$	10 ± 9
Total Bkg	$21\,110 \pm 140$	$66\,240 \pm 250$	$37\,530 \pm 200$	$533\,100 \pm 700$	$4\,500 \pm 60$
$bb\Phi$ (UL)	37^{+14}_{-10}	45^{+18}_{-13}			
ggF (UL)	4^{+2}_{-1}	73^{+28}_{-21}			
Data	21 154	66 300	37 527	533 134	4 511

7 Systematic uncertainties

The sources of systematic uncertainty can be divided into three groups: those of experimental origin, those related to the modelling of the simulated backgrounds, and those associated with signal simulation. The finite size of the simulated background samples is also an important source of uncertainty.

7.1 Experimental uncertainties

The dominant experimental uncertainties originate from residual mismodelling of the muon reconstruction and selection after the simulation-to-data efficiency correction factors have been applied. They include the uncertainty obtained from $Z \rightarrow \mu\mu$ data studies and a high- p_T extrapolation uncertainty corresponding to the decrease in the muon reconstruction and selection efficiency with increasing p_T which is predicted by the MC simulation. The degradation of the muon reconstruction efficiency was found to be approximately 3% per TeV as a function of muon p_T . Uncertainties in the isolation and trigger efficiencies of muons [61], along with the uncertainty in their energy scale and resolution, are estimated from $Z \rightarrow \mu\mu$ data taken at $\sqrt{s} = 13$ TeV. These are found to have only a small impact (they account for < 0.4% of the total uncertainty

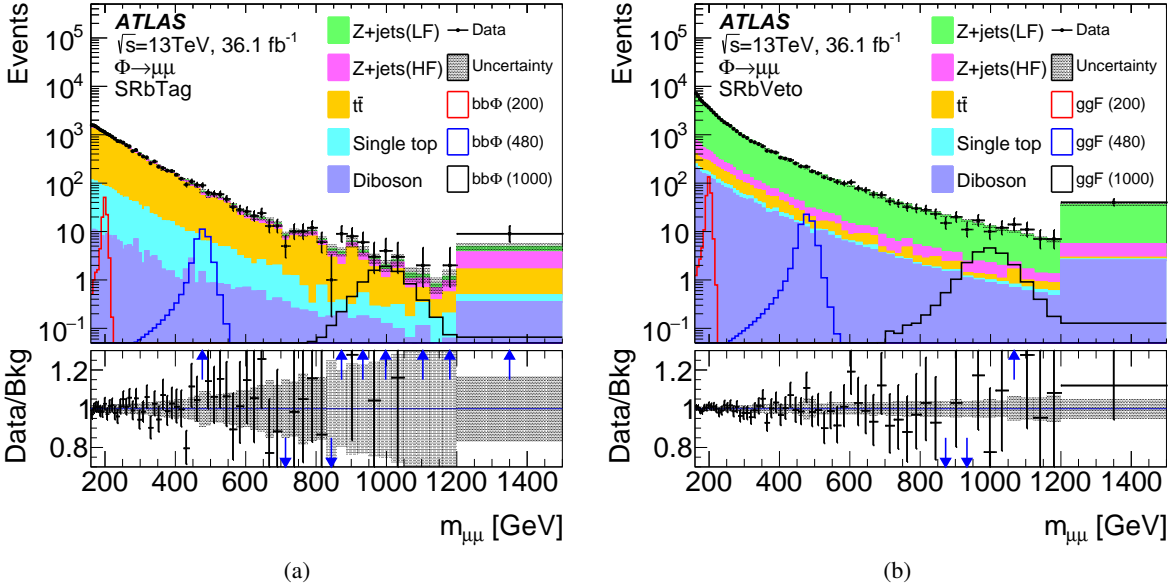


Figure 2: Distributions of the dimuon invariant mass, $m_{\mu\mu}$, after the combined fit to data are shown normalized: (a) in the SRbTag, under the background plus signal hypothesis (480 GeV $bb\Phi$ signal) and (b) in the SRbVeto, under the background plus signal hypothesis (480 GeV ggF signal). The fit for a $m_\Phi = 480$ GeV signal corresponds to the largest excess observed above the background expectation. Each background process is normalized according to its post-fit cross-section. The templates for the $m_\Phi = 200$ GeV, $m_\Phi = 480$ GeV and $m_\Phi = 1$ TeV mass hypotheses are normalized to the expected upper limit. The data are shown by the points, while the size of the statistical uncertainty is shown by the error bars. The last bin includes the overflow. The blue arrows represent the data points outside of the frame. The hatched band shows the total systematic uncertainty of the post-fit yield.

on the fitted value of the signal cross-sections). Other sources of experimental uncertainties are the residual differences in the modelling of the flavour-tagging algorithm, the jet energy scale and the jet energy resolution after the simulation-to-data correction factors are applied. Flavour-tagging simulation-to-data efficiency correction factors are derived [67] separately for b -jets, c -jets, and light-flavour jets. All three correction factors depend on jet p_T (or p_T and $|\eta|$) and are affected by uncertainties from multiple sources. These are decomposed into uncorrelated components which are then treated independently, resulting in three uncertainties for b -jets and for c -jets, and five for light-flavour jets. The approximate size of the uncertainty in the tagging efficiency is 2% for b -jets, 10% for c -jets and 30% for light-flavour jets. Additional uncertainties are considered in the extrapolation of the b -jet efficiency calibration above $p_T = 300$ GeV and in the misidentification of hadronically decaying τ -leptons as b -jets. The uncertainties in the jet energy scale and resolution are based on their respective measurements in data [65]. The many sources of uncertainty in the jet energy scale correction are decomposed into 21 uncorrelated components which are treated as being independent of one another. An additional uncertainty that specifically affects the energy calibration of b - and c -jets is considered.

The uncertainties in the energy scale and resolution of the jets and leptons are propagated to the calculation of E_T^{miss} , which also has additional uncertainties from the scale, resolution, and efficiency of the tracks used to define the soft term, along with the modelling of the underlying event.

The pile-up modelling uncertainty is assessed by varying the number of pile-up interactions in simulated events. The variations are designed to cover the uncertainty in the ratio of the predicted and measured

cross-section of non-diffractive inelastic events producing a hadronic system of mass $m_X > 13$ GeV [75].

The uncertainty in the combined 2015+2016 integrated luminosity is 2.1%. It is derived, following a methodology similar to that detailed in Ref. [76], and using the LUCID-2 detector for the baseline luminosity measurements [77], from calibration of the luminosity scale using x - y beam-separation scans.

7.2 Theoretical uncertainties

Background processes

As discussed earlier, the rates of major backgrounds are measured using data control regions, thus theoretical uncertainties in the predicted cross-section for $Z/\gamma^* + \text{jets}$ and $t\bar{t}$ processes are not considered. Instead, the effects of theoretical uncertainties in the modelling of the $m_{\mu\mu}$ distribution and in the ratio of the event yields in signal regions to those in the control regions are evaluated. The dominant theoretical uncertainties are the shape uncertainty in the dimuon mass spectra of the $t\bar{t}$ and $Z + \text{HF}$ contributions.

For both the $Z + \text{LF}$ and $Z + \text{HF}$ processes, the following sources of theoretical and modelling uncertainties are considered: PDF uncertainties (estimated via eigenvector variations and by comparing different PDF sets), limited accuracy of the fixed-order calculation (estimated by QCD scale variations), variations in the choice of strong coupling constant value ($\alpha_S(M_Z)$), EW corrections, and photon-induced corrections. These variations are treated as fully correlated between $Z + \text{LF}$ and $Z + \text{HF}$ processes.

The PDF variation uncertainty is obtained using the 90% confidence level (CL) CT14NNLO PDF error set and by following the procedure described in Refs. [78, 79]. Rather than a single nuisance parameter to describe the 28 eigenvectors of this PDF error set, which could lead to an underestimation of its effect, a re-diagonalized set of 7 PDF eigenvectors was used [33]. This represents the minimal set of PDF eigenvectors that maintains the necessary correlations, and the sum in quadrature of these eigenvectors matches the original CT14NNLO error envelope well. They are treated as separate nuisance parameters. The uncertainties due to the variation of PDF scales and α_S are derived using VRAP. The former is obtained by varying the renormalization and factorization scales of the nominal CT14NNLO PDF up and down simultaneously by a factor of two. The value of α_S used (0.118) is varied by ± 0.002 . The EW correction uncertainty was assessed by comparing the nominal additive ($1 + \delta_{\text{EW}} + \delta_{\text{QCD}}$) treatment with the multiplicative approximation ($(1 + \delta_{\text{EW}})(1 + \delta_{\text{QCD}})$) treatment of the EW correction in the combination of the higher-order EW and QCD effects. The uncertainty in the photon-induced correction is calculated from the uncertainties in the quark masses and the photon PDF. Following the recommendations of the PDF4LHC forum [79], an additional uncertainty due to the choice of nominal PDF set is derived by comparing the central values of CT14NNLO with those from other PDF sets, namely MMHT14 [80] and NNPDF3.0 [81]. The maximum width of the envelope of these comparisons is used as the PDF choice uncertainty, but only if it is larger than the width of the CT14NNLO PDF eigenvector variation envelope.

An additional modelling uncertainty is considered for the $Z + \text{HF}$ process. The $m_{\mu\mu}$ spectrum simulated by POWHEG was compared with those simulated with SHERPA 2.2.1 [45] and with MADGRAPH5_AMC@NLO interfaced with PYTHIA 8.186. A functional form was chosen to describe the envelope of the differences in the $m_{\mu\mu}$ distribution shape between events with at least one b -quark simulated by SHERPA 2.2.1 and MADGRAPH5_AMC@NLO v2.

These systematic uncertainties not only imply uncertainties in the shape of the $m_{\mu\mu}$ distribution in the signal region, but they also affect the ratio of the expected number of events in the signal region to the

expected number in the control region. The effect on the $Z + \text{LF}$ normalization in the bVeto signal region is 2%, while the size of the uncertainty for $Z + \text{HF}$ in the bTag signal region is 7%.

Moreover, the ratio of the expected number of $Z + \text{LF}$ events in the bVeto control region to the events in bTag control and signal regions was estimated with the nominal PowHEG+PYTHIA $Z + \text{jet}$ sample, and with the alternative MADGRAPH5_AMC@NLO v2 sample. To cover the observed difference between the two, an additional uncertainty of 27% in the normalization of the $Z + \text{LF}$ process in the bTag signal and control region was applied.

For the $t\bar{t}$ process, theoretical uncertainties in the modelling of the $m_{\mu\mu}$ spectrum and in the extrapolation from control region to signal region are also considered. These are estimated by comparing the nominal prediction with alternative ones. To estimate the impact of initial and final state radiation modelling, two alternative PowHEG+PYTHIA samples were generated with the following parameters. In the first one, the renormalization (μ_R) and factorization (μ_F) scale were varied by a factor of 0.5, the value of h_{damp} was doubled ($2m_t$) and the corresponding Perugia 2012 radiation tune variation was used. In the second sample, the renormalization and factorization scales were varied by a factor of 2, while the h_{damp} parameter was not changed. The associated variation from the Perugia 2012 tune was used. These choices of parameters have been shown to encompass the cases where μ_R and μ_F are varied independently, and covered the measured uncertainties of the data for unfolded $t\bar{t}$ distributions [82, 83]. Differences in parton shower and hadronization models were investigated using a sample where PowHEG-Box was interfaced with HERWIG++ 2.7.1 [84] with the UE-EE-5 tune [37] and the corresponding CTEQ6L1 PDFs. The nominal sample was also compared with a sample generated with MADGRAPH5_AMC@NLO 2.2.1 [30] interfaced with HERWIG++. A NLO matrix element and CT10 PDF were used for the $t\bar{t}$ hard-scattering process. The parton shower, hadronization and the underlying events were modelled using the HERWIG++ 2.7.1 generator. The UE-EE-5 tune and the corresponding CTEQ6L1 PDF were used. A functional form was chosen to encompass the differences in the $m_{\mu\mu}$ distribution shape between the nominal sample and all these alternative samples. These samples were also used to estimate the 3.5% extrapolation uncertainty from CRttbar to the SRbTag.

Theoretical uncertainties that arise from higher-order contributions to the cross-sections and PDFs and affect the values of the predicted cross-sections for the diboson and single-top backgrounds are considered.

Signal processes

Uncertainties related to signal modelling include the uncertainties associated with the initial- and final-state radiation, the modelling of underlying events, the choice of the renormalization and factorization scales, and the parton distribution functions. None of them has a sizeable effect on the shape of the $m_{\mu\mu}$ spectra, but some of them do affect the acceptance in the signal regions. Uncertainties for the different mass hypotheses were evaluated, but for simplicity, only the largest of the values is used. In the calculation of the uncertainties, appropriate requirements on the muon and jets kinematics are applied at hadron level for the SRbTag and SRbVeto regions.

The factorization and renormalization scales were varied by a factor of two up and down, including correlated and anti-correlated variations, both in PowHEG-Box and in MG5_AMC@NLO. For the $\text{bb}\Phi$ process, the largest deviation from the value of the nominal acceptance is considered as the final scale uncertainty (2% in SRbTag, and 1% in SRbVeto). A 25% uncertainty for the acceptance of ggF events in the SRbTag is considered, as well as its anti-correlated effect in the SRbVeto region, following the procedure adopted in Ref. [85].

The PDF uncertainties are estimated by taking the envelope of the changes in the acceptance associated with the PDF4LHC15_nlo_100 (PDF4LC15_nlo_nf4_30) [79] error set for the ggF ($bb\Phi$) signal process. They correspond to changes in acceptances not larger than 1%.

Systematic variations of the parameters of the A14 (for $bb\Phi$) and AZNLO (for ggF) tunes are used to account for the uncertainties associated with the initial and final state radiation and the modelling of underlying events. For $bb\Phi$, these uncertainties correspond to changes of 3.8% and 3.2% of the acceptance in the SRbTag and SRbVeto regions. They are associated with a migration of events from one signal region to the other, hence they are treated as anti-correlated between the two signal regions. For ggF, the uncertainty in the SRbVeto is negligible (< 0.5%), while it is 3.8% in the SRbTag.

As discussed in Section 3, the signal samples were simulated with the fast simulation framework of ATLAS, which replaces the full simulation of the electromagnetic and hadronic calorimeters by a parameterized model. No significant differences in acceptance and dimuon invariant mass were observed between a limited number of fast simulation signal samples and samples generated with full Geant4-based simulation, hence no systematic uncertainty is considered for the use of fast simulation.

The current result is dominated by the statistical uncertainty of the data (which accounts for 66% of the total uncertainty on the fitted value of the signal cross-section), and the systematic uncertainty due to the finite size of the simulated background samples (which accounts for 25% of the total uncertainty). Amongst the remaining systematic uncertainties, the modelling of the shape of the $m_{\mu\mu}$ distribution for the Z+jets and top–antitop backgrounds dominates (3% of the total uncertainty) followed by the muon identification efficiency (1.5%). All other considered sources of experimental and theoretical uncertainties (which individually have an impact < 0.4%) have a combined contribution of less than 5% to the total uncertainty on the upper limit.

8 Results

The observed p -values as a function of m_Φ , obtained applying the statistical analysis described in Section 6, are shown in Figure 3(a) for the $bb\Phi$ -only fit and in Figure 3(b) for the ggF-only fit. The lines in each figure correspond to separate fits. The dotted line represents the p -value for a fit including only SRbTag and all control regions (CRs), the dashed line represents the p -value for a fit including only SRbVeto+CRs, while the solid line corresponds to the combined SRbTag+SRbVeto+CRs fit. The dotted lines in the two figures show similar behaviour and so do the dashed lines, while the combined p -values are calculated for separate signal production modes implying very different contributions from the SRbVeto and SRbTag regions, which lead to substantially different limits. The largest excess of events above the expected background is observed for the b -quark associated production at about $m_\Phi = 480$ GeV and amounts to a local significance of 2.3σ , which becomes 0.6σ after considering the look-elsewhere effect over the mass range 0.2–1.0 TeV. The look-elsewhere effect is estimated using the method described in Ref. [86].

Since the data are in agreement with the predicted backgrounds the results are given in terms of exclusion limits. These are set using the modified frequentist CL_s method [87]. Upper limits on the cross section times branching ratio for a massive scalar particle are set at the 95% confidence level (CL) as a function of the particle mass. The upper limits at 95% CL on $\sigma_\Phi \times \mathcal{B}(\Phi \rightarrow \mu\mu)$ (where σ_Φ is the cross section and \mathcal{B} is the branching ratio) assume the natural width of the resonance to be negligible compared to the experimental resolution, and they cover the mass range 0.2–1.0 TeV. In Figure 4(a) and 4(b) the 95% CL upper limits are shown for b -quark associated production and gluon–gluon fusion, respectively. The

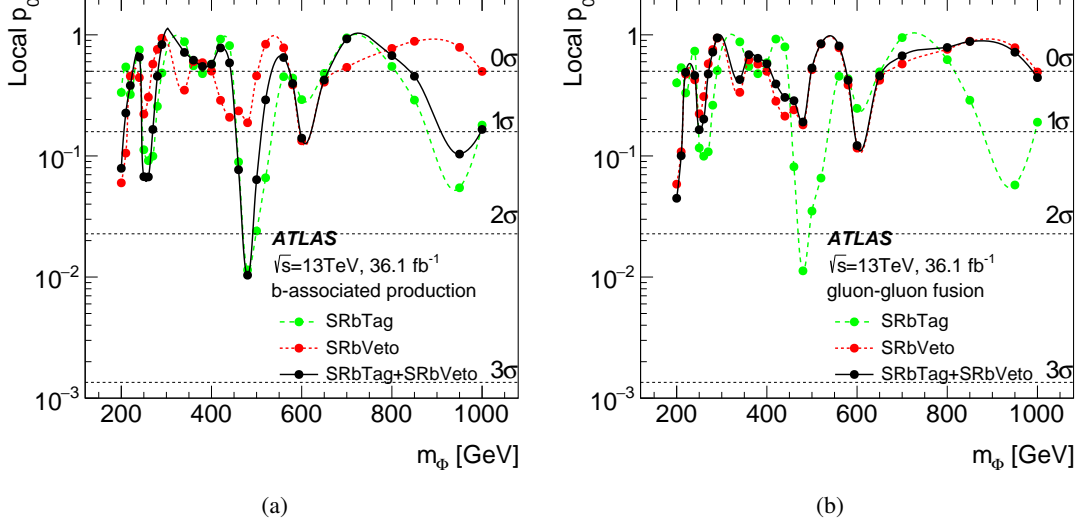


Figure 3: Observed p -values as a function of m_Φ for (a) a $bb\Phi$ -only fit and (b) a ggF -only fit. The dotted line corresponds to the data in the SRbTag only, the dashed line to the data in SRbVeto only, and the solid curve to the combination of the two data categories. All three fits include data from all control regions.

expected limits are in the ranges 1.3–25 fb and 1.8–25 fb, respectively. The observed limits are in the ranges 1.9–41 fb and 1.6–44 fb, respectively. Both the expected and observed limits are calculated in the asymptotic approximation [74], which was verified with MC pseudo-experiments for the $m_\Phi = 1000$ GeV hypothesis. The upper limit on the ggF production mode is dominated by the SRbVeto, while for the $bb\Phi$ production mode both the SRbTag and SRbVeto regions contribute to the result because of the relative acceptance of the $bb\Phi$ production mode in the two regions. Limits shown in Figure 4 are obtained in simultaneous fits of the SRbVeto and SRbTag data regions and correspond to the different signal production modes. Usage of the same data events in both the $bb\Phi$ -only and the ggF -only fits explains correlations in the behaviour of the observed limits.

Figures 5(a) and 5(b) show the observed and expected 95% CL upper limits on the production cross section times branching ratio for $\Phi \rightarrow \mu\mu$ as a function of the fractional contribution from b -quark associated production ($\sigma_{bb\Phi}/[\sigma_{bb\Phi} + \sigma_{ggF}]$) and the scalar resonance mass. These fractions are derived assuming that other production mechanisms do not affect the result.

A complete set of tables and figures are available at the Durham HepData repository [88].

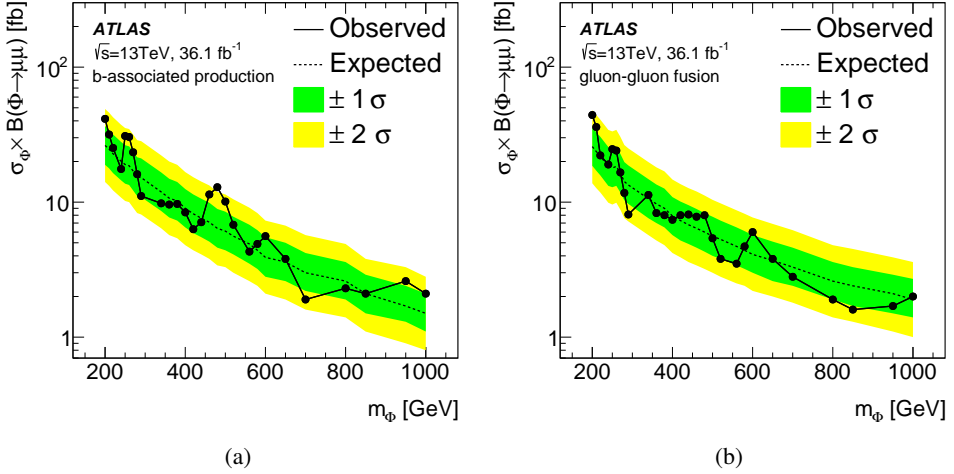


Figure 4: The observed and expected 95% CL upper limits on the production cross section times branching ratio for a massive scalar resonance produced via (a) b -quark associated production and (b) gluon—gluon fusion.

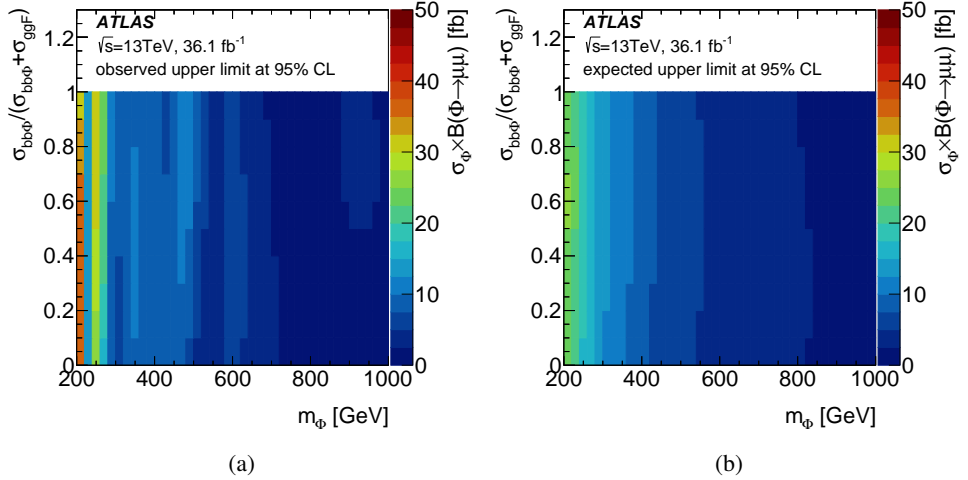


Figure 5: The (a) observed and (b) expected 95% CL upper limit on the production cross section times branching ratio for $\Phi \rightarrow \mu\mu$ as a function of the fractional contribution from b -quark associated production and the scalar boson mass.

9 Conclusion

The ATLAS detector at the LHC has been used to search for a massive scalar resonance decaying into two opposite-sign muons, produced via b -quark associated production or via gluon–gluon fusion, assuming that the natural width of the resonance is negligible compared to the experimental resolution. The search is conducted with 36.1 fb^{-1} of pp collision data at $\sqrt{s} = 13 \text{ TeV}$, recorded during 2015 and 2016. The observed dimuon invariant mass spectrum is consistent with the Standard Model prediction within uncertainties for events both with and without a b -tagged jet over the 0.2 – 1.0 TeV range. The observed

upper limits at 95% confidence level on the cross-section times branching ratio for b -quark associated production and gluon–gluon fusion are between 1.9 and 41 fb and 1.6 and 44 fb respectively, which is consistent with expectations.

Acknowledgements

We thank CERN for the very successful operation of the LHC, as well as the support staff from our institutions without whom ATLAS could not be operated efficiently.

We acknowledge the support of ANPCyT, Argentina; YerPhI, Armenia; ARC, Australia; BMWFW and FWF, Austria; ANAS, Azerbaijan; SSTC, Belarus; CNPq and FAPESP, Brazil; NSERC, NRC and CFI, Canada; CERN; CONICYT, Chile; CAS, MOST and NSFC, China; COLCIENCIAS, Colombia; MSMT CR, MPO CR and VSC CR, Czech Republic; DNRF and DNSRC, Denmark; IN2P3-CNRS, CEA-DRF/IRFU, France; SRNSFG, Georgia; BMBF, HGF, and MPG, Germany; GSRT, Greece; RGC, Hong Kong SAR, China; ISF and Benoziyo Center, Israel; INFN, Italy; MEXT and JSPS, Japan; CNRST, Morocco; NWO, Netherlands; RCN, Norway; MNiSW and NCN, Poland; FCT, Portugal; MNE/IFA, Romania; MES of Russia and NRC KI, Russian Federation; JINR; MESTD, Serbia; MSSR, Slovakia; ARRS and MIZŠ, Slovenia; DST/NRF, South Africa; MINECO, Spain; SRC and Wallenberg Foundation, Sweden; SERI, SNSF and Cantons of Bern and Geneva, Switzerland; MOST, Taiwan; TAEK, Turkey; STFC, United Kingdom; DOE and NSF, United States of America. In addition, individual groups and members have received support from BCKDF, CANARIE, CRC and Compute Canada, Canada; COST, ERC, ERDF, Horizon 2020, and Marie Skłodowska-Curie Actions, European Union; Investissements d’Avenir Labex and Idex, ANR, France; DFG and AvH Foundation, Germany; Herakleitos, Thales and Aristeia programmes co-financed by EU-ESF and the Greek NSRF, Greece; BSF-NSF and GIF, Israel; CERCA Programme Generalitat de Catalunya, Spain; The Royal Society and Leverhulme Trust, United Kingdom.

The crucial computing support from all WLCG partners is acknowledged gratefully, in particular from CERN, the ATLAS Tier-1 facilities at TRIUMF (Canada), NDGF (Denmark, Norway, Sweden), CC-IN2P3 (France), KIT/GridKA (Germany), INFN-CNAF (Italy), NL-T1 (Netherlands), PIC (Spain), ASGC (Taiwan), RAL (UK) and BNL (USA), the Tier-2 facilities worldwide and large non-WLCG resource providers. Major contributors of computing resources are listed in Ref. [89].

References

- [1] ATLAS Collaboration, *Observation of a new particle in the search for the Standard Model Higgs boson with the ATLAS detector at the LHC*, *Phys. Lett. B* **716** (2012) 1, arXiv: [1207.7214 \[hep-ex\]](#).
- [2] CMS Collaboration, *Observation of a new boson at a mass of 125 GeV with the CMS experiment at the LHC*, *Phys. Lett. B* **716** (2012) 30, arXiv: [1207.7235 \[hep-ex\]](#).
- [3] ATLAS Collaboration, *Measurements of the Higgs boson production and decay rates and coupling strengths using pp collision data at $\sqrt{s} = 7$ and 8 TeV in the ATLAS experiment*, *Eur. Phys. J. C* **76** (2016) 6, arXiv: [1507.04548 \[hep-ex\]](#).
- [4] ATLAS Collaboration, *Evidence for the spin-0 nature of the Higgs boson using ATLAS data*, *Phys. Lett. B* **726** (2013) 120, arXiv: [1307.1432 \[hep-ex\]](#).

- [5] CMS Collaboration, *Precise determination of the mass of the Higgs boson and tests of compatibility of its couplings with the standard model predictions using proton collisions at 7 and 8 TeV*, *Eur. Phys. J. C* **75** (2015) 212, arXiv: [1412.8662 \[hep-ex\]](#).
- [6] CMS Collaboration, *Constraints on the spin-parity and anomalous HVV couplings of the Higgs boson in proton collisions at 7 and 8 TeV*, *Phys. Rev. D* **92** (2015) 012004, arXiv: [1411.3441 \[hep-ex\]](#).
- [7] ATLAS and CMS Collaborations, *Measurements of the Higgs boson production and decay rates and constraints on its couplings from a combined ATLAS and CMS analysis of the LHC pp collision data at $\sqrt{s} = 7$ and 8 TeV*, *JHEP* **08** (2016) 045, arXiv: [1606.02266 \[hep-ex\]](#).
- [8] F. Englert and R. Brout, *Broken Symmetry and the Mass of Gauge Vector Mesons*, *Phys. Rev. Lett.* **13** (1964) 321.
- [9] P. W. Higgs, *Broken symmetries, massless particles and gauge fields*, *Phys. Lett.* **12** (1964) 132.
- [10] P. W. Higgs, *Broken Symmetries and the Masses of Gauge Bosons*, *Phys. Rev. Lett.* **13** (1964) 508.
- [11] P. W. Higgs, *Spontaneous Symmetry Breakdown without Massless Bosons*, *Phys. Rev.* **145** (1966) 1156.
- [12] G. Guralnik, C. Hagen and T. Kibble, *Global Conservation Laws and Massless Particles*, *Phys. Rev. Lett.* **13** (1964) 585.
- [13] T. Kibble, *Symmetry Breaking in Non-Abelian Gauge Theories*, *Phys. Rev.* **155** (1967) 1554.
- [14] A. Djouadi, *The anatomy of electro-weak symmetry breaking. Tome II: The Higgs bosons in the Minimal Supersymmetric Model*, *Phys. Rept.* **459** (2008) 1, arXiv: [hep-ph/0503173](#).
- [15] G. Branco et al., *Theory and phenomenology of two-Higgs-doublet models*, *Phys. Rept.* **516** (2012) 1, arXiv: [1106.0034 \[hep-ph\]](#).
- [16] W. Altmannshofer et al., *Collider signatures of flavorful Higgs bosons*, *Phys. Rev. D* **94** (2016) 115032, arXiv: [1610.02398 \[hep-ph\]](#).
- [17] ATLAS Collaboration, *Search for additional heavy neutral Higgs and gauge bosons in the ditau final state produced in 36fb^{-1} of pp collisions at $\sqrt{s} = 13\text{ TeV}$ with the ATLAS detector*, *JHEP* **01** (2018) 055, arXiv: [1709.07242 \[hep-ex\]](#).
- [18] CMS Collaboration, *Search for beyond the standard model Higgs bosons decaying into a $b\bar{b}$ pair in pp collisions at $\sqrt{s} = 13\text{ TeV}$* , *JHEP* **08** (2018) 113, arXiv: [1805.12191 \[hep-ex\]](#).
- [19] J. E. Camargo-Molina, A. Celis and D. A. Faroughy, *Anomalies in bottom from new physics in top*, *Phys. Lett. B* **784** (2018) 284, arXiv: [1805.04917 \[hep-ph\]](#).
- [20] ATLAS Collaboration, *Search for new high-mass phenomena in the dilepton final state using 36fb^{-1} of proton–proton collision data at $\sqrt{s} = 13\text{ TeV}$ with the ATLAS detector*, *JHEP* **10** (2017) 182, arXiv: [1707.02424 \[hep-ex\]](#).
- [21] ATLAS Collaboration, *Search for the neutral Higgs bosons of the Minimal Supersymmetric Standard Model in pp collisions at $\sqrt{s} = 7\text{ TeV}$ with the ATLAS detector*, *JHEP* **02** (2013) 095, arXiv: [1211.6956 \[hep-ex\]](#).
- [22] CMS Collaboration, *Search for neutral MSSM Higgs bosons decaying to $\mu^+\mu^-$ in pp collisions at $\sqrt{s} = 7$ and 8 TeV*, *Phys. Lett. B* **752** (2016) 221, arXiv: [1508.01437 \[hep-ex\]](#).
- [23] ATLAS Collaboration, *The ATLAS Experiment at the CERN Large Hadron Collider*, *JINST* **3** (2008) S08003.

- [24] ATLAS Collaboration, *ATLAS Insertable B-Layer Technical Design Report*, ATLAS-TDR-19, 2010, URL: <https://cds.cern.ch/record/1291633>, *ATLAS Insertable B-Layer Technical Design Report Addendum*, ATLAS-TDR-19-ADD-1, 2012, URL: <https://cds.cern.ch/record/1451888>.
- [25] ATLAS Collaboration, *Performance of the ATLAS trigger system in 2015*, *Eur. Phys. J. C* **77** (2017) 317, arXiv: [1611.09661 \[hep-ex\]](1611.09661).
- [26] P. Nason, *A New method for combining NLO QCD with shower Monte Carlo algorithms*, *JHEP* **11** (2004) 040, arXiv: <hep-ph/0409146>.
- [27] S. Frixione, P. Nason and C. Oleari, *Matching NLO QCD computations with parton shower simulations: the POWHEG method*, *JHEP* **11** (2007) 070, arXiv: [0709.2092 \[hep-ph\]](0709.2092).
- [28] S. Alioli, P. Nason, C. Oleari and E. Re, *A general framework for implementing NLO calculations in shower Monte Carlo programs: the POWHEG BOX*, *JHEP* **06** (2010) 043, arXiv: [1002.2581 \[hep-ph\]](1002.2581).
- [29] E. Bagnaschi, G. Degrassi, P. Slavich and A. Vicini, *Higgs production via gluon fusion in the POWHEG approach in the SM and in the MSSM*, *JHEP* **02** (2012) 88, arXiv: [1111.2854 \[hep-ph\]](1111.2854).
- [30] J. Alwall et al., *The automated computation of tree-level and next-to-leading order differential cross sections, and their matching to parton shower simulations*, *JHEP* **07** (2014) 079, arXiv: [1405.0301 \[hep-ph\]](1405.0301).
- [31] M. Wiesemann et al., *Higgs production in association with bottom quarks*, *JHEP* **02** (2015) 132, arXiv: [1409.5301 \[hep-ph\]](1409.5301).
- [32] H.-L. Lai et al., *New parton distributions for collider physics*, *Phys. Rev. D* **82** (2010) 074024, arXiv: [1007.2241 \[hep-ph\]](1007.2241).
- [33] S. Dulat et al., *New parton distribution functions from a global analysis of quantum chromodynamics*, *Phys. Rev. D* **93** (2016) 033006, arXiv: [1506.07443 \[hep-ph\]](1506.07443).
- [34] T. Sjöstrand et al., *An introduction to PYTHIA 8.2*, *Comput. Phys. Commun.* **191** (2015) 159, arXiv: [1410.3012 \[hep-ph\]](1410.3012).
- [35] ATLAS Collaboration, *Measurement of the Z/γ^* boson transverse momentum distribution in pp collisions at $\sqrt{s} = 7$ TeV with the ATLAS detector*, *JHEP* **09** (2014) 145, arXiv: [1406.3660 \[hep-ex\]](1406.3660).
- [36] J. Pumplin et al., *New Generation of Parton Distributions with Uncertainties from Global QCD Analysis*, *JHEP* **07** (2002) 012, arXiv: <hep-ph/0201195>.
- [37] ATLAS Collaboration, *ATLAS Pythia 8 tunes to 7 TeV data*, ATL-PHYS-PUB-2014-021, 2014, URL: <https://cds.cern.ch/record/1966419>.
- [38] R. D. Ball et al., *Parton distributions with LHC data*, *Nucl. Phys. B* **867** (2013) 244, arXiv: [1207.1303 \[hep-ph\]](1207.1303).
- [39] D. J. Lange, *The EvtGen particle decay simulation package*, *Nucl. Instrum. Meth. A* **462** (2001) 152.
- [40] S. Alioli, P. Nason, C. Oleari and E. Re, *Vector boson plus one jet production in POWHEG*, *JHEP* **01** (2011) 095, arXiv: [1009.5594 \[hep-ph\]](1009.5594).
- [41] N. Davidson, T. Przedzinski and Z. Was, *PHOTOS interface in C++: Technical and physics documentation*, *Comput. Phys. Commun.* **199** (2016) 86, arXiv: [1011.0937 \[hep-ph\]](1011.0937).

- [42] C. Anastasiou, L. J. Dixon, K. Melnikov and F. Petriello, *High precision QCD at hadron colliders: Electroweak gauge boson rapidity distributions at next-to-leading order*, Phys. Rev. D **69** (2004) 094008, arXiv: [hep-ph/0312266](#).
- [43] S. G. Bondarenko and A. A. Sapronov, *NLO EW and QCD proton-proton cross section calculations with mcsanc-v1.01*, Comput. Phys. Commun. **184** (2013) 2343, arXiv: [1301.3687 \[hep-ph\]](#).
- [44] A. D. Martin, R. G. Roberts, W. J. Stirling and R. S. Thorne, *Parton distributions incorporating QED contributions*, Eur. Phys. J. C **39** (2005) 155, arXiv: [hep-ph/0411040](#).
- [45] T. Gleisberg et al., *Event generation with SHERPA 1.1*, JHEP **02** (2009) 007, arXiv: [0811.4622 \[hep-ph\]](#).
- [46] L. Lönnblad, *Correcting the Color-Dipole Cascade Model with Fixed Order Matrix Elements*, JHEP **05** (2002) 046, arXiv: [hep-ph/0112284](#).
- [47] N. Lavesson and L. Lönnblad, *W+jets matrix elements and the dipole cascade*, JHEP **07** (2005) 054, arXiv: [hep-ph/0503293](#).
- [48] P. Z. Skands, *Tuning Monte Carlo generators: The Perugia tunes*, Phys. Rev. D **82** (2010) 074018, arXiv: [1005.3457 \[hep-ph\]](#).
- [49] M. Czakon and A. Mitov, *Top++: A program for the calculation of the top-pair cross-section at hadron colliders*, Comput. Phys. Commun. **185** (2014) 2930, arXiv: [1112.5675 \[hep-ph\]](#).
- [50] M. Aliev et al., *HATHOR: HAdronic Top and Heavy quarks cross section calculatoR*, Comput. Phys. Commun. **182** (2011) 1034, arXiv: [1007.1327 \[hep-ph\]](#).
- [51] P. Kant et al., *HATHOR for single top-quark production: Updated predictions and uncertainty estimates for single top-quark production in hadronic collisions*, Comput. Phys. Commun. **191** (2015) 74, arXiv: [1406.4403 \[hep-ph\]](#).
- [52] T. Gleisberg and S. Höche, *Comix, a new matrix element generator*, JHEP **12** (2008) 039, arXiv: [0808.3674 \[hep-ph\]](#).
- [53] F. Cascioli, P. Maierhofer and S. Pozzorini, *Scattering Amplitudes with Open Loops*, Phys. Rev. Lett. **108** (2012) 111601, arXiv: [1111.5206 \[hep-ph\]](#).
- [54] S. Schumann and F. Krauss, *A parton shower algorithm based on Catani-Seymour dipole factorisation*, JHEP **03** (2008) 038, arXiv: [0709.1027 \[hep-ph\]](#).
- [55] S. Höche, F. Krauss, M. Schönherr and F. Siegert, *QCD matrix elements + parton showers: The NLO case*, JHEP **04** (2013) 027, arXiv: [1207.5030 \[hep-ph\]](#).
- [56] ATLAS Collaboration, *The ATLAS Simulation Infrastructure*, Eur. Phys. J. C **70** (2010) 823, arXiv: [1005.4568 \[physics.ins-det\]](#).
- [57] ATLAS Collaboration, *The simulation principle and performance of the ATLAS fast calorimeter simulation FastCaloSim*, ATL-PHYS-PUB-2010-013, 2010, URL: <https://cds.cern.ch/record/1300517>.
- [58] S. Agostinelli et al., *GEANT4: A simulation toolkit*, Nucl. Instrum. Meth. A **506** (2003) 250.
- [59] ATLAS Collaboration, *Summary of ATLAS Pythia 8 tunes*, ATL-PHYS-PUB-2012-003, 2012, URL: <https://cds.cern.ch/record/1474107>.
- [60] ATLAS Collaboration, *Reconstruction of primary vertices at the ATLAS experiment in Run 1 proton–proton collisions at the LHC*, Eur. Phys. J. C **77** (2017) 332, arXiv: [1611.10235 \[physics.ins-det\]](#).

- [61] ATLAS Collaboration, *Muon reconstruction performance of the ATLAS detector in proton–proton collision data at $\sqrt{s} = 13\text{ TeV}$* , *Eur. Phys. J. C* **76** (2016) 292, arXiv: [1603.05598 \[hep-ex\]](#).
- [62] ATLAS Collaboration, *Topological cell clustering in the ATLAS calorimeters and its performance in LHC Run 1*, *Eur. Phys. J. C* **77** (2017) 490, arXiv: [1603.02934 \[hep-ex\]](#).
- [63] M. Cacciari, G. P. Salam and G. Soyez, *The anti- k_t jet clustering algorithm*, *JHEP* **04** (2008) 063, arXiv: [0802.1189 \[hep-ph\]](#).
- [64] M. Cacciari, G. P. Salam and G. Soyez, *FastJet user manual*, *Eur. Phys. J. C* **72** (2012) 1896, arXiv: [1111.6097 \[hep-ph\]](#).
- [65] ATLAS Collaboration, *Jet energy scale measurements and their systematic uncertainties in proton–proton collisions at $\sqrt{s} = 13\text{ TeV}$ with the ATLAS detector*, *Phys. Rev. D* **96** (2017) 072002, arXiv: [1703.09665 \[hep-ex\]](#).
- [66] ATLAS Collaboration, *Performance of pile-up mitigation techniques for jets in pp collisions at $\sqrt{s} = 8\text{ TeV}$ using the ATLAS detector*, *Eur. Phys. J. C* **76** (2016) 581, arXiv: [1510.03823 \[hep-ex\]](#).
- [67] ATLAS Collaboration, *Performance of b-jet identification in the ATLAS experiment*, *JINST* **11** (2016) P04008, arXiv: [1512.01094 \[hep-ex\]](#).
- [68] ATLAS Collaboration, *Optimisation of the ATLAS b-tagging performance for the 2016 LHC Run*, ATL-PHYS-PUB-2016-012, 2016, URL: <https://cds.cern.ch/record/2160731>.
- [69] ATLAS Collaboration, *Measurements of b-jet tagging efficiency with the ATLAS detector using $t\bar{t}$ events at $\sqrt{s} = 13\text{ TeV}$* , *JHEP* **08** (2018) 089, arXiv: [1805.01845 \[hep-ex\]](#).
- [70] ATLAS Collaboration, *Electron efficiency measurements with the ATLAS detector using the 2015 LHC proton–proton collision data*, ATLAS-CONF-2016-024, 2016, URL: <https://cds.cern.ch/record/2157687>.
- [71] ATLAS Collaboration, *Selection of jets produced in 13 TeV proton–proton collisions with the ATLAS detector*, ATLAS-CONF-2015-029, 2015, URL: <https://cds.cern.ch/record/2037702>.
- [72] ATLAS Collaboration, *Performance of missing transverse momentum reconstruction with the ATLAS detector using proton–proton collisions at $\sqrt{s} = 13\text{ TeV}$* , *Eur. Phys. J. C* **78** (2018) 903, arXiv: [1802.08168 \[hep-ex\]](#).
- [73] ATLAS Collaboration, *Search for resonances in diphoton events at $\sqrt{s} = 13\text{ TeV}$ with the ATLAS detector*, *JHEP* **09** (2016) 001, arXiv: [1606.03833 \[hep-ex\]](#).
- [74] G. Cowan, K. Cranmer, E. Gross and O. Vitells, *Asymptotic formulae for likelihood-based tests of new physics*, *Eur. Phys. J. C* **71** (2011) 1554, arXiv: [1007.1727 \[physics.data-an\]](#).
- [75] ATLAS Collaboration, *Measurement of the Inelastic Proton–Proton Cross Section at $\sqrt{s} = 13\text{ TeV}$ with the ATLAS Detector at the LHC*, *Phys. Rev. Lett.* **117** (2016) 182002, arXiv: [1606.02625 \[hep-ex\]](#).
- [76] ATLAS Collaboration, *Luminosity determination in pp collisions at $\sqrt{s} = 8\text{ TeV}$ using the ATLAS detector at the LHC*, *Eur. Phys. J. C* **76** (2016) 653, arXiv: [1608.03953 \[hep-ex\]](#).
- [77] G. Avoni et al., *The new LUCID-2 detector for luminosity measurement and monitoring in ATLAS*, *JINST* **13** (2018) P07017.
- [78] J. Gao and P. Nadolsky, *A meta-analysis of parton distribution functions*, *JHEP* **07** (2014) 035, arXiv: [1401.0013 \[hep-ph\]](#).

- [79] J. Butterworth et al., *PDF4LHC recommendations for LHC Run II*, *J. Phys. G* **43** (2016) 023001, arXiv: [1510.03865 \[hep-ph\]](#).
- [80] P. Motylinski, L. Harland-Lang, A. D. Martin and R. S. Thorne, *Updates of PDFs for the 2nd LHC run*, *Nucl. Part. Phys. Proc.* **273-275** (2016) 2136, arXiv: [1411.2560 \[hep-ph\]](#).
- [81] R. D. Ball et al., *Parton distributions for the LHC Run II*, *JHEP* **04** (2015) 040, arXiv: [1410.8849 \[hep-ph\]](#).
- [82] ATLAS Collaboration, *Simulation of top-quark production for the ATLAS experiment at $\sqrt{s} = 13 \text{ TeV}$* , ATL-PHYS-PUB-2016-004, 2016, URL: <https://cds.cern.ch/record/2120417>.
- [83] ATLAS Collaboration, *Comparison of Monte Carlo generator predictions to ATLAS measurements of top pair production at 7 TeV*, ATL-PHYS-PUB-2015-002, 2015, URL: <https://cds.cern.ch/record/1981319>.
- [84] M. Bahr et al., *Herwig++ physics and manual*, *Eur. Phys. J. C* **58** (2008) 639, arXiv: [0803.0883 \[hep-ph\]](#).
- [85] I. Stewart and F. Tackmann, *Theory Uncertainties for Higgs mass and other searches using jet bins*, *Phys. Rev. D* **85** (2012) 034011, arXiv: [1107.2117 \[hep-ph\]](#).
- [86] E. Gross and O. Vitells, *Trial factors for the look elsewhere effect in high energy physics*, *Eur. Phys. J. C* **70** (2010) 525, arXiv: [1005.1891 \[physics.data-an\]](#).
- [87] A. L. Read, *Presentation of search results: The CL_s technique*, *J. Phys. G* **28** (2002) 2693.
- [88] HEPdata record, <https://www.hepdata.net/record/84708>.
- [89] ATLAS Collaboration, *ATLAS Computing Acknowledgements*, ATL-GEN-PUB-2016-002, URL: <https://cds.cern.ch/record/2202407>.

The ATLAS Collaboration

M. Aaboud^{34d}, G. Aad⁹⁹, B. Abbott¹²⁵, D.C. Abbott¹⁰⁰, O. Abdinov^{13,*}, B. Abeloos¹²⁹,
D.K. Abhayasinghe⁹¹, S.H. Abidi¹⁶⁴, O.S. AbouZeid³⁹, N.L. Abraham¹⁵³, H. Abramowicz¹⁵⁸,
H. Abreu¹⁵⁷, Y. Abulaiti⁶, B.S. Acharya^{64a,64b,p}, S. Adachi¹⁶⁰, L. Adam⁹⁷, L. Adamczyk^{81a}, L. Adamek¹⁶⁴,
J. Adelman¹¹⁹, M. Adlersberger¹¹², A. Adiguzel^{12c,ai}, T. Adye¹⁴¹, A.A. Affolder¹⁴³, Y. Afik¹⁵⁷,
C. Agheorghiesei^{27c}, J.A. Aguilar-Saavedra^{137f,137a,ah}, F. Ahmadov^{77,af}, G. Aielli^{71a,71b}, S. Akatsuka⁸³,
T.P.A. Åkesson⁹⁴, E. Akilli⁵², A.V. Akimov¹⁰⁸, G.L. Alberghi^{23b,23a}, J. Albert¹⁷³, P. Albicocco⁴⁹,
M.J. Alconada Verzini⁸⁶, S. Alderweireldt¹¹⁷, M. Aleksa³⁵, I.N. Aleksandrov⁷⁷, C. Alexa^{27b},
D. Alexandre¹⁹, T. Alexopoulos¹⁰, M. Alhroob¹²⁵, B. Ali¹³⁹, G. Alimonti^{66a}, J. Alison³⁶, S.P. Alkire¹⁴⁵,
C. Allaire¹²⁹, B.M.M. Allbrooke¹⁵³, B.W. Allen¹²⁸, P.P. Allport²¹, A. Aloisio^{67a,67b}, A. Alonso³⁹,
F. Alonso⁸⁶, C. Alpigiani¹⁴⁵, A.A. Alshehri⁵⁵, M.I. Alstaty⁹⁹, B. Alvarez Gonzalez³⁵,
D. Álvarez Piqueras¹⁷¹, M.G. Alviggi^{67a,67b}, B.T. Amadio¹⁸, Y. Amaral Coutinho^{78b}, A. Ambler¹⁰¹,
L. Ambroz¹³², C. Amelung²⁶, D. Amidei¹⁰³, S.P. Amor Dos Santos^{137a,137c}, S. Amoroso⁴⁴,
C.S. Amrouche⁵², F. An⁷⁶, C. Anastopoulos¹⁴⁶, L.S. Ancu⁵², N. Andari¹⁴², T. Andeen¹¹, C.F. Anders^{59b},
J.K. Anders²⁰, K.J. Anderson³⁶, A. Andreazza^{66a,66b}, V. Andrei^{59a}, C.R. Anelli¹⁷³, S. Angelidakis³⁷,
I. Angelozzi¹¹⁸, A. Angerami³⁸, A.V. Anisenkov^{120b,120a}, A. Annovi^{69a}, C. Antel^{59a}, M.T. Anthony¹⁴⁶,
M. Antonelli⁴⁹, D.J.A. Antrim¹⁶⁸, F. Anulli^{70a}, M. Aoki⁷⁹, J.A. Aparisi Pozo¹⁷¹, L. Aperio Bella³⁵,
G. Arabidze¹⁰⁴, J.P. Araque^{137a}, V. Araujo Ferraz^{78b}, R. Araujo Pereira^{78b}, A.T.H. Arce⁴⁷, R.E. Ardell⁹¹,
F.A. Arduh⁸⁶, J-F. Arguin¹⁰⁷, S. Argyropoulos⁷⁵, J.-H. Arling⁴⁴, A.J. Armbruster³⁵, L.J. Armitage⁹⁰,
A. Armstrong¹⁶⁸, O. Arnaez¹⁶⁴, H. Arnold¹¹⁸, M. Arratia³¹, O. Arslan²⁴, A. Artamonov^{109,*}, G. Artoni¹³²,
S. Artz⁹⁷, S. Asai¹⁶⁰, N. Asbah⁵⁷, E.M. Asimakopoulou¹⁶⁹, L. Asquith¹⁵³, K. Assamagan²⁹, R. Astalos^{28a},
R.J. Atkin^{32a}, M. Atkinson¹⁷⁰, N.B. Atlay¹⁴⁸, K. Augsten¹³⁹, G. Avolio³⁵, R. Avramidou^{58a},
M.K. Ayoub^{15a}, A.M. Azoulay^{165b}, G. Azuelos^{107,av}, A.E. Baas^{59a}, M.J. Baca²¹, H. Bachacou¹⁴²,
K. Bachas^{65a,65b}, M. Backes¹³², P. Bagnaia^{70a,70b}, M. Bahmani⁸², H. Bahrasemani¹⁴⁹, A.J. Bailey¹⁷¹,
V.R. Bailey¹⁷⁰, J.T. Baines¹⁴¹, M. Bajic³⁹, C. Bakalis¹⁰, O.K. Baker¹⁸⁰, P.J. Bakker¹¹⁸, D. Bakshi Gupta⁸,
S. Balaji¹⁵⁴, E.M. Baldin^{120b,120a}, P. Balek¹⁷⁷, F. Balli¹⁴², W.K. Balunas¹³⁴, J. Balz⁹⁷, E. Banas⁸²,
A. Bandyopadhyay²⁴, S. Banerjee^{178,l}, A.A.E. Bannoura¹⁷⁹, L. Barak¹⁵⁸, W.M. Barbe³⁷, E.L. Barberio¹⁰²,
D. Barberis^{53b,53a}, M. Barbero⁹⁹, T. Barillari¹¹³, M-S. Barisits³⁵, J. Barkeloo¹²⁸, T. Barklow¹⁵⁰,
R. Barnea¹⁵⁷, S.L. Barnes^{58c}, B.M. Barnett¹⁴¹, R.M. Barnett¹⁸, Z. Barnovska-Blenessy^{58a},
A. Baroncelli^{72a}, G. Barone²⁹, A.J. Barr¹³², L. Barranco Navarro¹⁷¹, F. Barreiro⁹⁶,
J. Barreiro Guimarães da Costa^{15a}, R. Bartoldus¹⁵⁰, A.E. Barton⁸⁷, P. Bartos^{28a}, A. Basalaev¹³⁵,
A. Bassalat¹²⁹, R.L. Bates⁵⁵, S.J. Batista¹⁶⁴, S. Batlamous^{34e}, J.R. Batley³¹, M. Battaglia¹⁴³,
M. Bauce^{70a,70b}, F. Bauer¹⁴², K.T. Bauer¹⁶⁸, H.S. Bawa¹⁵⁰, J.B. Beacham¹²³, T. Beau¹³³,
P.H. Beauchemin¹⁶⁷, P. Bechtle²⁴, H.C. Beck⁵¹, H.P. Beck^{20,s}, K. Becker⁵⁰, M. Becker⁹⁷, C. Becot⁴⁴,
A. Beddall^{12d}, A.J. Beddall^{12a}, V.A. Bednyakov⁷⁷, M. Bedognetti¹¹⁸, C.P. Bee¹⁵², T.A. Beermann⁷⁴,
M. Begalli^{78b}, M. Begel²⁹, A. Behera¹⁵², J.K. Behr⁴⁴, F. Beisiegel²⁴, A.S. Bell⁹², G. Bella¹⁵⁸,
L. Bellagamba^{23b}, A. Bellerive³³, M. Bellomo¹⁵⁷, P. Bellos⁹, K. Belotskiy¹¹⁰, N.L. Belyaev¹¹⁰,
O. Benary^{158,*}, D. Benchekroun^{34a}, M. Bender¹¹², N. Benekos¹⁰, Y. Benhammou¹⁵⁸,
E. Benhar Noccioli¹⁸⁰, J. Benitez⁷⁵, D.P. Benjamin⁶, M. Benoit⁵², J.R. Bensinger²⁶, S. Bentvelsen¹¹⁸,
L. Beresford¹³², M. Beretta⁴⁹, D. Berge⁴⁴, E. Bergeaas Kuutmann¹⁶⁹, N. Berger⁵, B. Bergmann¹³⁹,
L.J. Bergsten²⁶, J. Beringer¹⁸, S. Berlendis⁷, N.R. Bernard¹⁰⁰, G. Bernardi¹³³, C. Bernius¹⁵⁰,
F.U. Bernlochner²⁴, T. Berry⁹¹, P. Berta⁹⁷, C. Bertella^{15a}, G. Bertoli^{43a,43b}, I.A. Bertram⁸⁷, G.J. Besjes³⁹,
O. Bessidskaia Bylund¹⁷⁹, M. Bessner⁴⁴, N. Besson¹⁴², A. Bethani⁹⁸, S. Bethke¹¹³, A. Betti²⁴,
A.J. Bevan⁹⁰, J. Beyer¹¹³, R. Bi¹³⁶, R.M. Bianchi¹³⁶, O. Biebel¹¹², D. Biedermann¹⁹, R. Bielski³⁵,
K. Bierwagen⁹⁷, N.V. Biesuz^{69a,69b}, M. Biglietti^{72a}, T.R.V. Billoud¹⁰⁷, M. Bindi⁵¹, A. Bingul^{12d},

C. Bini^{70a,70b}, S. Biondi^{23b,23a}, M. Birman¹⁷⁷, T. Bisanz⁵¹, J.P. Biswal¹⁵⁸, C. Bittrich⁴⁶, D.M. Bjergaard⁴⁷, J.E. Black¹⁵⁰, K.M. Black²⁵, T. Blazek^{28a}, I. Bloch⁴⁴, C. Blocker²⁶, A. Blue⁵⁵, U. Blumenschein⁹⁰, Dr. Blunier^{144a}, G.J. Bobbink¹¹⁸, V.S. Bobrovnikov^{120b,120a}, S.S. Bocchetta⁹⁴, A. Bocci⁴⁷, D. Boerner¹⁷⁹, D. Bogavac¹¹², A.G. Bogdanchikov^{120b,120a}, C. Bohm^{43a}, V. Boisvert⁹¹, P. Bokan^{51,169}, T. Bold^{81a}, A.S. Boldyrev¹¹¹, A.E. Bolz^{59b}, M. Bomben¹³³, M. Bona⁹⁰, J.S. Bonilla¹²⁸, M. Boonekamp¹⁴², H.M. Borecka-Bielska⁸⁸, A. Borisov¹²¹, G. Borissov⁸⁷, J. Bortfeldt³⁵, D. Bortoletto¹³², V. Bortolotto^{71a,71b}, D. Boscherini^{23b}, M. Bosman¹⁴, J.D. Bossio Sola³⁰, K. Bouaouda^{34a}, J. Boudreau¹³⁶, E.V. Bouhova-Thacker⁸⁷, D. Boumediene³⁷, C. Bourdarios¹²⁹, S.K. Boutle⁵⁵, A. Boveia¹²³, J. Boyd³⁵, D. Boye^{32b}, I.R. Boyko⁷⁷, A.J. Bozson⁹¹, J. Bracinik²¹, N. Brahimi⁹⁹, A. Brandt⁸, G. Brandt¹⁷⁹, O. Brandt^{59a}, F. Braren⁴⁴, U. Bratzler¹⁶¹, B. Brau¹⁰⁰, J.E. Brau¹²⁸, W.D. Breaden Madden⁵⁵, K. Brendlinger⁴⁴, L. Brenner⁴⁴, R. Brenner¹⁶⁹, S. Bressler¹⁷⁷, B. Brickwedde⁹⁷, D.L. Briglin²¹, D. Britton⁵⁵, D. Britzger¹¹³, I. Brock²⁴, R. Brock¹⁰⁴, G. Brooijmans³⁸, T. Brooks⁹¹, W.K. Brooks^{144b}, E. Brost¹¹⁹, J.H. Broughton²¹, P.A. Bruckman de Renstrom⁸², D. Bruncko^{28b}, A. Bruni^{23b}, G. Bruni^{23b}, L.S. Bruni¹¹⁸, S. Bruno^{71a,71b}, B.H. Brunt³¹, M. Bruschi^{23b}, N. Bruscino¹³⁶, P. Bryant³⁶, L. Bryngemark⁹⁴, T. Buanes¹⁷, Q. Buat³⁵, P. Buchholz¹⁴⁸, A.G. Buckley⁵⁵, I.A. Budagov⁷⁷, M.K. Bugge¹³¹, F. Bührer⁵⁰, O. Bulekov¹¹⁰, D. Bullock⁸, T.J. Burch¹¹⁹, S. Burdin⁸⁸, C.D. Burgard¹¹⁸, A.M. Burger⁵, B. Burghgrave¹¹⁹, K. Burk⁸², S. Burke¹⁴¹, I. Burmeister⁴⁵, J.T.P. Burr¹³², V. Büscher⁹⁷, E. Buschmann⁵¹, P. Bussey⁵⁵, J.M. Butler²⁵, C.M. Buttar⁵⁵, J.M. Butterworth⁹², P. Butti³⁵, W. Buttlinger³⁵, A. Buzatu¹⁵⁵, A.R. Buzykaev^{120b,120a}, G. Cabras^{23b,23a}, S. Cabrera Urbán¹⁷¹, D. Caforio¹³⁹, H. Cai¹⁷⁰, V.M.M. Cairo², O. Cakir^{4a}, N. Calace³⁵, P. Calafiura¹⁸, A. Calandri⁹⁹, G. Calderini¹³³, P. Calfayan⁶³, G. Callea⁵⁵, L.P. Caloba^{78b}, S. Calvente Lopez⁹⁶, D. Calvet³⁷, S. Calvet³⁷, T.P. Calvet¹⁵², M. Calvetti^{69a,69b}, R. Camacho Toro¹³³, S. Camarda³⁵, D. Camarero Munoz⁹⁶, P. Camarri^{71a,71b}, D. Cameron¹³¹, R. Caminal Armadans¹⁰⁰, C. Camincher³⁵, S. Campana³⁵, M. Campanelli⁹², A. Camplani³⁹, A. Campoverde¹⁴⁸, V. Canale^{67a,67b}, M. Cano Bret^{58c}, J. Cantero¹²⁶, T. Cao¹⁵⁸, Y. Cao¹⁷⁰, M.D.M. Capeans Garrido³⁵, I. Caprini^{27b}, M. Caprini^{27b}, M. Capua^{40b,40a}, R.M. Carbone³⁸, R. Cardarelli^{71a}, F.C. Cardillo¹⁴⁶, I. Carli¹⁴⁰, T. Carli³⁵, G. Carlino^{67a}, B.T. Carlson¹³⁶, L. Carminati^{66a,66b}, R.M.D. Carney^{43a,43b}, S. Caron¹¹⁷, E. Carquin^{144b}, S. Carrá^{66a,66b}, J.W.S. Carter¹⁶⁴, D. Casadei^{32b}, M.P. Casado^{14,g}, A.F. Casha¹⁶⁴, D.W. Casper¹⁶⁸, R. Castelijn¹¹⁸, F.L. Castillo¹⁷¹, V. Castillo Gimenez¹⁷¹, N.F. Castro^{137a,137e}, A. Catinaccio³⁵, J.R. Catmore¹³¹, A. Cattai³⁵, J. Caudron²⁴, V. Cavalieri²⁹, E. Cavallaro¹⁴, D. Cavalli^{66a}, M. Cavalli-Sforza¹⁴, V. Cavasinni^{69a,69b}, E. Celebi^{12b}, F. Ceradini^{72a,72b}, L. Cerdà Alberich¹⁷¹, A.S. Cerqueira^{78a}, A. Cerri¹⁵³, L. Cerrito^{71a,71b}, F. Cerutti¹⁸, A. Cervelli^{23b,23a}, S.A. Cetin^{12b}, A. Chafaq^{34a}, D. Chakraborty¹¹⁹, S.K. Chan⁵⁷, W.S. Chan¹¹⁸, W.Y. Chan⁸⁸, J.D. Chapman³¹, B. Chargeishvili^{156b}, D.G. Charlton²¹, C.C. Chau³³, C.A. Chavez Barajas¹⁵³, S. Che¹²³, A. Chegwidden¹⁰⁴, S. Chekanov⁶, S.V. Chekulaev^{165a}, G.A. Chelkov^{77,au}, M.A. Chelstowska³⁵, B. Chen⁷⁶, C. Chen^{58a}, C.H. Chen⁷⁶, H. Chen²⁹, J. Chen^{58a}, J. Chen³⁸, S. Chen¹³⁴, S.J. Chen^{15c}, X. Chen^{15b,at}, Y. Chen⁸⁰, Y-H. Chen⁴⁴, H.C. Cheng^{61a}, H.J. Cheng^{15d}, A. Cheplakov⁷⁷, E. Cheremushkina¹²¹, R. Cherkaoui El Moursli^{34e}, E. Cheu⁷, K. Cheung⁶², T.J.A. Chevaléries¹⁴², L. Chevalier¹⁴², V. Chiarella⁴⁹, G. Chiarelli^{69a}, G. Chiodini^{65a}, A.S. Chisholm^{35,21}, A. Chitan^{27b}, I. Chiu¹⁶⁰, Y.H. Chiu¹⁷³, M.V. Chizhov⁷⁷, K. Choi⁶³, A.R. Chomont¹²⁹, S. Chouridou¹⁵⁹, Y.S. Chow¹¹⁸, V. Christodoulou⁹², M.C. Chu^{61a}, J. Chudoba¹³⁸, A.J. Chuinard¹⁰¹, J.J. Chwastowski⁸², L. Chytka¹²⁷, D. Cinca⁴⁵, V. Cindro⁸⁹, I.A. Cioară²⁴, A. Ciocio¹⁸, F. Cirotto^{67a,67b}, Z.H. Citron¹⁷⁷, M. Citterio^{66a}, A. Clark⁵², M.R. Clark³⁸, P.J. Clark⁴⁸, C. Clement^{43a,43b}, Y. Coadou⁹⁹, M. Cobal^{64a,64c}, A. Coccato^{53b}, J. Cochran⁷⁶, H. Cohen¹⁵⁸, A.E.C. Coimbra¹⁷⁷, L. Colasurdo¹¹⁷, B. Cole³⁸, A.P. Colijn¹¹⁸, J. Collot⁵⁶, P. Conde Muñoz^{137a,i}, E. Coniavitis⁵⁰, S.H. Connell^{32b}, I.A. Connelly⁹⁸, S. Constantinescu^{27b}, F. Conventi^{67a,aw}, A.M. Cooper-Sarkar¹³², F. Cormier¹⁷², K.J.R. Cormier¹⁶⁴, L.D. Corpe⁹², M. Corradi^{70a,70b}, E.E. Corrigan⁹⁴, F. Corriveau^{101,ad}, A. Cortes-Gonzalez³⁵, M.J. Costa¹⁷¹, F. Costanza⁵, D. Costanzo¹⁴⁶, G. Cottin³¹, G. Cowan⁹¹, J.W. Cowley³¹, B.E. Cox⁹⁸, J. Crane⁹⁸, K. Cranmer¹²², S.J. Crawley⁵⁵,

R.A. Creager¹³⁴, G. Cree³³, S. Crépé-Renaudin⁵⁶, F. Crescioli¹³³, M. Cristinziani²⁴, V. Croft¹²²,
 G. Crosetti^{40b,40a}, A. Cueto⁹⁶, T. Cuhadar Donszelmann¹⁴⁶, A.R. Cukierman¹⁵⁰, S. Czekierda⁸²,
 P. Czodrowski³⁵, M.J. Da Cunha Sargedas De Sousa^{58b}, C. Da Via⁹⁸, W. Dabrowski^{81a}, T. Dado^{28a,y},
 S. Dahbi^{34e}, T. Dai¹⁰³, F. Dallaire¹⁰⁷, C. Dallapiccola¹⁰⁰, M. Dam³⁹, G. D'amen^{23b,23a}, J. Damp⁹⁷,
 J.R. Dandoy¹³⁴, M.F. Daneri³⁰, N.P. Dang^{178,l}, N.D Dann⁹⁸, M. Danninger¹⁷², V. Dao³⁵, G. Darbo^{53b},
 S. Darmora⁸, O. Dartsi⁵, A. Dattagupta¹²⁸, T. Daubney⁴⁴, S. D'Auria^{66a,66b}, W. Davey²⁴, C. David⁴⁴,
 T. Davidek¹⁴⁰, D.R. Davis⁴⁷, E. Dawe¹⁰², I. Dawson¹⁴⁶, K. De⁸, R. De Asmundis^{67a}, A. De Benedetti¹²⁵,
 M. De Beurs¹¹⁸, S. De Castro^{23b,23a}, S. De Cecco^{70a,70b}, N. De Groot¹¹⁷, P. de Jong¹¹⁸, H. De la Torre¹⁰⁴,
 F. De Lorenzi⁷⁶, A. De Maria^{69a,69b}, D. De Pedis^{70a}, A. De Salvo^{70a}, U. De Sanctis^{71a,71b},
 M. De Santis^{71a,71b}, A. De Santo¹⁵³, K. De Vasconcelos Corga⁹⁹, J.B. De Vivie De Regie¹²⁹,
 C. Debenedetti¹⁴³, D.V. Dedovich⁷⁷, N. Dehghanian³, M. Del Gaudio^{40b,40a}, J. Del Peso⁹⁶,
 Y. Delabat Diaz⁴⁴, D. Delgove¹²⁹, F. Deliot¹⁴², C.M. Delitzsch⁷, M. Della Pietra^{67a,67b}, D. Della Volpe⁵²,
 A. Dell'Acqua³⁵, L. Dell'Asta²⁵, M. Delmastro⁵, C. Delporte¹²⁹, P.A. Delsart⁵⁶, D.A. DeMarco¹⁶⁴,
 S. Demers¹⁸⁰, M. Demichev⁷⁷, S.P. Denisov¹²¹, D. Denysiuk¹¹⁸, L. D'Eramo¹³³, D. Derendarz⁸²,
 J.E. Derkaoui^{34d}, F. Derue¹³³, P. Dervan⁸⁸, K. Desch²⁴, C. Deterre⁴⁴, K. Dette¹⁶⁴, M.R. Devesa³⁰,
 P.O. Deviveiros³⁵, A. Dewhurst¹⁴¹, S. Dhaliwal²⁶, F.A. Di Bello⁵², A. Di Ciaccio^{71a,71b}, L. Di Ciaccio⁵,
 W.K. Di Clemente¹³⁴, C. Di Donato^{67a,67b}, A. Di Girolamo³⁵, G. Di Gregorio^{69a,69b}, B. Di Micco^{72a,72b},
 R. Di Nardo¹⁰⁰, K.F. Di Petrillo⁵⁷, R. Di Sipio¹⁶⁴, D. Di Valentino³³, C. Diaconu⁹⁹, M. Diamond¹⁶⁴,
 F.A. Dias³⁹, T. Dias Do Vale^{137a}, M.A. Diaz^{144a}, J. Dickinson¹⁸, E.B. Diehl¹⁰³, J. Dietrich¹⁹,
 S. Díez Cornell⁴⁴, A. Dimitrievska¹⁸, J. Dingfelder²⁴, F. Dittus³⁵, F. Djama⁹⁹, T. Djobava^{156b},
 J.I. Djuvsland¹⁷, M.A.B. Do Vale^{78c}, M. Dobre^{27b}, D. Dodsworth²⁶, C. Doglioni⁹⁴, J. Dolejsi¹⁴⁰,
 Z. Dolezal¹⁴⁰, M. Donadelli^{78d}, J. Donini³⁷, A. D'onofrio⁹⁰, M. D'Onofrio⁸⁸, J. Dopke¹⁴¹, A. Doria^{67a},
 M.T. Dova⁸⁶, A.T. Doyle⁵⁵, E. Drechsler¹⁴⁹, E. Dreyer¹⁴⁹, T. Dreyer⁵¹, Y. Du^{58b}, F. Dubinin¹⁰⁸,
 M. Dubovsky^{28a}, A. Dubreuil⁵², E. Duchovni¹⁷⁷, G. Duckeck¹¹², A. Ducourthial¹³³, O.A. Ducu^{107,x},
 D. Duda¹¹³, A. Dudarev³⁵, A.C. Dudder⁹⁷, E.M. Duffield¹⁸, L. Duflot¹²⁹, M. Dührssen³⁵, C. Dülsen¹⁷⁹,
 M. Dumancic¹⁷⁷, A.E. Dumitriu^{27b,e}, A.K. Duncan⁵⁵, M. Dunford^{59a}, A. Duperrin⁹⁹, H. Duran Yildiz^{4a},
 M. Düren⁵⁴, A. Durglishvili^{156b}, D. Duschinger⁴⁶, B. Dutta⁴⁴, D. Duvnjak¹, G. Dyckes¹³⁴, M. Dyndal⁴⁴,
 S. Dysch⁹⁸, B.S. Dziedzic⁸², K.M. Ecker¹¹³, R.C. Edgar¹⁰³, T. Eifert³⁵, G. Eigen¹⁷, K. Einsweiler¹⁸,
 T. Ekelof¹⁶⁹, M. El Kacimi^{34c}, R. El Kosseifi⁹⁹, V. Ellajosyula⁹⁹, M. Ellert¹⁶⁹, F. Ellinghaus¹⁷⁹,
 A.A. Elliot⁹⁰, N. Ellis³⁵, J. Elmsheuser²⁹, M. Elsing³⁵, D. Emeliyanov¹⁴¹, A. Emerman³⁸, Y. Enari¹⁶⁰,
 J.S. Ennis¹⁷⁵, M.B. Epland⁴⁷, J. Erdmann⁴⁵, A. Ereditato²⁰, S. Errede¹⁷⁰, M. Escalier¹²⁹, C. Escobar¹⁷¹,
 O. Estrada Pastor¹⁷¹, A.I. Etienne¹⁴², E. Etzion¹⁵⁸, H. Evans⁶³, A. Ezhilov¹³⁵, M. Ezzi^{34e}, F. Fabbri⁵⁵,
 L. Fabbri^{23b,23a}, V. Fabiani¹¹⁷, G. Facini⁹², R.M. Faisca Rodrigues Pereira^{137a}, R.M. Fakhrutdinov¹²¹,
 S. Falciano^{70a}, P.J. Falke⁵, S. Falke⁵, J. Faltova¹⁴⁰, Y. Fang^{15a}, M. Fanti^{66a,66b}, A. Farbin⁸, A. Farilla^{72a},
 E.M. Farina^{68a,68b}, T. Farooque¹⁰⁴, S. Farrell¹⁸, S.M. Farrington¹⁷⁵, P. Farthouat³⁵, F. Fassi^{34e},
 P. Fassnacht³⁵, D. Fassouliotis⁹, M. Fucci Giannelli⁴⁸, W.J. Fawcett³¹, L. Fayard¹²⁹, O.L. Fedin^{135,q},
 W. Fedorko¹⁷², M. Feickert⁴¹, S. Feigl¹³¹, L. Feligioni⁹⁹, C. Feng^{58b}, E.J. Feng³⁵, M. Feng⁴⁷,
 M.J. Fenton⁵⁵, A.B. Fenyuk¹²¹, J. Ferrando⁴⁴, A. Ferrari¹⁶⁹, P. Ferrari¹¹⁸, R. Ferrari^{68a},
 D.E. Ferreira de Lima^{59b}, A. Ferrer¹⁷¹, D. Ferrere⁵², C. Ferretti¹⁰³, F. Fiedler⁹⁷, A. Filipčič⁸⁹, F. Filthaut¹¹⁷,
 K.D. Finelli²⁵, M.C.N. Fiolhais^{137a,137c,a}, L. Fiorini¹⁷¹, C. Fischer¹⁴, W.C. Fisher¹⁰⁴, N. Flaschel⁴⁴,
 I. Fleck¹⁴⁸, P. Fleischmann¹⁰³, R.R.M. Fletcher¹³⁴, T. Flick¹⁷⁹, B.M. Flierl¹¹², L.M. Flores¹³⁴,
 L.R. Flores Castillo^{61a}, F.M. Follega^{73a,73b}, N. Fomin¹⁷, G.T. Forcolin^{73a,73b}, A. Formica¹⁴², F.A. Förster¹⁴,
 A.C. Forti⁹⁸, A.G. Foster²¹, D. Fournier¹²⁹, H. Fox⁸⁷, S. Fracchia¹⁴⁶, P. Francavilla^{69a,69b},
 M. Franchini^{23b,23a}, S. Franchino^{59a}, D. Francis³⁵, L. Franconi¹⁴³, M. Franklin⁵⁷, M. Frate¹⁶⁸,
 M. Fraternali^{68a,68b}, A.N. Fray⁹⁰, D. Freeborn⁹², B. Freund¹⁰⁷, W.S. Freund^{78b}, E.M. Freundlich⁴⁵,
 D.C. Frizzell¹²⁵, D. Froidevaux³⁵, J.A. Frost¹³², C. Fukunaga¹⁶¹, E. Fullana Torregrosa¹⁷¹,
 E. Fumagalli^{53b,53a}, T. Fusayasu¹¹⁴, J. Fuster¹⁷¹, O. Gabizon¹⁵⁷, A. Gabrielli^{23b,23a}, A. Gabrielli¹⁸,

G.P. Gach^{81a}, S. Gadatsch⁵², P. Gadow¹¹³, G. Gagliardi^{53b,53a}, L.G. Gagnon¹⁰⁷, C. Galea^{27b},
 B. Galhardo^{137a,137c}, E.J. Gallas¹³², B.J. Gallop¹⁴¹, P. Gallus¹³⁹, G. Galster³⁹, R. Gamboa Goni⁹⁰,
 K.K. Gan¹²³, S. Ganguly¹⁷⁷, J. Gao^{58a}, Y. Gao⁸⁸, Y.S. Gao^{150,n}, C. García¹⁷¹, J.E. García Navarro¹⁷¹,
 J.A. García Pascual^{15a}, C. Garcia-Argos⁵⁰, M. Garcia-Sciveres¹⁸, R.W. Gardner³⁶, N. Garelli¹⁵⁰,
 S. Gargiulo⁵⁰, V. Garonne¹³¹, K. Gasnikova⁴⁴, A. Gaudiello^{53b,53a}, G. Gaudio^{68a}, I.L. Gavrilenko¹⁰⁸,
 A. Gavrilyuk¹⁰⁹, C. Gay¹⁷², G. Gaycken²⁴, E.N. Gazis¹⁰, C.N.P. Gee¹⁴¹, J. Geisen⁵¹, M. Geisen⁹⁷,
 M.P. Geisler^{59a}, C. Gemme^{53b}, M.H. Genest⁵⁶, C. Geng¹⁰³, S. Gentile^{70a,70b}, S. George⁹¹, D. Gerbaudo¹⁴,
 G. Gessner⁴⁵, S. Ghasemi¹⁴⁸, M. Ghasemi Bostanabad¹⁷³, M. Ghneimat²⁴, B. Giacobbe^{23b},
 S. Giagu^{70a,70b}, N. Giangiacomi^{23b,23a}, P. Giannetti^{69a}, A. Giannini^{67a,67b}, S.M. Gibson⁹¹, M. Gignac¹⁴³,
 D. Gillberg³³, G. Gilles¹⁷⁹, D.M. Gingrich^{3,av}, M.P. Giordani^{64a,64c}, F.M. Giorgi^{23b}, P.F. Giraud¹⁴²,
 P. Giromini⁵⁷, G. Giugliarelli^{64a,64c}, D. Giugni^{66a}, F. Giuli¹³², M. Giulini^{59b}, S. Gkaitatzis¹⁵⁹, I. Gkialas^{9,k},
 E.L. Gkougkousis¹⁴, P. Gkountoumis¹⁰, L.K. Gladilin¹¹¹, C. Glasman⁹⁶, J. Glatzer¹⁴, P.C.F. Glaysher⁴⁴,
 A. Glazov⁴⁴, M. Goblirsch-Kolb²⁶, J. Godlewski⁸², S. Goldfarb¹⁰², T. Golling⁵², D. Golubkov¹²¹,
 A. Gomes^{137a,137b}, R. Goncalves Gama⁵¹, R. Gonçalo^{137a}, G. Gonella⁵⁰, L. Gonella²¹, A. Gongadze⁷⁷,
 F. Gonnella²¹, J.L. Gonski⁵⁷, S. González de la Hoz¹⁷¹, S. Gonzalez-Sevilla⁵², L. Goossens³⁵,
 P.A. Gorbounov¹⁰⁹, H.A. Gordon²⁹, B. Gorini³⁵, E. Gorini^{65a,65b}, A. Gorišek⁸⁹, A.T. Goshaw⁴⁷,
 C. Gössling⁴⁵, M.I. Gostkin⁷⁷, C.A. Gottardo²⁴, C.R. Goudet¹²⁹, D. Goujdami^{34c}, A.G. Goussiou¹⁴⁵,
 N. Govender^{32b,c}, C. Goy⁵, E. Gozani¹⁵⁷, I. Grabowska-Bold^{81a}, P.O.J. Gradin¹⁶⁹, E.C. Graham⁸⁸,
 J. Gramling¹⁶⁸, E. Gramstad¹³¹, S. Grancagnolo¹⁹, V. Gratchev¹³⁵, P.M. Gravila^{27f}, F.G. Gravili^{65a,65b},
 C. Gray⁵⁵, H.M. Gray¹⁸, Z.D. Greenwood^{93,al}, C. Grefe²⁴, K. Gregersen⁹⁴, I.M. Gregor⁴⁴, P. Grenier¹⁵⁰,
 K. Grevtsov⁴⁴, N.A. Grieser¹²⁵, J. Griffiths⁸, A.A. Grillo¹⁴³, K. Grimm^{150,b}, S. Grinstein^{14,z}, Ph. Gris³⁷,
 J.-F. Grivaz¹²⁹, S. Groh⁹⁷, E. Gross¹⁷⁷, J. Grosse-Knetter⁵¹, G.C. Grossi⁹³, Z.J. Grout⁹², C. Grud¹⁰³,
 A. Grummer¹¹⁶, L. Guan¹⁰³, W. Guan¹⁷⁸, J. Guenther³⁵, A. Guerguichon¹²⁹, F. Guescini^{165a}, D. Guest¹⁶⁸,
 R. Gugel⁵⁰, B. Gui¹²³, T. Guillemin⁵, S. Guindon³⁵, U. Gul⁵⁵, J. Guo^{58c}, W. Guo¹⁰³, Y. Guo^{58a,t}, Z. Guo⁹⁹,
 R. Gupta⁴⁴, S. Gurbuz^{12c}, G. Gustavino¹²⁵, P. Gutierrez¹²⁵, C. Gutschow⁹², C. Guyot¹⁴², M.P. Guzik^{81a},
 C. Gwenlan¹³², C.B. Gwilliam⁸⁸, A. Haas¹²², C. Haber¹⁸, H.K. Hadavand⁸, N. Haddad^{34e}, A. Hadef^{58a},
 S. Hageböck²⁴, M. Hagihara¹⁶⁶, M. Haleem¹⁷⁴, J. Haley¹²⁶, G. Halladjian¹⁰⁴, G.D. Hallewell⁹⁹,
 K. Hamacher¹⁷⁹, P. Hamal¹²⁷, K. Hamano¹⁷³, A. Hamilton^{32a}, G.N. Hamity¹⁴⁶, K. Han^{58a,ak}, L. Han^{58a},
 S. Han^{15d}, K. Hanagaki^{79,v}, M. Hance¹⁴³, D.M. Handl¹¹², B. Haney¹³⁴, R. Hankache¹³³, P. Hanke^{59a},
 E. Hansen⁹⁴, J.B. Hansen³⁹, J.D. Hansen³⁹, M.C. Hansen²⁴, P.H. Hansen³⁹, K. Hara¹⁶⁶, A.S. Hard¹⁷⁸,
 T. Harenberg¹⁷⁹, S. Harkusha¹⁰⁵, P.F. Harrison¹⁷⁵, N.M. Hartmann¹¹², Y. Hasegawa¹⁴⁷, A. Hasib⁴⁸,
 S. Hassani¹⁴², S. Haug²⁰, R. Hauser¹⁰⁴, L. Hauswald⁴⁶, L.B. Havener³⁸, M. Havranek¹³⁹, C.M. Hawkes²¹,
 R.J. Hawkings³⁵, D. Hayden¹⁰⁴, C. Hayes¹⁵², C.P. Hays¹³², J.M. Hays⁹⁰, H.S. Hayward⁸⁸,
 S.J. Haywood¹⁴¹, F. He^{58a}, M.P. Heath⁴⁸, V. Hedberg⁹⁴, L. Heelan⁸, S. Heer²⁴, K.K. Heidegger⁵⁰,
 J. Heilman³³, S. Heim⁴⁴, T. Heim¹⁸, B. Heinemann^{44,aq}, J.J. Heinrich¹¹², L. Heinrich¹²², C. Heinz⁵⁴,
 J. Hejbal¹³⁸, L. Helary³⁵, A. Held¹⁷², S. Hellesund¹³¹, C.M. Helling¹⁴³, S. Hellman^{43a,43b}, C. Helsens³⁵,
 R.C.W. Henderson⁸⁷, Y. Heng¹⁷⁸, S. Henkelmann¹⁷², A.M. Henriques Correia³⁵, G.H. Herbert¹⁹,
 H. Herde²⁶, V. Herget¹⁷⁴, Y. Hernández Jiménez^{32c}, H. Herr⁹⁷, M.G. Herrmann¹¹², T. Herrmann⁴⁶,
 G. Herten⁵⁰, R. Hertenberger¹¹², L. Hervas³⁵, T.C. Herwig¹³⁴, G.G. Hesketh⁹², N.P. Hessey^{165a},
 A. Higashida¹⁶⁰, S. Higashino⁷⁹, E. Higón-Rodriguez¹⁷¹, K. Hildebrand³⁶, E. Hill¹⁷³, J.C. Hill³¹,
 K.K. Hill²⁹, K.H. Hiller⁴⁴, S.J. Hillier²¹, M. Hils⁴⁶, I. Hinchliffe¹⁸, F. Hinterkeuser²⁴, M. Hirose¹³⁰,
 D. Hirschbuehl¹⁷⁹, B. Hiti⁸⁹, O. Hladik¹³⁸, D.R. Hlaluku^{32c}, X. Hoad⁴⁸, J. Hobbs¹⁵², N. Hod^{165a},
 M.C. Hodgkinson¹⁴⁶, A. Hoecker³⁵, M.R. Hoeferkamp¹¹⁶, F. Hoenig¹¹², D. Hohn⁵⁰, D. Hohov¹²⁹,
 T.R. Holmes³⁶, M. Holzbock¹¹², M. Homann⁴⁵, B.H. Hommels³¹, S. Honda¹⁶⁶, T. Honda⁷⁹, T.M. Hong¹³⁶,
 A. Höngle¹¹³, B.H. Hooberman¹⁷⁰, W.H. Hopkins¹²⁸, Y. Horii¹¹⁵, P. Horn⁴⁶, A.J. Horton¹⁴⁹, L.A. Horyn³⁶,
 J-Y. Hostachy⁵⁶, A. Hostiuc¹⁴⁵, S. Hou¹⁵⁵, A. Hoummada^{34a}, J. Howarth⁹⁸, J. Hoya⁸⁶, M. Hrabovsky¹²⁷,
 J. Hrdinka³⁵, I. Hristova¹⁹, J. Hrivnac¹²⁹, A. Hrynevich¹⁰⁶, T. Hrynev'ova⁵, P.J. Hsu⁶², S.-C. Hsu¹⁴⁵, Q. Hu²⁹,

S. Hu^{58c}, Y. Huang^{15a}, Z. Hubacek¹³⁹, F. Hubaut⁹⁹, M. Huebner²⁴, F. Huegging²⁴, T.B. Huffman¹³², M. Huhtinen³⁵, R.F.H. Hunter³³, P. Huo¹⁵², A.M. Hupe³³, N. Huseynov^{77,af}, J. Huston¹⁰⁴, J. Huth⁵⁷, R. Hyneman¹⁰³, G. Iacobucci⁵², G. Iakovidis²⁹, I. Ibragimov¹⁴⁸, L. Iconomidou-Fayard¹²⁹, Z. Idrissi^{34e}, P. Iengo³⁵, R. Ignazzi³⁹, O. Igonkina^{118,ab}, R. Iguchi¹⁶⁰, T. Iizawa⁵², Y. Ikegami⁷⁹, M. Ikeno⁷⁹, D. Iliadis¹⁵⁹, N. Ilic¹¹⁷, F. Iltzsche⁴⁶, G. Introzzi^{68a,68b}, M. Iodice^{72a}, K. Iordanidou³⁸, V. Ippolito^{70a,70b}, M.F. Isacson¹⁶⁹, N. Ishijima¹³⁰, M. Ishino¹⁶⁰, M. Ishitsuka¹⁶², W. Islam¹²⁶, C. Issever¹³², S. Istin¹⁵⁷, F. Ito¹⁶⁶, J.M. Iturbe Ponce^{61a}, R. Iuppa^{73a,73b}, A. Ivina¹⁷⁷, H. Iwasaki⁷⁹, J.M. Izen⁴², V. Izzo^{67a}, P. Jacka¹³⁸, P. Jackson¹, R.M. Jacobs²⁴, V. Jain², G. Jäkel¹⁷⁹, K.B. Jakobi⁹⁷, K. Jakobs⁵⁰, S. Jakobsen⁷⁴, T. Jakoubek¹³⁸, D.O. Jamin¹²⁶, R. Jansky⁵², J. Janssen²⁴, M. Janus⁵¹, P.A. Janus^{81a}, G. Jarlskog⁹⁴, N. Javadov^{77,af}, T. Javůrek³⁵, M. Javurkova⁵⁰, F. Jeanneau¹⁴², L. Jeanty¹⁸, J. Jejelava^{156a,ag}, A. Jelinskas¹⁷⁵, P. Jenni^{50,d}, J. Jeong⁴⁴, N. Jeong⁴⁴, S. Jézéquel⁵, H. Ji¹⁷⁸, J. Jia¹⁵², H. Jiang⁷⁶, Y. Jiang^{58a}, Z. Jiang^{150,r}, S. Jiggins⁵⁰, F.A. Jimenez Morales³⁷, J. Jimenez Pena¹⁷¹, S. Jin^{15c}, A. Jinaru^{27b}, O. Jinnouchi¹⁶², H. Jivan^{32c}, P. Johansson¹⁴⁶, K.A. Johns⁷, C.A. Johnson⁶³, K. Jon-And^{43a,43b}, R.W.L. Jones⁸⁷, S.D. Jones¹⁵³, S. Jones⁷, T.J. Jones⁸⁸, J. Jongmanns^{59a}, P.M. Jorge^{137a,137b}, J. Jovicevic^{165a}, X. Ju¹⁸, J.J. Junggeburth¹¹³, A. Juste Rozas^{14,z}, A. Kaczmarska⁸², M. Kado¹²⁹, H. Kagan¹²³, M. Kagan¹⁵⁰, T. Kaji¹⁷⁶, E. Kajomovitz¹⁵⁷, C.W. Kalderon⁹⁴, A. Kaluza⁹⁷, S. Kama⁴¹, A. Kamenshchikov¹²¹, L. Kanjur⁸⁹, Y. Kano¹⁶⁰, V.A. Kantserov¹¹⁰, J. Kanzaki⁷⁹, L.S. Kaplan¹⁷⁸, D. Kar^{32c}, M.J. Kareem^{165b}, E. Karentzos¹⁰, S.N. Karpov⁷⁷, Z.M. Karpova⁷⁷, V. Kartvelishvili⁸⁷, A.N. Karyukhin¹²¹, L. Kashif¹⁷⁸, R.D. Kass¹²³, A. Kastanas^{43a,43b}, Y. Kataoka¹⁶⁰, C. Kato^{58d,58c}, J. Katzy⁴⁴, K. Kawade⁸⁰, K. Kawagoe⁸⁵, T. Kawaguchi¹¹⁵, T. Kawamoto¹⁶⁰, G. Kawamura⁵¹, E.F. Kay⁸⁸, V.F. Kazanin^{120b,120a}, R. Keeler¹⁷³, R. Kehoe⁴¹, J.S. Keller³³, E. Kellermann⁹⁴, J.J. Kempster²¹, J. Kendrick²¹, O. Kepka¹³⁸, S. Kersten¹⁷⁹, B.P. Kerševan⁸⁹, S. Ketabchi Haghigat¹⁶⁴, R.A. Keyes¹⁰¹, M. Khader¹⁷⁰, F. Khalil-Zada¹³, A. Khanov¹²⁶, A.G. Kharlamov^{120b,120a}, T. Kharlamova^{120b,120a}, E.E. Khoda¹⁷², A. Khodinov¹⁶³, T.J. Khoo⁵², E. Khramov⁷⁷, J. Khubua^{156b}, S. Kido⁸⁰, M. Kiehn⁵², C.R. Kilby⁹¹, Y.K. Kim³⁶, N. Kimura^{64a,64c}, O.M. Kind¹⁹, B.T. King⁸⁸, D. Kirchmeier⁴⁶, J. Kirk¹⁴¹, A.E. Kiryunin¹¹³, T. Kishimoto¹⁶⁰, D. Kisielewska^{81a}, V. Kitali⁴⁴, O. Kivernyk⁵, E. Kladiva^{28b,*}, T. Klapdor-Kleingrothaus⁵⁰, M.H. Klein¹⁰³, M. Klein⁸⁸, U. Klein⁸⁸, K. Kleinknecht⁹⁷, P. Klimek¹¹⁹, A. Klimentov²⁹, T. Klingl²⁴, T. Klioutchnikova³⁵, F.F. Klitzner¹¹², P. Kluit¹¹⁸, S. Kluth¹¹³, E. Kneringer⁷⁴, E.B.F.G. Knoops⁹⁹, A. Knue⁵⁰, A. Kobayashi¹⁶⁰, D. Kobayashi⁸⁵, T. Kobayashi¹⁶⁰, M. Kobel⁴⁶, M. Kocian¹⁵⁰, P. Kodys¹⁴⁰, P.T. Koenig²⁴, T. Koffas³³, E. Koffeman¹¹⁸, N.M. Köhler¹¹³, T. Koi¹⁵⁰, M. Kolb^{59b}, I. Koletsou⁵, T. Kondo⁷⁹, N. Kondrashova^{58c}, K. Köneke⁵⁰, A.C. König¹¹⁷, T. Kono⁷⁹, R. Konoplich^{122,an}, V. Konstantinides⁹², N. Konstantinidis⁹², B. Konya⁹⁴, R. Kopeliansky⁶³, S. Koperny^{81a}, K. Korcyl⁸², K. Kordas¹⁵⁹, G. Koren¹⁵⁸, A. Korn⁹², I. Korolkov¹⁴, E.V. Korolkova¹⁴⁶, N. Korotkova¹¹¹, O. Kortner¹¹³, S. Kortner¹¹³, T. Kosek¹⁴⁰, V.V. Kostyukhin²⁴, A. Kotwal⁴⁷, A. Koumouris¹⁰, A. Kourkoumeli-Charalampidi^{68a,68b}, C. Kourkoumelis⁹, E. Kourlitis¹⁴⁶, V. Kouskoura²⁹, A.B. Kowalewska⁸², R. Kowalewski¹⁷³, T.Z. Kowalski^{81a}, C. Kozakai¹⁶⁰, W. Kozanecki¹⁴², A.S. Kozhin¹²¹, V.A. Kramarenko¹¹¹, G. Kramberger⁸⁹, D. Krasnopevtsev^{58a}, M.W. Krasny¹³³, A. Krasznahorkay³⁵, D. Krauss¹¹³, J.A. Kremer^{81a}, J. Kretzschmar⁸⁸, P. Krieger¹⁶⁴, K. Krizka¹⁸, K. Kroeninger⁴⁵, H. Kroha¹¹³, J. Kroll¹³⁸, J. Kroll¹³⁴, J. Krstic¹⁶, U. Kruchonak⁷⁷, H. Krüger²⁴, N. Krumnack⁷⁶, M.C. Kruse⁴⁷, T. Kubota¹⁰², S. Kuday^{4b}, J.T. Kuechler¹⁷⁹, S. Kuehn³⁵, A. Kugel^{59a}, T. Kuhl⁴⁴, V. Kukhtin⁷⁷, R. Kukla⁹⁹, Y. Kulchitsky^{105,aj}, S. Kuleshov^{144b}, Y.P. Kulinich¹⁷⁰, M. Kuna⁵⁶, T. Kunigo⁸³, A. Kupco¹³⁸, T. Kupfer⁴⁵, O. Kuprash¹⁵⁸, H. Kurashige⁸⁰, L.L. Kurchaninov^{165a}, Y.A. Kurochkin¹⁰⁵, A. Kurova¹¹⁰, M.G. Kurth^{15d}, E.S. Kuwertz³⁵, M. Kuze¹⁶², J. Kvita¹²⁷, T. Kwan¹⁰¹, A. La Rosa¹¹³, J.L. La Rosa Navarro^{78d}, L. La Rotonda^{40b,40a}, F. La Ruffa^{40b,40a}, C. Lacasta¹⁷¹, F. Lacava^{70a,70b}, J. Lacey⁴⁴, D.P.J. Lack⁹⁸, H. Lacker¹⁹, D. Lacour¹³³, E. Ladygin⁷⁷, R. Lafaye⁵, B. Laforge¹³³, T. Lagouri^{32c}, S. Lai⁵¹, S. Lammers⁶³, W. Lampl⁷, E. Lançon²⁹, U. Landgraf⁵⁰, M.P.J. Landon⁹⁰, M.C. Lanfermann⁵², V.S. Lang⁴⁴, J.C. Lange⁵¹, R.J. Langenberg³⁵, A.J. Lankford¹⁶⁸, F. Lanni²⁹, K. Lantzsch²⁴, A. Lanza^{68a}, A. Lapertosa^{53b,53a}, S. Laplace¹³³, J.F. Laporte¹⁴², T. Lari^{66a},

F. Lasagni Manghi^{23b,23a}, M. Lassnig³⁵, T.S. Lau^{61a}, A. Laudrain¹²⁹, M. Lavorgna^{67a,67b},
 M. Lazzaroni^{66a,66b}, B. Le¹⁰², O. Le Dertz¹³³, E. Le Guirriec⁹⁹, E.P. Le Quilleuc¹⁴², M. LeBlanc⁷,
 T. LeCompte⁶, F. Ledroit-Guillon⁵⁶, C.A. Lee²⁹, G.R. Lee^{144a}, L. Lee⁵⁷, S.C. Lee¹⁵⁵, B. Lefebvre¹⁰¹,
 M. Lefebvre¹⁷³, F. Legger¹¹², C. Leggett¹⁸, K. Lehmann¹⁴⁹, N. Lehmann¹⁷⁹, G. Lehmann Miotto³⁵,
 W.A. Leight⁴⁴, A. Leisos^{159,w}, M.A.L. Leite^{78d}, R. Leitner¹⁴⁰, D. Lellouch¹⁷⁷, K.J.C. Leney⁹², T. Lenz²⁴,
 B. Lenzi³⁵, R. Leone⁷, S. Leone^{69a}, C. Leonidopoulos⁴⁸, G. Lerner¹⁵³, C. Leroy¹⁰⁷, R. Les¹⁶⁴,
 A.A.J. Lesage¹⁴², C.G. Lester³¹, M. Levchenko¹³⁵, J. Levêque⁵, D. Levin¹⁰³, L.J. Levinson¹⁷⁷, D. Lewis⁹⁰,
 B. Li^{15b}, B. Li¹⁰³, C-Q. Li^{58a,am}, H. Li^{58a}, H. Li^{58b}, K. Li¹⁵⁰, L. Li^{58c}, M. Li^{15a}, Q. Li^{15d}, Q.Y. Li^{58a},
 S. Li^{58d,58c}, X. Li^{58c}, Y. Li¹⁴⁸, Z. Liang^{15a}, B. Liberti^{71a}, A. Liblong¹⁶⁴, K. Lie^{61c}, S. Liem¹¹⁸,
 A. Limosani¹⁵⁴, C.Y. Lin³¹, K. Lin¹⁰⁴, T.H. Lin⁹⁷, R.A. Linck⁶³, J.H. Lindon²¹, B.E. Lindquist¹⁵²,
 A.L. Lioni⁵², E. Lipeles¹³⁴, A. Lipniacka¹⁷, M. Lisovyi^{59b}, T.M. Liss^{170,as}, A. Lister¹⁷², A.M. Litke¹⁴³,
 J.D. Little⁸, B. Liu⁷⁶, B.L. Liu⁶, H.B. Liu²⁹, H. Liu¹⁰³, J.B. Liu^{58a}, J.K.K. Liu¹³², K. Liu¹³³, M. Liu^{58a},
 P. Liu¹⁸, Y. Liu^{15a}, Y.L. Liu^{58a}, Y.W. Liu^{58a}, M. Livan^{68a,68b}, A. Lleres⁵⁶, J. Llorente Merino^{15a},
 S.L. Lloyd⁹⁰, C.Y. Lo^{61b}, F. Lo Sterzo⁴¹, E.M. Lobodzinska⁴⁴, P. Loch⁷, T. Lohse¹⁹, K. Lohwasser¹⁴⁶,
 M. Lokajicek¹³⁸, J.D. Long¹⁷⁰, R.E. Long⁸⁷, L. Longo^{65a,65b}, K.A.Looper¹²³, J.A. Lopez^{144b},
 I. Lopez Paz⁹⁸, A. Lopez Solis¹⁴⁶, J. Lorenz¹¹², N. Lorenzo Martinez⁵, M. Losada²², P.J. Lösel¹¹²,
 A. Lösle⁵⁰, X. Lou⁴⁴, X. Lou^{15a}, A. Lounis¹²⁹, J. Love⁶, P.A. Love⁸⁷, J.J. Lozano Bahilo¹⁷¹, H. Lu^{61a},
 M. Lu^{58a}, Y.J. Lu⁶², H.J. Lubatti¹⁴⁵, C. Luci^{70a,70b}, A. Lucotte⁵⁶, C. Luedtke⁵⁰, F. Luehring⁶³, I. Luise¹³³,
 L. Luminari^{70a}, B. Lund-Jensen¹⁵¹, M.S. Lutz¹⁰⁰, P.M. Luzi¹³³, D. Lynn²⁹, R. Lysak¹³⁸, E. Lytken⁹⁴,
 F. Lyu^{15a}, V. Lyubushkin⁷⁷, T. Lyubushkina⁷⁷, H. Ma²⁹, L.L. Ma^{58b}, Y. Ma^{58b}, G. Maccarrone⁴⁹,
 A. Macchioli¹¹³, C.M. Macdonald¹⁴⁶, J. Machado Miguens^{134,137b}, D. Madaffari¹⁷¹, R. Madar³⁷,
 W.F. Mader⁴⁶, N. Madysa⁴⁶, J. Maeda⁸⁰, K. Maekawa¹⁶⁰, S. Maeland¹⁷, T. Maeno²⁹, M. Maerker⁴⁶,
 A.S. Maevskiy¹¹¹, V. Magerl⁵⁰, D.J. Mahon³⁸, C. Maidantchik^{78b}, T. Maier¹¹², A. Maio^{137a,137b,137d},
 O. Majersky^{28a}, S. Majewski¹²⁸, Y. Makida⁷⁹, N. Makovec¹²⁹, B. Malaescu¹³³, Pa. Malecki⁸²,
 V.P. Maleev¹³⁵, F. Malek⁵⁶, U. Mallik⁷⁵, D. Malon⁶, C. Malone³¹, S. Maltezos¹⁰, S. Malyukov³⁵,
 J. Mamuzic¹⁷¹, G. Mancini⁴⁹, I. Mandić⁸⁹, J. Maneira^{137a}, L. Manhaes de Andrade Filho^{78a},
 J. Manjarres Ramos⁴⁶, K.H. Mankinen⁹⁴, A. Mann¹¹², A. Manousos⁷⁴, B. Mansoulie¹⁴²,
 S. Manzoni^{66a,66b}, A. Marantis¹⁵⁹, G. Marceca³⁰, L. March⁵², L. Marchese¹³², G. Marchiori¹³³,
 M. Marcisovsky¹³⁸, C. Marcon⁹⁴, C.A. Marin Tobon³⁵, M. Marjanovic³⁷, F. Marroquim^{78b}, Z. Marshall¹⁸,
 M.U.F Martensson¹⁶⁹, S. Marti-Garcia¹⁷¹, C.B. Martin¹²³, T.A. Martin¹⁷⁵, V.J. Martin⁴⁸,
 B. Martin dit Latour¹⁷, M. Martinez^{14,z}, V.I. Martinez Outschoorn¹⁰⁰, S. Martin-Haugh¹⁴¹,
 V.S. Martoiu^{27b}, A.C. Martyniuk⁹², A. Marzin³⁵, L. Masetti⁹⁷, T. Mashimo¹⁶⁰, R. Mashinistov¹⁰⁸,
 J. Masik⁹⁸, A.L. Maslennikov^{120b,120a}, L.H. Mason¹⁰², L. Massa^{71a,71b}, P. Massarotti^{67a,67b},
 P. Mastrandrea¹⁵², A. Mastroberardino^{40b,40a}, T. Masubuchi¹⁶⁰, P. Mättig²⁴, J. Maurer^{27b}, B. Maček⁸⁹,
 S.J. Maxfield⁸⁸, D.A. Maximov^{120b,120a}, R. Mazini¹⁵⁵, I. Maznas¹⁵⁹, S.M. Mazza¹⁴³, S.P. Mc Kee¹⁰³,
 A. McCarn⁴¹, T.G. McCarthy¹¹³, L.I. McClymont⁹², W.P. McCormack¹⁸, E.F. McDonald¹⁰²,
 J.A. McFayden³⁵, G. Mchedlidze⁵¹, M.A. McKay⁴¹, K.D. McLean¹⁷³, S.J. McMahon¹⁴¹,
 P.C. McNamara¹⁰², C.J. McNicol¹⁷⁵, R.A. McPherson^{173,ad}, J.E. Mdhluli^{32c}, Z.A. Meadows¹⁰⁰,
 S. Meehan¹⁴⁵, T.M. Megy⁵⁰, S. Mehlhase¹¹², A. Mehta⁸⁸, T. Meideck⁵⁶, B. Meirose⁴², D. Melini^{171,h},
 B.R. Mellado Garcia^{32c}, J.D. Mellenthin⁵¹, M. Melo^{28a}, F. Meloni⁴⁴, A. Melzer²⁴, S.B. Menary⁹⁸,
 E.D. Mendes Gouveia^{137a}, L. Meng⁸⁸, X.T. Meng¹⁰³, S. Menke¹¹³, E. Meoni^{40b,40a}, S. Mergelmeyer¹⁹,
 S.A.M. Merkt¹³⁶, C. Merlassino²⁰, P. Mermod⁵², L. Merola^{67a,67b}, C. Meroni^{66a}, F.S. Merritt³⁶,
 A. Messina^{70a,70b}, J. Metcalfe⁶, A.S. Mete¹⁶⁸, C. Meyer⁶³, J. Meyer¹⁵⁷, J-P. Meyer¹⁴²,
 H. Meyer Zu Theenhausen^{59a}, F. Miano¹⁵³, R.P. Middleton¹⁴¹, L. Mijović⁴⁸, G. Mikenberg¹⁷⁷,
 M. Mikestikova¹³⁸, M. Mikuz⁸⁹, M. Milesi¹⁰², A. Milic¹⁶⁴, D.A. Millar⁹⁰, D.W. Miller³⁶, A. Milov¹⁷⁷,
 D.A. Milstead^{43a,43b}, R.A. Mina^{150,r}, A.A. Minaenko¹²¹, M. Miñano Moya¹⁷¹, I.A. Minashvili^{156b},
 A.I. Mincer¹²², B. Mindur^{81a}, M. Mineev⁷⁷, Y. Minegishi¹⁶⁰, Y. Ming¹⁷⁸, L.M. Mir¹⁴, A. Mirto^{65a,65b},

K.P. Mistry¹³⁴, T. Mitani¹⁷⁶, J. Mitrevski¹¹², V.A. Mitsou¹⁷¹, M. Mittal^{58c}, A. Miucci²⁰, P.S. Miyagawa¹⁴⁶, A. Mizukami⁷⁹, J.U. Mjörnmark⁹⁴, T. Mkrtchyan¹⁸¹, M. Mlynarikova¹⁴⁰, T. Moa^{43a,43b}, K. Mochizuki¹⁰⁷, P. Mogg⁵⁰, S. Mohapatra³⁸, S. Molander^{43a,43b}, R. Moles-Valls²⁴, M.C. Mondragon¹⁰⁴, K. Mönig⁴⁴, J. Monk³⁹, E. Monnier⁹⁹, A. Montalbano¹⁴⁹, J. Montejo Berlingen³⁵, F. Monticelli⁸⁶, S. Monzani^{66a}, N. Morange¹²⁹, D. Moreno²², M. Moreno Llácer³⁵, P. Morettini^{53b}, M. Morgenstern¹¹⁸, S. Morgenstern⁴⁶, D. Mori¹⁴⁹, M. Mori⁵⁷, M. Morinaga¹⁷⁶, V. Morisbak¹³¹, A.K. Morley³⁵, G. Mornacchi³⁵, A.P. Morris⁹², J.D. Morris⁹⁰, L. Morvaj¹⁵², P. Moschovakos¹⁰, M. Mosidze^{156b}, H.J. Moss¹⁴⁶, J. Moss^{150,o}, K. Motohashi¹⁶², R. Mount¹⁵⁰, E. Mountricha³⁵, E.J.W. Moyse¹⁰⁰, S. Muanza⁹⁹, F. Mueller¹¹³, J. Mueller¹³⁶, R.S.P. Mueller¹¹², D. Muenstermann⁸⁷, G.A. Mullier⁹⁴, F.J. Munoz Sanchez⁹⁸, P. Murin^{28b}, W.J. Murray^{175,141}, A. Murrone^{66a,66b}, M. Muškinja⁸⁹, C. Mwewa^{32a}, A.G. Myagkov^{121,ao}, J. Myers¹²⁸, M. Myska¹³⁹, B.P. Nachman¹⁸, O. Nackenhorst⁴⁵, K. Nagai¹³², K. Nagano⁷⁹, Y. Nagasaka⁶⁰, M. Nagel⁵⁰, E. Nagy⁹⁹, A.M. Nairz³⁵, Y. Nakahama¹¹⁵, K. Nakamura⁷⁹, T. Nakamura¹⁶⁰, I. Nakano¹²⁴, H. Nanjo¹³⁰, F. Napolitano^{59a}, R.F. Naranjo Garcia⁴⁴, R. Narayan¹¹, D.I. Narrias Villar^{59a}, I. Naryshkin¹³⁵, T. Naumann⁴⁴, G. Navarro²², R. Nayyar⁷, H.A. Neal^{103,*}, P.Y. Nechaeva¹⁰⁸, T.J. Neep¹⁴², A. Negri^{68a,68b}, M. Negrini^{23b}, S. Nektarijevic¹¹⁷, C. Nellist⁵¹, M.E. Nelson¹³², S. Nemecek¹³⁸, P. Nemethy¹²², M. Nessi^{35,f}, M.S. Neubauer¹⁷⁰, M. Neumann¹⁷⁹, P.R. Newman²¹, T.Y. Ng^{61c}, Y.S. Ng¹⁹, Y.W.Y. Ng¹⁶⁸, H.D.N. Nguyen⁹⁹, T. Nguyen Manh¹⁰⁷, E. Nibigira³⁷, R.B. Nickerson¹³², R. Nicolaïdou¹⁴², D.S. Nielsen³⁹, J. Nielsen¹⁴³, N. Nikiforou¹¹, V. Nikolaenko^{121,ao}, I. Nikolic-Audit¹³³, K. Nikolopoulos²¹, P. Nilsson²⁹, H.R. Nindhito⁵², Y. Ninomiya⁷⁹, A. Nisati^{70a}, N. Nishu^{58c}, R. Nisius¹¹³, I. Nitsche⁴⁵, T. Nitta¹⁷⁶, T. Nobe¹⁶⁰, Y. Noguchi⁸³, M. Nomachi¹³⁰, I. Nomidis¹³³, M.A. Nomura²⁹, T. Nooney⁹⁰, M. Nordberg³⁵, N. Norjoharuddeen¹³², T. Novak⁸⁹, O. Novgorodova⁴⁶, R. Novotny¹³⁹, L. Nozka¹²⁷, K. Ntekas¹⁶⁸, E. Nurse⁹², F. Nuti¹⁰², F.G. Oakham^{33,av}, H. Oberlack¹¹³, J. Ocariz¹³³, A. Ochi⁸⁰, I. Ochoa³⁸, J.P. Ochoa-Ricoux^{144a}, K. O'Connor²⁶, S. Oda⁸⁵, S. Odaka⁷⁹, S. Oerdekk⁵¹, A. Oh⁹⁸, S.H. Oh⁴⁷, C.C. Ohm¹⁵¹, H. Oide^{53b,53a}, M.L. Ojeda¹⁶⁴, H. Okawa¹⁶⁶, Y. Okazaki⁸³, Y. Okumura¹⁶⁰, T. Okuyama⁷⁹, A. Olariu^{27b}, L.F. Oleiro Seabra^{137a}, S.A. Olivares Pino^{144a}, D. Oliveira Damazio²⁹, J.L. Oliver¹, M.J.R. Olsson³⁶, A. Olszewski⁸², J. Olszowska⁸², D.C. O'Neil¹⁴⁹, A. Onofre^{137a,137e}, K. Onogi¹¹⁵, P.U.E. Onyisi¹¹, H. Oppen¹³¹, M.J. Oreglia³⁶, G.E. Orellana⁸⁶, Y. Oren¹⁵⁸, D. Orestano^{72a,72b}, E.C. Orgill⁹⁸, N. Orlando^{61b}, A.A. O'Rourke⁴⁴, R.S. Orr¹⁶⁴, B. Osculati^{53b,53a,*}, V. O'Shea⁵⁵, R. Ospanov^{58a}, G. Otero y Garzon³⁰, H. Otono⁸⁵, M. Ouchrif^{34d}, F. Ould-Saada¹³¹, A. Ouraou¹⁴², Q. Ouyang^{15a}, M. Owen⁵⁵, R.E. Owen²¹, V.E. Ozcan^{12c}, N. Ozturk⁸, J. Pacalt¹²⁷, H.A. Pacey³¹, K. Pachal¹⁴⁹, A. Pacheco Pages¹⁴, L. Pacheco Rodriguez¹⁴², C. Padilla Aranda¹⁴, S. Pagan Griso¹⁸, M. Paganini¹⁸⁰, G. Palacino⁶³, S. Palazzo⁴⁸, S. Palestini³⁵, M. Palka^{81b}, D. Pallin³⁷, I. Panagoulias¹⁰, C.E. Pandini³⁵, J.G. Panduro Vazquez⁹¹, P. Pani³⁵, G. Panizzo^{64a,64c}, L. Paolozzi⁵², T.D. Papadopoulou¹⁰, K. Papageorgiou^{9,k}, A. Paramonov⁶, D. Paredes Hernandez^{61b}, S.R. Paredes Saenz¹³², B. Parida¹⁶³, T.H. Park³³, A.J. Parker⁸⁷, K.A. Parker⁴⁴, M.A. Parker³¹, F. Parodi^{53b,53a}, J.A. Parsons³⁸, U. Parzefall⁵⁰, V.R. Pascuzzi¹⁶⁴, J.M.P. Pasner¹⁴³, E. Pasqualucci^{70a}, S. Passaggio^{53b}, F. Pastore⁹¹, P. Pasuwan^{43a,43b}, S. Pataraia⁹⁷, J.R. Pater⁹⁸, A. Pathak^{178,1}, T. Pauly³⁵, B. Pearson¹¹³, M. Pedersen¹³¹, L. Pedraza Diaz¹¹⁷, R. Pedro^{137a,137b}, S.V. Peleganchuk^{120b,120a}, O. Penc¹³⁸, C. Peng^{15d}, H. Peng^{58a}, B.S. Peralva^{78a}, M.M. Perego¹²⁹, A.P. Pereira Peixoto^{137a}, D.V. Perepelitsa²⁹, F. Peri¹⁹, L. Perini^{66a,66b}, H. Pernegger³⁵, S. Perrella^{67a,67b}, V.D. Peshekhonov^{77,*}, K. Peters⁴⁴, R.F.Y. Peters⁹⁸, B.A. Petersen³⁵, T.C. Petersen³⁹, E. Petit⁵⁶, A. Petridis¹, C. Petridou¹⁵⁹, P. Petroff¹²⁹, M. Petrov¹³², F. Petrucci^{72a,72b}, M. Pettee¹⁸⁰, N.E. Pettersson¹⁰⁰, A. Peyaud¹⁴², R. Pezoa^{144b}, T. Pham¹⁰², F.H. Phillips¹⁰⁴, P.W. Phillips¹⁴¹, M.W. Phipps¹⁷⁰, G. Piacquadio¹⁵², E. Pianori¹⁸, A. Picazio¹⁰⁰, R.H. Pickles⁹⁸, R. Piegaia³⁰, J.E. Pilcher³⁶, A.D. Pilkington⁹⁸, M. Pinamonti^{71a,71b}, J.L. Pinfold³, M. Pitt¹⁷⁷, L. Pizzimento^{71a,71b}, M.-A. Pleier²⁹, V. Pleskot¹⁴⁰, E. Plotnikova⁷⁷, D. Pluth⁷⁶, P. Podberezko^{120b,120a}, R. Poettgen⁹⁴, R. Poggi⁵², L. Poggiali¹²⁹, I. Pogrebnyak¹⁰⁴, D. Pohl²⁴, I. Pokharel⁵¹, G. Polesello^{68a}, A. Poley¹⁸, A. Policicchio^{70a,70b}, R. Polifka³⁵, A. Polini^{23b}, C.S. Pollard⁴⁴, V. Polychronakos²⁹, D. Ponomarenko¹¹⁰, L. Pontecorvo³⁵, G.A. Popeneciu^{27d},

D.M. Portillo Quintero¹³³, S. Pospisil¹³⁹, K. Potamianos⁴⁴, I.N. Potrap⁷⁷, C.J. Potter³¹, H. Potti¹¹,
 T. Poulsen⁹⁴, J. Poveda³⁵, T.D. Powell¹⁴⁶, M.E. Pozo Astigarraga³⁵, P. Pralavorio⁹⁹, S. Prell⁷⁶, D. Price⁹⁸,
 M. Primavera^{65a}, S. Prince¹⁰¹, M.L. Proffitt¹⁴⁵, N. Proklova¹¹⁰, K. Prokofiev^{61c}, F. Prokoshin^{144b},
 S. Protopopescu²⁹, J. Proudfoot⁶, M. Przybycien^{81a}, A. Puri¹⁷⁰, P. Puzo¹²⁹, J. Qian¹⁰³, Y. Qin⁹⁸,
 A. Quadt⁵¹, M. Queitsch-Maitland⁴⁴, A. Qureshi¹, P. Rados¹⁰², F. Ragusa^{66a,66b}, G. Rahal⁹⁵, J.A. Raine⁵²,
 S. Rajagopalan²⁹, A. Ramirez Morales⁹⁰, K. Ran^{15a}, T. Rashid¹²⁹, S. Raspovov⁵, M.G. Ratti^{66a,66b},
 D.M. Rauch⁴⁴, F. Rauscher¹¹², S. Rave⁹⁷, B. Ravina¹⁴⁶, I. Ravinovich¹⁷⁷, J.H. Rawling⁹⁸, M. Raymond³⁵,
 A.L. Read¹³¹, N.P. Readioff⁵⁶, M. Reale^{65a,65b}, D.M. Rebuzzi^{68a,68b}, A. Redelbach¹⁷⁴, G. Redlinger²⁹,
 R. Reece¹⁴³, R.G. Reed^{32c}, K. Reeves⁴², L. Rehnisch¹⁹, J. Reichert¹³⁴, D. Reikher¹⁵⁸, A. Reiss⁹⁷,
 A. Rej¹⁴⁸, C. Rembser³⁵, H. Ren^{15d}, M. Rescigno^{70a}, S. Resconi^{66a}, E.D. Ressegue¹³⁴, S. Rettie¹⁷²,
 E. Reynolds²¹, O.L. Rezanova^{120b,120a}, P. Reznicek¹⁴⁰, E. Ricci^{73a,73b}, R. Richter¹¹³, S. Richter⁴⁴,
 E. Richter-Was^{81b}, O. Ricken²⁴, M. Ridel¹³³, P. Rieck¹¹³, C.J. Riegel¹⁷⁹, O. Rifki⁴⁴, M. Rijssenbeek¹⁵²,
 A. Rimoldi^{68a,68b}, M. Rimoldi²⁰, L. Rinaldi^{23b}, G. Ripellino¹⁵¹, B. Ristic⁸⁷, E. Ritsch³⁵, I. Riu¹⁴,
 J.C. Rivera Vergara^{144a}, F. Rizatdinova¹²⁶, E. Rizvi⁹⁰, C. Rizzi¹⁴, R.T. Roberts⁹⁸, S.H. Robertson^{101,ad},
 D. Robinson³¹, J.E.M. Robinson⁴⁴, A. Robson⁵⁵, E. Rocco⁹⁷, C. Roda^{69a,69b}, Y. Rodina⁹⁹,
 S. Rodriguez Bosca¹⁷¹, A. Rodriguez Perez¹⁴, D. Rodriguez Rodriguez¹⁷¹, A.M. Rodríguez Vera^{165b},
 S. Roe³⁵, C.S. Rogan⁵⁷, O. Røhne¹³¹, R. Röhrlig¹¹³, C.P.A. Roland⁶³, J. Roloff⁵⁷, A. Romaniouk¹¹⁰,
 M. Romano^{23b,23a}, N. Rompotis⁸⁸, M. Ronzani¹²², L. Roos¹³³, S. Rosati^{70a}, K. Rosbach⁵⁰, N-A. Rosien⁵¹,
 B.J. Rosser¹³⁴, E. Rossi⁴⁴, E. Rossi^{72a,72b}, E. Rossi^{67a,67b}, L.P. Rossi^{53b}, L. Rossini^{66a,66b}, J.H.N. Rosten³¹,
 R. Rosten¹⁴, M. Rotaru^{27b}, J. Rothberg¹⁴⁵, D. Rousseau¹²⁹, D. Roy^{32c}, A. Rozanov⁹⁹, Y. Rozen¹⁵⁷,
 X. Ruan^{32c}, F. Rubbo¹⁵⁰, F. Rühr⁵⁰, A. Ruiz-Martinez¹⁷¹, Z. Rurikova⁵⁰, N.A. Rusakovich⁷⁷,
 H.L. Russell¹⁰¹, J.P. Rutherford⁷, E.M. Rüttinger^{44,m}, Y.F. Ryabov¹³⁵, M. Rybar³⁸, G. Rybkin¹²⁹, S. Ryu⁶,
 A. Ryzhov¹²¹, G.F. Rzehorž⁵¹, P. Sabatini⁵¹, G. Sabato¹¹⁸, S. Sacerdoti¹²⁹, H.F-W. Sadrozinski¹⁴³,
 R. Sadykov⁷⁷, F. Safai Tehrani^{70a}, P. Saha¹¹⁹, M. Sahinsoy^{59a}, A. Sahu¹⁷⁹, M. Saimpert⁴⁴, M. Saito¹⁶⁰,
 T. Saito¹⁶⁰, H. Sakamoto¹⁶⁰, A. Sakharov^{122,an}, D. Salamani⁵², G. Salamanna^{72a,72b},
 J.E. Salazar Loyola^{144b}, P.H. Sales De Bruin¹⁶⁹, D. Salihagic^{113,*}, A. Salnikov¹⁵⁰, J. Salt¹⁷¹,
 D. Salvatore^{40b,40a}, F. Salvatore¹⁵³, A. Salvucci^{61a,61b,61c}, A. Salzburger³⁵, J. Samarati³⁵, D. Sammel⁵⁰,
 D. Sampsonidis¹⁵⁹, D. Sampsonidou¹⁵⁹, J. Sánchez¹⁷¹, A. Sanchez Pineda^{64a,64c}, H. Sandaker¹³¹,
 C.O. Sander⁴⁴, M. Sandhoff¹⁷⁹, C. Sandoval²², D.P.C. Sankey¹⁴¹, M. Sannino^{53b,53a}, Y. Sano¹¹⁵,
 A. Sansoni⁴⁹, C. Santoni³⁷, H. Santos^{137a}, I. Santoyo Castillo¹⁵³, A. Santra¹⁷¹, A. Sapronov⁷⁷,
 J.G. Saraiva^{137a,137d}, O. Sasaki⁷⁹, K. Sato¹⁶⁶, E. Sauvan⁵, P. Savard^{164,av}, N. Savic¹¹³, R. Sawada¹⁶⁰,
 C. Sawyer¹⁴¹, L. Sawyer^{93,al}, C. Sbarra^{23b}, A. Sbrizzi^{23a}, T. Scanlon⁹², J. Schaarschmidt¹⁴⁵, P. Schacht¹¹³,
 B.M. Schachtner¹¹², D. Schaefer³⁶, L. Schaefer¹³⁴, J. Schaeffer⁹⁷, S. Schaepe³⁵, U. Schäfer⁹⁷,
 A.C. Schaffer¹²⁹, D. Schaile¹¹², R.D. Schamberger¹⁵², N. Scharmberg⁹⁸, V.A. Schegelsky¹³⁵,
 D. Scheirich¹⁴⁰, F. Schenck¹⁹, M. Schernau¹⁶⁸, C. Schiavi^{53b,53a}, S. Schier¹⁴³, L.K. Schildgen²⁴,
 Z.M. Schillaci²⁶, E.J. Schioppa³⁵, M. Schioppa^{40b,40a}, K.E. Schleicher⁵⁰, S. Schlenker³⁵,
 K.R. Schmidt-Sommerfeld¹¹³, K. Schmieden³⁵, C. Schmitt⁹⁷, S. Schmitt⁴⁴, S. Schmitz⁹⁷,
 J.C. Schmoeckel⁴⁴, U. Schnoor⁵⁰, L. Schoeffel¹⁴², A. Schoening^{59b}, E. Schopf¹³², M. Schott⁹⁷,
 J.F.P. Schouwenberg¹¹⁷, J. Schovancova³⁵, S. Schramm⁵², A. Schulte⁹⁷, H-C. Schultz-Coulon^{59a},
 M. Schumacher⁵⁰, B.A. Schumm¹⁴³, Ph. Schune¹⁴², A. Schwartzman¹⁵⁰, T.A. Schwarz¹⁰³,
 Ph. Schwemling¹⁴², R. Schwienhorst¹⁰⁴, A. Sciandra²⁴, G. Sciolla²⁶, M. Scornajenghi^{40b,40a}, F. Scuri^{69a},
 F. Scutti¹⁰², L.M. Scyboz¹¹³, C.D. Sebastiani^{70a,70b}, P. Seema¹⁹, S.C. Seidel¹¹⁶, A. Seiden¹⁴³, T. Seiss³⁶,
 J.M. Seixas^{78b}, G. Sekhniaidze^{67a}, K. Sekhon¹⁰³, S.J. Sekula⁴¹, N. Semprini-Cesari^{23b,23a}, S. Sen⁴⁷,
 S. Senkin³⁷, C. Serfon¹³¹, L. Serin¹²⁹, L. Serkin^{64a,64b}, M. Sessa^{58a}, H. Severini¹²⁵, F. Sforza¹⁶⁷,
 A. Sfyrla⁵², E. Shabalina⁵¹, J.D. Shahinian¹⁴³, N.W. Shaikh^{43a,43b}, D. Shaked Renous¹⁷⁷, L.Y. Shan^{15a},
 R. Shang¹⁷⁰, J.T. Shank²⁵, M. Shapiro¹⁸, A.S. Sharma¹, A. Sharma¹³², P.B. Shatalov¹⁰⁹, K. Shaw¹⁵³,
 S.M. Shaw⁹⁸, A. Shcherbakova¹³⁵, Y. Shen¹²⁵, N. Sherafati³³, A.D. Sherman²⁵, P. Sherwood⁹², L. Shi^{155,ar},

S. Shimizu⁷⁹, C.O. Shimmin¹⁸⁰, Y. Shimogama¹⁷⁶, M. Shimojima¹¹⁴, I.P.J. Shipsey¹³², S. Shirabe⁸⁵,
 M. Shiyakova⁷⁷, J. Shlomi¹⁷⁷, A. Shmeleva¹⁰⁸, D. Shoaleh Saadi¹⁰⁷, M.J. Shochet³⁶, S. Shojaii¹⁰²,
 D.R. Shope¹²⁵, S. Shrestha¹²³, E. Shulga¹¹⁰, P. Sicho¹³⁸, A.M. Sickles¹⁷⁰, P.E. Sidebo¹⁵¹,
 E. Sideras Haddad^{32c}, O. Sidiropoulou³⁵, A. Sidoti^{23b,23a}, F. Siegert⁴⁶, Dj. Sijacki¹⁶, J. Silva^{137a},
 M. Silva Jr.¹⁷⁸, M.V. Silva Oliveira^{78a}, S.B. Silverstein^{43a}, S. Simion¹²⁹, E. Simioni⁹⁷, M. Simon⁹⁷,
 R. Simoniello⁹⁷, P. Sinervo¹⁶⁴, N.B. Sinev¹²⁸, M. Sioli^{23b,23a}, I. Siral¹⁰³, S.Yu. Sivoklokov¹¹¹,
 J. Sjölin^{43a,43b}, P. Skubic¹²⁵, M. Slater²¹, T. Slavicek¹³⁹, M. Slawinska⁸², K. Sliwa¹⁶⁷, R. Slovak¹⁴⁰,
 V. Smakhtin¹⁷⁷, B.H. Smart⁵, J. Smiesko^{28a}, N. Smirnov¹¹⁰, S.Yu. Smirnov¹¹⁰, Y. Smirnov¹¹⁰,
 L.N. Smirnova¹¹¹, O. Smirnova⁹⁴, J.W. Smith⁵¹, M. Smizanska⁸⁷, K. Smolek¹³⁹, A. Smykiewicz⁸²,
 A.A. Snesarev¹⁰⁸, I.M. Snyder¹²⁸, S. Snyder²⁹, R. Sobie^{173,ad}, A.M. Soffa¹⁶⁸, A. Soffer¹⁵⁸, A. Søgaard⁴⁸,
 F. Sohns⁵¹, G. Sokhrannyi⁸⁹, C.A. Solans Sanchez³⁵, M. Solar¹³⁹, E.Yu. Soldatov¹¹⁰, U. Soldevila¹⁷¹,
 A.A. Solodkov¹²¹, A. Soloshenko⁷⁷, O.V. Solovyanov¹²¹, V. Solovyev¹³⁵, P. Sommer¹⁴⁶, H. Son¹⁶⁷,
 W. Song¹⁴¹, W.Y. Song^{165b}, A. Sopczak¹³⁹, F. Sopkova^{28b}, C.L. Sotiropoulou^{69a,69b}, S. Sottocornola^{68a,68b},
 R. Soualah^{64a,64c,j}, A.M. Soukharev^{120b,120a}, D. South⁴⁴, S. Spagnolo^{65a,65b}, M. Spalla¹¹³,
 M. Spangenberg¹⁷⁵, F. Spanò⁹¹, D. Sperlich¹⁹, T.M. Spieker^{59a}, R. Spighi^{23b}, G. Spigo³⁵, L.A. Spiller¹⁰²,
 D.P. Spiteri⁵⁵, M. Spousta¹⁴⁰, A. Stabile^{66a,66b}, R. Stamen^{59a}, S. Stamm¹⁹, E. Stanecka⁸², R.W. Stanek⁶,
 C. Stanescu^{72a}, B. Stanislaus¹³², M.M. Stanitzki⁴⁴, B. Stapf¹¹⁸, S. Stapnes¹³¹, E.A. Starchenko¹²¹,
 G.H. Stark¹⁴³, J. Stark⁵⁶, S.H Stark³⁹, P. Staroba¹³⁸, P. Starovoitov^{59a}, S. Stärz¹⁰¹, R. Staszewski⁸²,
 M. Stegler⁴⁴, P. Steinberg²⁹, B. Stelzer¹⁴⁹, H.J. Stelzer³⁵, O. Stelzer-Chilton^{165a}, H. Stenzel⁵⁴,
 T.J. Stevenson¹⁵³, G.A. Stewart³⁵, M.C. Stockton³⁵, G. Stoica^{27b}, P. Stolte⁵¹, S. Stonjek¹¹³,
 A. Straessner⁴⁶, J. Strandberg¹⁵¹, S. Strandberg^{43a,43b}, M. Strauss¹²⁵, P. Strizenec^{28b}, R. Ströhmer¹⁷⁴,
 D.M. Strom¹²⁸, R. Stroynowski⁴¹, A. Strubig⁴⁸, S.A. Stucci²⁹, B. Stugu¹⁷, J. Stupak¹²⁵, N.A. Styles⁴⁴,
 D. Su¹⁵⁰, J. Su¹³⁶, S. Suchek^{59a}, Y. Sugaya¹³⁰, M. Suk¹³⁹, V.V. Sulin¹⁰⁸, M.J. Sullivan⁸⁸, D.M.S. Sultan⁵²,
 S. Sultansoy^{4c}, T. Sumida⁸³, S. Sun¹⁰³, X. Sun³, K. Suruliz¹⁵³, C.J.E. Suster¹⁵⁴, M.R. Sutton¹⁵³,
 S. Suzuki⁷⁹, M. Svatos¹³⁸, M. Swiatlowski³⁶, S.P. Swift², A. Sydorenko⁹⁷, I. Sykora^{28a}, M. Sykora¹⁴⁰,
 T. Sykora¹⁴⁰, D. Ta⁹⁷, K. Tackmann^{44,aa}, J. Taenzer¹⁵⁸, A. Taffard¹⁶⁸, R. Tafirout^{165a}, E. Tahirovic⁹⁰,
 N. Taiblum¹⁵⁸, H. Takai²⁹, R. Takashima⁸⁴, E.H. Takasugi¹¹³, K. Takeda⁸⁰, T. Takeshita¹⁴⁷, Y. Takubo⁷⁹,
 M. Talby⁹⁹, A.A. Talyshев^{120b,120a}, J. Tanaka¹⁶⁰, M. Tanaka¹⁶², R. Tanaka¹²⁹, B.B. Tannenwald¹²³,
 S. Tapia Araya^{144b}, S. Tapprogge⁹⁷, A. Tarek Abouelfadl Mohamed¹³³, S. Tarem¹⁵⁷, G. Tarna^{27b,e},
 G.F. Tartarelli^{66a}, P. Tas¹⁴⁰, M. Tasevsky¹³⁸, T. Tashiro⁸³, E. Tassi^{40b,40a}, A. Tavares Delgado^{137a,137b},
 Y. Tayalati^{34e}, A.J. Taylor⁴⁸, G.N. Taylor¹⁰², P.T.E. Taylor¹⁰², W. Taylor^{165b}, A.S. Tee⁸⁷,
 R. Teixeira De Lima¹⁵⁰, P. Teixeira-Dias⁹¹, H. Ten Kate³⁵, J.J. Teoh¹¹⁸, S. Terada⁷⁹, K. Terashi¹⁶⁰,
 J. Terron⁹⁶, S. Terzo¹⁴, M. Testa⁴⁹, R.J. Teuscher^{164,ad}, S.J. Thais¹⁸⁰, T. Theveneaux-Pelzer⁴⁴, F. Thiele³⁹,
 D.W. Thomas⁹¹, J.P. Thomas²¹, A.S. Thompson⁵⁵, P.D. Thompson²¹, L.A. Thomsen¹⁸⁰, E. Thomson¹³⁴,
 Y. Tian³⁸, R.E. Ticse Torres⁵¹, V.O. Tikhomirov^{108,ap}, Yu.A. Tikhonov^{120b,120a}, S. Timoshenko¹¹⁰,
 P. Tipton¹⁸⁰, S. Tisserant⁹⁹, K. Todome¹⁶², S. Todorova-Nova⁵, S. Todt⁴⁶, J. Tojo⁸⁵, S. Tokár^{28a},
 K. Tokushuku⁷⁹, E. Tolley¹²³, K.G. Tomiwa^{32c}, M. Tomoto¹¹⁵, L. Tompkins^{150,r}, K. Toms¹¹⁶, B. Tong⁵⁷,
 P. Tornambe⁵⁰, E. Torrence¹²⁸, H. Torres⁴⁶, E. Torró Pastor¹⁴⁵, C. Tosciri¹³², J. Toth^{99,ac}, F. Touchard⁹⁹,
 D.R. Tovey¹⁴⁶, C.J. Treado¹²², T. Trefzger¹⁷⁴, F. Tresoldi¹⁵³, A. Tricoli²⁹, I.M. Trigger^{165a},
 S. Trincaz-Duvold¹³³, W. Trischuk¹⁶⁴, B. Trocmé⁵⁶, A. Trofymov¹²⁹, C. Troncon^{66a}, M. Trovatelli¹⁷³,
 F. Trovato¹⁵³, L. Truong^{32b}, M. Trzebinski⁸², A. Trzupek⁸², F. Tsai⁴⁴, J.C-L. Tseng¹³², P.V. Tsiareshka^{105,aj},
 A. Tsirigotis¹⁵⁹, N. Tsirintanis⁹, V. Tsiskaridze¹⁵², E.G. Tskhadadze^{156a}, I.I. Tsukerman¹⁰⁹, V. Tsulaia¹⁸,
 S. Tsuno⁷⁹, D. Tsybychev^{152,163}, Y. Tu^{61b}, A. Tudorache^{27b}, V. Tudorache^{27b}, T.T. Tulbure^{27a}, A.N. Tuna⁵⁷,
 S. Turchikhin⁷⁷, D. Turgeman¹⁷⁷, I. Turk Cakir^{4b,u}, R.J. Turner²¹, R.T. Turra^{66a}, P.M. Tuts³⁸,
 S. Tzamarias¹⁵⁹, E. Tzovara⁹⁷, G. Uccielli⁴⁵, I. Ueda⁷⁹, M. Ughetto^{43a,43b}, F. Ukegawa¹⁶⁶, G. Unal³⁵,
 A. Undrus²⁹, G. Unei¹⁶⁸, F.C. Ungaro¹⁰², Y. Unno⁷⁹, K. Uno¹⁶⁰, J. Urban^{28b}, P. Urquijo¹⁰², G. Usai⁸,
 J. Usui⁷⁹, L. Vacavant⁹⁹, V. Vacek¹³⁹, B. Vachon¹⁰¹, K.O.H. Vadla¹³¹, A. Vaidya⁹², C. Valderanis¹¹²,

E. Valdes Santurio^{43a,43b}, M. Valente⁵², S. Valentini^{23b,23a}, A. Valero¹⁷¹, L. Valéry⁴⁴, R.A. Vallance²¹,
 A. Vallier⁵, J.A. Valls Ferrer¹⁷¹, T.R. Van Daalen¹⁴, H. Van der Graaf¹¹⁸, P. Van Gemmeren⁶,
 I. Van Vulpen¹¹⁸, M. Vanadia^{71a,71b}, W. Vandelli³⁵, A. Vaniachine¹⁶³, P. Vankov¹¹⁸, R. Vari^{70a},
 E.W. Varnes⁷, C. Varni^{53b,53a}, T. Varol⁴¹, D. Varouchas¹²⁹, K.E. Varvell¹⁵⁴, G.A. Vasquez^{144b},
 J.G. Vasquez¹⁸⁰, F. Vazeille³⁷, D. Vazquez Furelos¹⁴, T. Vazquez Schroeder³⁵, J. Veatch⁵¹,
 V. Vecchio^{72a,72b}, L.M. Veloce¹⁶⁴, F. Veloso^{137a,137c}, S. Veneziano^{70a}, A. Ventura^{65a,65b}, N. Venturi³⁵,
 V. Vercesi^{68a}, M. Verducci^{72a,72b}, C.M. Vergel Infante⁷⁶, C. Vergis²⁴, W. Verkerke¹¹⁸, A.T. Vermeulen¹¹⁸,
 J.C. Vermeulen¹¹⁸, M.C. Vetterli^{149,av}, N. Viaux Maira^{144b}, M. Vicente Barreto Pinto⁵², I. Vichou^{170,*},
 T. Vickey¹⁴⁶, O.E. Vickey Boeriu¹⁴⁶, G.H.A. Viehhauser¹³², S. Viel¹⁸, L. Vigani¹³², M. Villa^{23b,23a},
 M. Villaplana Perez^{66a,66b}, E. Vilucchi⁴⁹, M.G. Vinchter³³, V.B. Vinogradov⁷⁷, A. Vishwakarma⁴⁴,
 C. Vittori^{23b,23a}, I. Vivarelli¹⁵³, S. Vlachos¹⁰, M. Vogel¹⁷⁹, P. Vokac¹³⁹, G. Volpi¹⁴,
 S.E. von Buddenbrock^{32c}, E. Von Toerne²⁴, V. Vorobel¹⁴⁰, K. Vorobev¹¹⁰, M. Vos¹⁷¹, J.H. Vossebeld⁸⁸,
 N. Vranjes¹⁶, M. Vranjes Milosavljevic¹⁶, V. Vrba¹³⁹, M. Vreeswijk¹¹⁸, T. Šfiligoj⁸⁹, R. Vuillermet³⁵,
 I. Vukotic³⁶, T. Ženiš^{28a}, L. Živkovic¹⁶, P. Wagner²⁴, W. Wagner¹⁷⁹, J. Wagner-Kuhr¹¹², H. Wahlberg⁸⁶,
 S. Wahrmund⁴⁶, K. Wakamiya⁸⁰, V.M. Walbrecht¹¹³, J. Walder⁸⁷, R. Walker¹¹², S.D. Walker⁹¹,
 W. Walkowiak¹⁴⁸, V. Wallangen^{43a,43b}, A.M. Wang⁵⁷, C. Wang^{58b}, F. Wang¹⁷⁸, H. Wang¹⁸, H. Wang³,
 J. Wang¹⁵⁴, J. Wang^{59b}, P. Wang⁴¹, Q. Wang¹²⁵, R.-J. Wang¹³³, R. Wang^{58a}, R. Wang⁶, S.M. Wang¹⁵⁵,
 W.T. Wang^{58a}, W. Wang^{15c,ae}, W.X. Wang^{58a,ae}, Y. Wang^{58a,am}, Z. Wang^{58c}, C. Wanotayaroj⁴⁴,
 A. Warburton¹⁰¹, C.P. Ward³¹, D.R. Wardrope⁹², A. Washbrook⁴⁸, P.M. Watkins²¹, A.T. Watson²¹,
 M.F. Watson²¹, G. Watts¹⁴⁵, S. Watts⁹⁸, B.M. Waugh⁹², A.F. Webb¹¹, S. Webb⁹⁷, C. Weber¹⁸⁰,
 M.S. Weber²⁰, S.A. Weber³³, S.M. Weber^{59a}, A.R. Weidberg¹³², J. Weingarten⁴⁵, M. Weirich⁹⁷,
 C. Weiser⁵⁰, P.S. Wells³⁵, T. Wenaus²⁹, T. Wengler³⁵, S. Wenig³⁵, N. Wermes²⁴, M.D. Werner⁷⁶,
 P. Werner³⁵, M. Wessels^{59a}, T.D. Weston²⁰, K. Whalen¹²⁸, N.L. Whallon¹⁴⁵, A.M. Wharton⁸⁷,
 A.S. White¹⁰³, A. White⁸, M.J. White¹, R. White^{144b}, D. Whiteson¹⁶⁸, B.W. Whitmore⁸⁷, F.J. Wickens¹⁴¹,
 W. Wiedenmann¹⁷⁸, M. Wielers¹⁴¹, C. Wiglesworth³⁹, L.A.M. Wiik-Fuchs⁵⁰, F. Wilk⁹⁸, H.G. Wilkens³⁵,
 L.J. Wilkins⁹¹, H.H. Williams¹³⁴, S. Williams³¹, C. Willis¹⁰⁴, S. Willocq¹⁰⁰, J.A. Wilson²¹,
 I. Wingerter-Seez⁵, E. Winkels¹⁵³, F. Winklmeier¹²⁸, O.J. Winston¹⁵³, B.T. Winter⁵⁰, M. Wittgen¹⁵⁰,
 M. Wobisch⁹³, A. Wolf⁹⁷, T.M.H. Wolf¹⁸, R. Wolff⁹⁹, J. Wollrath⁵⁰, M.W. Wolter⁸², H. Wolters^{137a,137c},
 V.W.S. Wong¹⁷², N.L. Woods¹⁴³, S.D. Worm²¹, B.K. Wosiek⁸², K.W. Woźniak⁸², K. Wraight⁵⁵, M. Wu³⁶,
 S.L. Wu¹⁷⁸, X. Wu⁵², Y. Wu^{58a}, T.R. Wyatt⁹⁸, B.M. Wynne⁴⁸, S. Xella³⁹, Z. Xi¹⁰³, L. Xia¹⁷⁵, D. Xu^{15a},
 H. Xu^{58a,e}, L. Xu²⁹, T. Xu¹⁴², W. Xu¹⁰³, Z. Xu¹⁵⁰, B. Yabsley¹⁵⁴, S. Yacoob^{32a}, K. Yajima¹³⁰,
 D.P. Yallup⁹², D. Yamaguchi¹⁶², Y. Yamaguchi¹⁶², A. Yamamoto⁷⁹, T. Yamanaka¹⁶⁰, F. Yamane⁸⁰,
 M. Yamatani¹⁶⁰, T. Yamazaki¹⁶⁰, Y. Yamazaki⁸⁰, Z. Yan²⁵, H.J. Yang^{58c,58d}, H.T. Yang¹⁸, S. Yang⁷⁵,
 Y. Yang¹⁶⁰, Z. Yang¹⁷, W.-M. Yao¹⁸, Y.C. Yap⁴⁴, Y. Yasu⁷⁹, E. Yatsenko^{58c,58d}, J. Ye⁴¹, S. Ye²⁹,
 I. Yeletskikh⁷⁷, E. Yigitbasi²⁵, E. Yildirim⁹⁷, K. Yorita¹⁷⁶, K. Yoshihara¹³⁴, C.J.S. Young³⁵, C. Young¹⁵⁰,
 J. Yu⁸, J. Yu⁷⁶, X. Yue^{59a}, S.P.Y. Yuen²⁴, B. Zabinski⁸², G. Zacharis¹⁰, E. Zaffaroni⁵², R. Zaidan¹⁴,
 A.M. Zaitsev^{121,ao}, T. Zakareishvili^{156b}, N. Zakharchuk³³, S. Zambito⁵⁷, D. Zanzi³⁵, D.R. Zaripovas⁵⁵,
 S.V. Zeißner⁴⁵, C. Zeitnitz¹⁷⁹, G. Zemaitytė¹³², J.C. Zeng¹⁷⁰, Q. Zeng¹⁵⁰, O. Zenin¹²¹, D. Zerwas¹²⁹,
 M. Zgubić¹³², D.F. Zhang^{58b}, D. Zhang¹⁰³, F. Zhang¹⁷⁸, G. Zhang^{58a}, G. Zhang^{15b}, H. Zhang^{15c},
 J. Zhang⁶, L. Zhang^{15c}, L. Zhang^{58a}, M. Zhang¹⁷⁰, P. Zhang^{15c}, R. Zhang^{58a}, R. Zhang²⁴, X. Zhang^{58b},
 Y. Zhang^{15d}, Z. Zhang¹²⁹, P. Zhao⁴⁷, Y. Zhao^{58b,129,ak}, Z. Zhao^{58a}, A. Zhemchugov⁷⁷, Z. Zheng¹⁰³,
 D. Zhong¹⁷⁰, B. Zhou¹⁰³, C. Zhou¹⁷⁸, M.S. Zhou^{15d}, M. Zhou¹⁵², N. Zhou^{58c}, Y. Zhou⁷, C.G. Zhu^{58b},
 H.L. Zhu^{58a}, H. Zhu^{15a}, J. Zhu¹⁰³, Y. Zhu^{58a}, X. Zhuang^{15a}, K. Zhukov¹⁰⁸, V. Zhulanov^{120b,120a},
 A. Zibell¹⁷⁴, D. Ziemińska⁶³, N.I. Zimine⁷⁷, S. Zimmermann⁵⁰, Z. Zinonos¹¹³, M. Ziolkowski¹⁴⁸,
 G. Zobernig¹⁷⁸, A. Zoccoli^{23b,23a}, K. Zoch⁵¹, T.G. Zorbas¹⁴⁶, R. Zou³⁶, M. Zur Nedden¹⁹, L. Zwalski³⁵.

¹Department of Physics, University of Adelaide, Adelaide; Australia.

- ²Physics Department, SUNY Albany, Albany NY; United States of America.
- ³Department of Physics, University of Alberta, Edmonton AB; Canada.
- ^{4(a)}Department of Physics, Ankara University, Ankara; ^(b)Istanbul Aydin University, Istanbul; ^(c)Division of Physics, TOBB University of Economics and Technology, Ankara; Turkey.
- ⁵LAPP, Université Grenoble Alpes, Université Savoie Mont Blanc, CNRS/IN2P3, Annecy; France.
- ⁶High Energy Physics Division, Argonne National Laboratory, Argonne IL; United States of America.
- ⁷Department of Physics, University of Arizona, Tucson AZ; United States of America.
- ⁸Department of Physics, University of Texas at Arlington, Arlington TX; United States of America.
- ⁹Physics Department, National and Kapodistrian University of Athens, Athens; Greece.
- ¹⁰Physics Department, National Technical University of Athens, Zografou; Greece.
- ¹¹Department of Physics, University of Texas at Austin, Austin TX; United States of America.
- ^{12(a)}Bahcesehir University, Faculty of Engineering and Natural Sciences, Istanbul; ^(b)Istanbul Bilgi University, Faculty of Engineering and Natural Sciences, Istanbul; ^(c)Department of Physics, Bogazici University, Istanbul; ^(d)Department of Physics Engineering, Gaziantep University, Gaziantep; Turkey.
- ¹³Institute of Physics, Azerbaijan Academy of Sciences, Baku; Azerbaijan.
- ¹⁴Institut de Física d'Altes Energies (IFAE), Barcelona Institute of Science and Technology, Barcelona; Spain.
- ^{15(a)}Institute of High Energy Physics, Chinese Academy of Sciences, Beijing; ^(b)Physics Department, Tsinghua University, Beijing; ^(c)Department of Physics, Nanjing University, Nanjing; ^(d)University of Chinese Academy of Science (UCAS), Beijing; China.
- ¹⁶Institute of Physics, University of Belgrade, Belgrade; Serbia.
- ¹⁷Department for Physics and Technology, University of Bergen, Bergen; Norway.
- ¹⁸Physics Division, Lawrence Berkeley National Laboratory and University of California, Berkeley CA; United States of America.
- ¹⁹Institut für Physik, Humboldt Universität zu Berlin, Berlin; Germany.
- ²⁰Albert Einstein Center for Fundamental Physics and Laboratory for High Energy Physics, University of Bern, Bern; Switzerland.
- ²¹School of Physics and Astronomy, University of Birmingham, Birmingham; United Kingdom.
- ²²Centro de Investigaciones, Universidad Antonio Nariño, Bogota; Colombia.
- ^{23(a)}Dipartimento di Fisica e Astronomia, Università di Bologna, Bologna; ^(b)INFN Sezione di Bologna; Italy.
- ²⁴Physikalisches Institut, Universität Bonn, Bonn; Germany.
- ²⁵Department of Physics, Boston University, Boston MA; United States of America.
- ²⁶Department of Physics, Brandeis University, Waltham MA; United States of America.
- ^{27(a)}Transilvania University of Brasov, Brasov; ^(b)Horia Hulubei National Institute of Physics and Nuclear Engineering, Bucharest; ^(c)Department of Physics, Alexandru Ioan Cuza University of Iasi, Iasi; ^(d)National Institute for Research and Development of Isotopic and Molecular Technologies, Physics Department, Cluj-Napoca; ^(e)University Politehnica Bucharest, Bucharest; ^(f)West University in Timisoara, Timisoara; Romania.
- ^{28(a)}Faculty of Mathematics, Physics and Informatics, Comenius University, Bratislava; ^(b)Department of Subnuclear Physics, Institute of Experimental Physics of the Slovak Academy of Sciences, Kosice; Slovak Republic.
- ²⁹Physics Department, Brookhaven National Laboratory, Upton NY; United States of America.
- ³⁰Departamento de Física, Universidad de Buenos Aires, Buenos Aires; Argentina.
- ³¹Cavendish Laboratory, University of Cambridge, Cambridge; United Kingdom.
- ^{32(a)}Department of Physics, University of Cape Town, Cape Town; ^(b)Department of Mechanical Engineering Science, University of Johannesburg, Johannesburg; ^(c)School of Physics, University of the

Witwatersrand, Johannesburg; South Africa.

³³Department of Physics, Carleton University, Ottawa ON; Canada.

^{34(a)}Faculté des Sciences Ain Chock, Réseau Universitaire de Physique des Hautes Energies - Université Hassan II, Casablanca;^(b)Centre National de l'Energie des Sciences Techniques Nucleaires (CNESTEN), Rabat;^(c)Faculté des Sciences Semlalia, Université Cadi Ayyad, LPHEA-Marrakech;^(d)Faculté des Sciences, Université Mohamed Premier and LPTPM, Oujda;^(e)Faculté des sciences, Université Mohammed V, Rabat; Morocco.

³⁵CERN, Geneva; Switzerland.

³⁶Enrico Fermi Institute, University of Chicago, Chicago IL; United States of America.

³⁷LPC, Université Clermont Auvergne, CNRS/IN2P3, Clermont-Ferrand; France.

³⁸Nevis Laboratory, Columbia University, Irvington NY; United States of America.

³⁹Niels Bohr Institute, University of Copenhagen, Copenhagen; Denmark.

^{40(a)}Dipartimento di Fisica, Università della Calabria, Rende;^(b)INFN Gruppo Collegato di Cosenza, Laboratori Nazionali di Frascati; Italy.

⁴¹Physics Department, Southern Methodist University, Dallas TX; United States of America.

⁴²Physics Department, University of Texas at Dallas, Richardson TX; United States of America.

^{43(a)}Department of Physics, Stockholm University;^(b)Oskar Klein Centre, Stockholm; Sweden.

⁴⁴Deutsches Elektronen-Synchrotron DESY, Hamburg and Zeuthen; Germany.

⁴⁵Lehrstuhl für Experimentelle Physik IV, Technische Universität Dortmund, Dortmund; Germany.

⁴⁶Institut für Kern- und Teilchenphysik, Technische Universität Dresden, Dresden; Germany.

⁴⁷Department of Physics, Duke University, Durham NC; United States of America.

⁴⁸SUPA - School of Physics and Astronomy, University of Edinburgh, Edinburgh; United Kingdom.

⁴⁹INFN e Laboratori Nazionali di Frascati, Frascati; Italy.

⁵⁰Physikalisch Institut, Albert-Ludwigs-Universität Freiburg, Freiburg; Germany.

⁵¹II. Physikalisch Institut, Georg-August-Universität Göttingen, Göttingen; Germany.

⁵²Département de Physique Nucléaire et Corpusculaire, Université de Genève, Genève; Switzerland.

^{53(a)}Dipartimento di Fisica, Università di Genova, Genova;^(b)INFN Sezione di Genova; Italy.

⁵⁴II. Physikalisch Institut, Justus-Liebig-Universität Giessen, Giessen; Germany.

⁵⁵SUPA - School of Physics and Astronomy, University of Glasgow, Glasgow; United Kingdom.

⁵⁶LPSC, Université Grenoble Alpes, CNRS/IN2P3, Grenoble INP, Grenoble; France.

⁵⁷Laboratory for Particle Physics and Cosmology, Harvard University, Cambridge MA; United States of America.

^{58(a)}Department of Modern Physics and State Key Laboratory of Particle Detection and Electronics, University of Science and Technology of China, Hefei;^(b)Institute of Frontier and Interdisciplinary Science and Key Laboratory of Particle Physics and Particle Irradiation (MOE), Shandong University, Qingdao;^(c)School of Physics and Astronomy, Shanghai Jiao Tong University, KLPPAC-MoE, SKLPPC, Shanghai;^(d)Tsung-Dao Lee Institute, Shanghai; China.

^{59(a)}Kirchhoff-Institut für Physik, Ruprecht-Karls-Universität Heidelberg, Heidelberg;^(b)Physikalisch Institut, Ruprecht-Karls-Universität Heidelberg, Heidelberg; Germany.

⁶⁰Faculty of Applied Information Science, Hiroshima Institute of Technology, Hiroshima; Japan.

^{61(a)}Department of Physics, Chinese University of Hong Kong, Shatin, N.T., Hong Kong;^(b)Department of Physics, University of Hong Kong, Hong Kong;^(c)Department of Physics and Institute for Advanced Study, Hong Kong University of Science and Technology, Clear Water Bay, Kowloon, Hong Kong; China.

⁶²Department of Physics, National Tsing Hua University, Hsinchu; Taiwan.

⁶³Department of Physics, Indiana University, Bloomington IN; United States of America.

^{64(a)}INFN Gruppo Collegato di Udine, Sezione di Trieste, Udine;^(b)ICTP, Trieste;^(c)Dipartimento di Chimica, Fisica e Ambiente, Università di Udine, Udine; Italy.

- ^{65(a)}INFN Sezione di Lecce; ^(b)Dipartimento di Matematica e Fisica, Università del Salento, Lecce; Italy.
^{66(a)}INFN Sezione di Milano; ^(b)Dipartimento di Fisica, Università di Milano, Milano; Italy.
^{67(a)}INFN Sezione di Napoli; ^(b)Dipartimento di Fisica, Università di Napoli, Napoli; Italy.
^{68(a)}INFN Sezione di Pavia; ^(b)Dipartimento di Fisica, Università di Pavia, Pavia; Italy.
^{69(a)}INFN Sezione di Pisa; ^(b)Dipartimento di Fisica E. Fermi, Università di Pisa, Pisa; Italy.
^{70(a)}INFN Sezione di Roma; ^(b)Dipartimento di Fisica, Sapienza Università di Roma, Roma; Italy.
^{71(a)}INFN Sezione di Roma Tor Vergata; ^(b)Dipartimento di Fisica, Università di Roma Tor Vergata, Roma; Italy.
^{72(a)}INFN Sezione di Roma Tre; ^(b)Dipartimento di Matematica e Fisica, Università Roma Tre, Roma; Italy.
^{73(a)}INFN-TIFPA; ^(b)Università degli Studi di Trento, Trento; Italy.
⁷⁴Institut für Astro- und Teilchenphysik, Leopold-Franzens-Universität, Innsbruck; Austria.
⁷⁵University of Iowa, Iowa City IA; United States of America.
⁷⁶Department of Physics and Astronomy, Iowa State University, Ames IA; United States of America.
⁷⁷Joint Institute for Nuclear Research, Dubna; Russia.
^{78(a)}Departamento de Engenharia Elétrica, Universidade Federal de Juiz de Fora (UFJF), Juiz de Fora; ^(b)Universidade Federal do Rio De Janeiro COPPE/EE/IF, Rio de Janeiro; ^(c)Universidade Federal de São João del Rei (UFSJ), São João del Rei; ^(d)Instituto de Física, Universidade de São Paulo, São Paulo; Brazil.
⁷⁹KEK, High Energy Accelerator Research Organization, Tsukuba; Japan.
⁸⁰Graduate School of Science, Kobe University, Kobe; Japan.
^{81(a)}AGH University of Science and Technology, Faculty of Physics and Applied Computer Science, Krakow; ^(b)Marian Smoluchowski Institute of Physics, Jagiellonian University, Krakow; Poland.
⁸²Institute of Nuclear Physics Polish Academy of Sciences, Krakow; Poland.
⁸³Faculty of Science, Kyoto University, Kyoto; Japan.
⁸⁴Kyoto University of Education, Kyoto; Japan.
⁸⁵Research Center for Advanced Particle Physics and Department of Physics, Kyushu University, Fukuoka ; Japan.
⁸⁶Instituto de Física La Plata, Universidad Nacional de La Plata and CONICET, La Plata; Argentina.
⁸⁷Physics Department, Lancaster University, Lancaster; United Kingdom.
⁸⁸Oliver Lodge Laboratory, University of Liverpool, Liverpool; United Kingdom.
⁸⁹Department of Experimental Particle Physics, Jožef Stefan Institute and Department of Physics, University of Ljubljana, Ljubljana; Slovenia.
⁹⁰School of Physics and Astronomy, Queen Mary University of London, London; United Kingdom.
⁹¹Department of Physics, Royal Holloway University of London, Egham; United Kingdom.
⁹²Department of Physics and Astronomy, University College London, London; United Kingdom.
⁹³Louisiana Tech University, Ruston LA; United States of America.
⁹⁴Fysiska institutionen, Lunds universitet, Lund; Sweden.
⁹⁵Centre de Calcul de l’Institut National de Physique Nucléaire et de Physique des Particules (IN2P3), Villeurbanne; France.
⁹⁶Departamento de Física Teorica C-15 and CIAFF, Universidad Autónoma de Madrid, Madrid; Spain.
⁹⁷Institut für Physik, Universität Mainz, Mainz; Germany.
⁹⁸School of Physics and Astronomy, University of Manchester, Manchester; United Kingdom.
⁹⁹CPPM, Aix-Marseille Université, CNRS/IN2P3, Marseille; France.
¹⁰⁰Department of Physics, University of Massachusetts, Amherst MA; United States of America.
¹⁰¹Department of Physics, McGill University, Montreal QC; Canada.
¹⁰²School of Physics, University of Melbourne, Victoria; Australia.
¹⁰³Department of Physics, University of Michigan, Ann Arbor MI; United States of America.

- ¹⁰⁴Department of Physics and Astronomy, Michigan State University, East Lansing MI; United States of America.
- ¹⁰⁵B.I. Stepanov Institute of Physics, National Academy of Sciences of Belarus, Minsk; Belarus.
- ¹⁰⁶Research Institute for Nuclear Problems of Byelorussian State University, Minsk; Belarus.
- ¹⁰⁷Group of Particle Physics, University of Montreal, Montreal QC; Canada.
- ¹⁰⁸P.N. Lebedev Physical Institute of the Russian Academy of Sciences, Moscow; Russia.
- ¹⁰⁹Institute for Theoretical and Experimental Physics (ITEP), Moscow; Russia.
- ¹¹⁰National Research Nuclear University MEPhI, Moscow; Russia.
- ¹¹¹D.V. Skobeltsyn Institute of Nuclear Physics, M.V. Lomonosov Moscow State University, Moscow; Russia.
- ¹¹²Fakultät für Physik, Ludwig-Maximilians-Universität München, München; Germany.
- ¹¹³Max-Planck-Institut für Physik (Werner-Heisenberg-Institut), München; Germany.
- ¹¹⁴Nagasaki Institute of Applied Science, Nagasaki; Japan.
- ¹¹⁵Graduate School of Science and Kobayashi-Maskawa Institute, Nagoya University, Nagoya; Japan.
- ¹¹⁶Department of Physics and Astronomy, University of New Mexico, Albuquerque NM; United States of America.
- ¹¹⁷Institute for Mathematics, Astrophysics and Particle Physics, Radboud University Nijmegen/Nikhef, Nijmegen; Netherlands.
- ¹¹⁸Nikhef National Institute for Subatomic Physics and University of Amsterdam, Amsterdam; Netherlands.
- ¹¹⁹Department of Physics, Northern Illinois University, DeKalb IL; United States of America.
- ^{120(a)}Budker Institute of Nuclear Physics and NSU, SB RAS, Novosibirsk;^(b)Novosibirsk State University Novosibirsk; Russia.
- ¹²¹Institute for High Energy Physics of the National Research Centre Kurchatov Institute, Protvino; Russia.
- ¹²²Department of Physics, New York University, New York NY; United States of America.
- ¹²³Ohio State University, Columbus OH; United States of America.
- ¹²⁴Faculty of Science, Okayama University, Okayama; Japan.
- ¹²⁵Homer L. Dodge Department of Physics and Astronomy, University of Oklahoma, Norman OK; United States of America.
- ¹²⁶Department of Physics, Oklahoma State University, Stillwater OK; United States of America.
- ¹²⁷Palacký University, RCPTM, Joint Laboratory of Optics, Olomouc; Czech Republic.
- ¹²⁸Center for High Energy Physics, University of Oregon, Eugene OR; United States of America.
- ¹²⁹LAL, Université Paris-Sud, CNRS/IN2P3, Université Paris-Saclay, Orsay; France.
- ¹³⁰Graduate School of Science, Osaka University, Osaka; Japan.
- ¹³¹Department of Physics, University of Oslo, Oslo; Norway.
- ¹³²Department of Physics, Oxford University, Oxford; United Kingdom.
- ¹³³LPNHE, Sorbonne Université, Paris Diderot Sorbonne Paris Cité, CNRS/IN2P3, Paris; France.
- ¹³⁴Department of Physics, University of Pennsylvania, Philadelphia PA; United States of America.
- ¹³⁵Konstantinov Nuclear Physics Institute of National Research Centre "Kurchatov Institute", PNPI, St. Petersburg; Russia.
- ¹³⁶Department of Physics and Astronomy, University of Pittsburgh, Pittsburgh PA; United States of America.
- ^{137(a)}Laboratório de Instrumentação e Física Experimental de Partículas - LIP;^(b)Departamento de Física, Faculdade de Ciências, Universidade de Lisboa, Lisboa;^(c)Departamento de Física, Universidade de Coimbra, Coimbra;^(d)Centro de Física Nuclear da Universidade de Lisboa, Lisboa;^(e)Departamento de Física, Universidade do Minho, Braga;^(f)Departamento de Física Teórica y del Cosmos, Universidad de Granada, Granada (Spain);^(g)Dep Física and CEFITEC of Faculdade de Ciências e Tecnologia,

Universidade Nova de Lisboa, Caparica; Portugal.

¹³⁸Institute of Physics, Academy of Sciences of the Czech Republic, Prague; Czech Republic.

¹³⁹Czech Technical University in Prague, Prague; Czech Republic.

¹⁴⁰Charles University, Faculty of Mathematics and Physics, Prague; Czech Republic.

¹⁴¹Particle Physics Department, Rutherford Appleton Laboratory, Didcot; United Kingdom.

¹⁴²IRFU, CEA, Université Paris-Saclay, Gif-sur-Yvette; France.

¹⁴³Santa Cruz Institute for Particle Physics, University of California Santa Cruz, Santa Cruz CA; United States of America.

^{144(a)}Departamento de Física, Pontificia Universidad Católica de Chile, Santiago;^(b)Departamento de Física, Universidad Técnica Federico Santa María, Valparaíso; Chile.

¹⁴⁵Department of Physics, University of Washington, Seattle WA; United States of America.

¹⁴⁶Department of Physics and Astronomy, University of Sheffield, Sheffield; United Kingdom.

¹⁴⁷Department of Physics, Shinshu University, Nagano; Japan.

¹⁴⁸Department Physik, Universität Siegen, Siegen; Germany.

¹⁴⁹Department of Physics, Simon Fraser University, Burnaby BC; Canada.

¹⁵⁰SLAC National Accelerator Laboratory, Stanford CA; United States of America.

¹⁵¹Physics Department, Royal Institute of Technology, Stockholm; Sweden.

¹⁵²Departments of Physics and Astronomy, Stony Brook University, Stony Brook NY; United States of America.

¹⁵³Department of Physics and Astronomy, University of Sussex, Brighton; United Kingdom.

¹⁵⁴School of Physics, University of Sydney, Sydney; Australia.

¹⁵⁵Institute of Physics, Academia Sinica, Taipei; Taiwan.

^{156(a)}E. Andronikashvili Institute of Physics, Iv. Javakhishvili Tbilisi State University, Tbilisi;^(b)High Energy Physics Institute, Tbilisi State University, Tbilisi; Georgia.

¹⁵⁷Department of Physics, Technion, Israel Institute of Technology, Haifa; Israel.

¹⁵⁸Raymond and Beverly Sackler School of Physics and Astronomy, Tel Aviv University, Tel Aviv; Israel.

¹⁵⁹Department of Physics, Aristotle University of Thessaloniki, Thessaloniki; Greece.

¹⁶⁰International Center for Elementary Particle Physics and Department of Physics, University of Tokyo, Tokyo; Japan.

¹⁶¹Graduate School of Science and Technology, Tokyo Metropolitan University, Tokyo; Japan.

¹⁶²Department of Physics, Tokyo Institute of Technology, Tokyo; Japan.

¹⁶³Tomsk State University, Tomsk; Russia.

¹⁶⁴Department of Physics, University of Toronto, Toronto ON; Canada.

^{165(a)}TRIUMF, Vancouver BC;^(b)Department of Physics and Astronomy, York University, Toronto ON; Canada.

¹⁶⁶Division of Physics and Tomonaga Center for the History of the Universe, Faculty of Pure and Applied Sciences, University of Tsukuba, Tsukuba; Japan.

¹⁶⁷Department of Physics and Astronomy, Tufts University, Medford MA; United States of America.

¹⁶⁸Department of Physics and Astronomy, University of California Irvine, Irvine CA; United States of America.

¹⁶⁹Department of Physics and Astronomy, University of Uppsala, Uppsala; Sweden.

¹⁷⁰Department of Physics, University of Illinois, Urbana IL; United States of America.

¹⁷¹Instituto de Física Corpuscular (IFIC), Centro Mixto Universidad de Valencia - CSIC, Valencia; Spain.

¹⁷²Department of Physics, University of British Columbia, Vancouver BC; Canada.

¹⁷³Department of Physics and Astronomy, University of Victoria, Victoria BC; Canada.

¹⁷⁴Fakultät für Physik und Astronomie, Julius-Maximilians-Universität Würzburg, Würzburg; Germany.

¹⁷⁵Department of Physics, University of Warwick, Coventry; United Kingdom.

- ¹⁷⁶Waseda University, Tokyo; Japan.
- ¹⁷⁷Department of Particle Physics, Weizmann Institute of Science, Rehovot; Israel.
- ¹⁷⁸Department of Physics, University of Wisconsin, Madison WI; United States of America.
- ¹⁷⁹Fakultät für Mathematik und Naturwissenschaften, Fachgruppe Physik, Bergische Universität Wuppertal, Wuppertal; Germany.
- ¹⁸⁰Department of Physics, Yale University, New Haven CT; United States of America.
- ¹⁸¹Yerevan Physics Institute, Yerevan; Armenia.
- ^a Also at Borough of Manhattan Community College, City University of New York, NY; United States of America.
- ^b Also at California State University, East Bay; United States of America.
- ^c Also at Centre for High Performance Computing, CSIR Campus, Rosebank, Cape Town; South Africa.
- ^d Also at CERN, Geneva; Switzerland.
- ^e Also at CPPM, Aix-Marseille Université, CNRS/IN2P3, Marseille; France.
- ^f Also at Département de Physique Nucléaire et Corpusculaire, Université de Genève, Genève; Switzerland.
- ^g Also at Departament de Fisica de la Universitat Autonoma de Barcelona, Barcelona; Spain.
- ^h Also at Departamento de Física Teorica y del Cosmos, Universidad de Granada, Granada (Spain); Spain.
- ⁱ Also at Departamento de Física, Instituto Superior Técnico, Universidade de Lisboa, Lisboa; Portugal.
- ^j Also at Department of Applied Physics and Astronomy, University of Sharjah, Sharjah; United Arab Emirates.
- ^k Also at Department of Financial and Management Engineering, University of the Aegean, Chios; Greece.
- ^l Also at Department of Physics and Astronomy, University of Louisville, Louisville, KY; United States of America.
- ^m Also at Department of Physics and Astronomy, University of Sheffield, Sheffield; United Kingdom.
- ⁿ Also at Department of Physics, California State University, Fresno CA; United States of America.
- ^o Also at Department of Physics, California State University, Sacramento CA; United States of America.
- ^p Also at Department of Physics, King's College London, London; United Kingdom.
- ^q Also at Department of Physics, St. Petersburg State Polytechnical University, St. Petersburg; Russia.
- ^r Also at Department of Physics, Stanford University; United States of America.
- ^s Also at Department of Physics, University of Fribourg, Fribourg; Switzerland.
- ^t Also at Department of Physics, University of Michigan, Ann Arbor MI; United States of America.
- ^u Also at Giresun University, Faculty of Engineering, Giresun; Turkey.
- ^v Also at Graduate School of Science, Osaka University, Osaka; Japan.
- ^w Also at Hellenic Open University, Patras; Greece.
- ^x Also at Horia Hulubei National Institute of Physics and Nuclear Engineering, Bucharest; Romania.
- ^y Also at II. Physikalisch Institut, Georg-August-Universität Göttingen, Göttingen; Germany.
- ^z Also at Institucio Catalana de Recerca i Estudis Avancats, ICREA, Barcelona; Spain.
- ^{aa} Also at Institut für Experimentalphysik, Universität Hamburg, Hamburg; Germany.
- ^{ab} Also at Institute for Mathematics, Astrophysics and Particle Physics, Radboud University Nijmegen/Nikhef, Nijmegen; Netherlands.
- ^{ac} Also at Institute for Particle and Nuclear Physics, Wigner Research Centre for Physics, Budapest; Hungary.
- ^{ad} Also at Institute of Particle Physics (IPP); Canada.
- ^{ae} Also at Institute of Physics, Academia Sinica, Taipei; Taiwan.
- ^{af} Also at Institute of Physics, Azerbaijan Academy of Sciences, Baku; Azerbaijan.
- ^{ag} Also at Institute of Theoretical Physics, Ilia State University, Tbilisi; Georgia.
- ^{ah} Also at Instituto de Física Teórica de la Universidad Autónoma de Madrid; Spain.

- ai* Also at Istanbul University, Dept. of Physics, Istanbul; Turkey.
- aj* Also at Joint Institute for Nuclear Research, Dubna; Russia.
- ak* Also at LAL, Université Paris-Sud, CNRS/IN2P3, Université Paris-Saclay, Orsay; France.
- al* Also at Louisiana Tech University, Ruston LA; United States of America.
- am* Also at LPNHE, Sorbonne Université, Paris Diderot Sorbonne Paris Cité, CNRS/IN2P3, Paris; France.
- an* Also at Manhattan College, New York NY; United States of America.
- ao* Also at Moscow Institute of Physics and Technology State University, Dolgoprudny; Russia.
- ap* Also at National Research Nuclear University MEPhI, Moscow; Russia.
- aq* Also at Physikalisches Institut, Albert-Ludwigs-Universität Freiburg, Freiburg; Germany.
- ar* Also at School of Physics, Sun Yat-sen University, Guangzhou; China.
- as* Also at The City College of New York, New York NY; United States of America.
- at* Also at The Collaborative Innovation Center of Quantum Matter (CICQM), Beijing; China.
- au* Also at Tomsk State University, Tomsk, and Moscow Institute of Physics and Technology State University, Dolgoprudny; Russia.
- av* Also at TRIUMF, Vancouver BC; Canada.
- aw* Also at Universita di Napoli Parthenope, Napoli; Italy.
- * Deceased